

**SKELETAL MUSCLE AS A MECHANISM FOR PERIPHERAL REGULATION OF VOLUNTARY
PHYSICAL ACTIVITY**

A Dissertation

by

DAVID PAUL FERGUSON

Submitted to the Office of Graduate Studies of
Texas A&M University
in partial fulfillment of the requirements for the degree of

DOCTOR OF PHILOSOPHY

Chair of Committee, J. Timothy Lightfoot
Committee Members, James D. Fluckey
Michael Massett
Lawrence J. Dangott
Roger Sansom
Head of Department, Richard Kreider

August 2013

Major Subject: Kinesiology

Copyright 2013 David Paul Ferguson

ABSTRACT

Physical activity can prevent cardiovascular disease, obesity, type II diabetes and some types of cancer. With only 3.5% of adults meeting the recommended physical activity guidelines, research has focused on the regulatory factors that influence physical activity level. Genetic influence accounts for the majority of physical activity regulation. However, there is limited information on the mechanisms that affect physical activity, in part, because of a lack of reliable methods to silence genes *in vivo*. The purpose of this dissertation was to identify mechanisms in skeletal muscle that influence physical activity. The methods used to accomplish the purpose of this dissertation were the evaluation of Vivo-morpholinos as a gene silencing tool in skeletal muscle and brain, identification of proteins in skeletal muscle associated with increased physical activity level, and the use Vivo-morpholinos to transiently knockdown the identified skeletal muscle proteins as a means to elucidate mechanisms for the peripheral regulation of physical activity. Overall, this study showed that Vivo-morpholinos effectively silenced genes in skeletal muscle yet required the use of a pharmacological aid to achieve gene silencing in the brain. Additionally proteins associated with calcium regulation (Annexin A6 and Calsequestrin 1) and the Krebs's (TCA) cycle were found to be over expressed in the high active animals. The knockdown of Annexin A6 and Calsequestrin 1 resulted in a significant decrease in physical activity, thus showing that calcium regulation could influence the physical activity response. While these results provide a potential mechanism for the peripheral regulation of physical activity, a side effect observed was that Vivo-morpholinos can hybridize resulting in increased mortality rates of the treatment animals. Therefore, we developed methods to alleviate the toxic effects of Vivo-morpholinos. Thus, this dissertation refined a technique for

determining a gene's effect in an *in vivo* model and identified two candidate proteins (Annexin A6 and Calsequestrin 1) that play a role in regulating daily physical activity.

DEDICATION

I dedicate this dissertation to my dependable research assistant, best friend, and loving wife, Kayley. Despite illness, financial hardships, and emotional stress she has always encouraged me to never follow my dreams, but chase them down. Thank you for supporting me in the pursuit of this dream.

ACKNOWLEDGEMENTS

I could not have completed this work if it were not for the help of my committee and my lab group. I would like to thank Tim Lightfoot, Michael Massett, Jim Fluckey, Larry Dangott, and Roger Sansom for their guidance in this process. Each individual has left a lasting impression on me, which has shaped my education. Often this education came outside the class room such as learning the principles of tissue preservation while moving a lab in 24 hours from Charlotte, NC to College Station, TX with Dr. Lightfoot; the effects of genetics on performance from Dr. Massett's Spiderman candy bucket; the basics of muscle protein synthesis while traveling at █████ mph in Dr. Fluckey's Boss 302; the methods of proteomics while contemplating buying a kit car with Dr. Dangott; and discussions on lactate instead of philosophy with Dr. Sansom.

Over the years, I have worked with many fellow undergrad and graduate students. I would like to identify Bob Bowen, Amy Knab, Trudy Moore-Harrison, Alicia Hamilton, Tyrone Ceaser, Felicia Dangerfield-Persky, Greeshma Shenoy, Michelle Dawes, and Patrick "Blaise" Collins. Additionally, I would like to acknowledge some of the individuals that worked on the studies in this dissertation. I have worked with Emily Schmitt for six years from the time we were Masters Students in Clinical Exercise Physiology at UNC Charlotte to now as PhD students at Texas A&M. As fate would have it, Dr. Lightfoot assigned us to a group project in the fall of 2007, and from that moment we have been friends first and collaborators second. I could have not have had the success I have had if it were not for Emily. From our early days of working with NASCAR when she managed to "get" us two pit passes to the race at Martinsville to when she mastered the tail vein injection technique in 20 mins when it took me several weeks. She is

a great teacher, researcher, and friend. In fact, she is the model to which I will compare all future co-workers to.

Heather Vellers recently joined the lab and I have been very grateful for her willingness to help on all aspects of projects. I am impressed by how quickly Heather learned the molecular biology techniques used in our lab. More importantly, I am proud and honored to watch her grow in one of the crucial aspects of being a doctoral student - the playing of practical jokes on fellow graduate students. For a time Heather was known as the girl that disposed of distilled water by walking around campus and pouring a little out at each building. Now she is known as the student that enclosed another student's desk in masking tape. I was honored when it was thought that I performed the masking tape prank. I have no doubt that Heather is on her way to being a great scientist.

Every lab needs a little bit of trouble, for the Biology of Physical Activity Lab this was Sheril Marek. Sheril started working as an undergraduate and continued as a Masters Student. The thing that impressed me about Sheril was that she dedicated long hours to the lab with the only purpose being the desire to help others. I am very grateful for her dedication, input, and keeping me on my toes. She certainly earned her endearing nickname of "trouble."

Two of the smartest undergraduate students I have ever met are Analisa Jimenez and Conor Irwin. I had the pleasure of working with Analisa for several years and was always impressed by her maturity and diligence. She is the only undergraduate student I know of that could hold her own at a poster presentation with one of the pillars in the exercise physiology field. Conor recently joined the lab and mastered western blotting in the amount of time it takes a normal person to master walking and chewing gum. He has been a great addition to

the lab and I have enjoyed working with him. I look forward to seeing the bright careers both Analisa and Conor will achieve.

I would also like to thank the help of the Muscle Biology lab, specifically Mike Wiggs and Kevin Shimkus for their help in trouble shooting the western blot technique.

NOMENCLATURE

Mouse Gene *Italicized First Letter Capitalized (ex: Glut4)*

Human Gene *ALL CAPITALIZED ITALICIZED (ex: GLUT4)*

Mouse Protein First Letter Capitalized (ex: Glut4)

Human Protein ALL CAPITALIZED (ex: GLUT4)

The literature has used “over expression,” “over-expression,” and “overexpression” to characterize the increase in gene/protein amount. For this dissertation “over expression” will be used.

Figures are presented in the appendix and denoted by the section they are referenced in followed by the figure number (i.e. 2.3 represents figure 3 in section 2)

All tables in this dissertation are referenced in section 3. The tables are presented in the appendix.

TABLE OF CONTENTS

	Page
ABSTRACT.....	ii
DEDICATION.....	iv
ACKNOWLEDGEMENTS.....	v
NOMENCLATURE.....	viii
TABLE OF CONTENTS.....	ix
CHAPTER	
I INTRODUCTION AND LITERATURE REVIEW.....	1
1.1 Genomic Regions Associated with the Regulation of Voluntary Physical Activity.....	5
1.2 Central Drive and Reward Driven Behavior Regulate Voluntary Physical Activity.....	11
1.3 Peripheral Factors Affecting the Capability to be Physically Active.....	14
1.3.1 Substrate Utilization Influences Physical Activity.....	14
1.3.2 Skeletal Muscle Force of Contraction and Muscle Fatigue Influences Physical Activity.....	15
1.4 Methods to Elucidate the Proteome that is Associated with Voluntary Physical Activity.....	20
1.5 Confirming Candidate Gene's Involvement in Physical Activity.....	24
1.6 Summary.....	28
II VIVO-MORPHOLINOS INDUCED TRANSIENT KNOCKDOWN OF PHYSICAL ACTIVITY RELATED PROTEINS.....	29
2.1 Synopsis.....	29
2.2 Introduction.....	30
2.3 Methods.....	33
2.3.1 Experiment 1: Evaluation of Vivo-morpholinos' Gene Silencing in Mouse Activity Model.....	33
2.3.2 Experiment 2: Determination of Vivo-morpholino Washout Period.....	36
2.3.3 Experiment 3: Utilization of a Vivo-morpholino Cocktail.....	37

2.4 Results.....	38
2.4.1 Experiment 1: Evaluation of Vivo-morpholinos in Activity Model.....	38
2.4.2 Experiment 2: Determination of Vivo-morpholino Washout Period.....	39
2.4.3 Experiment 3: Utilization of a Vivo-morpholino Cocktail.....	40
2.5 Discussion.....	40
III THE DIFFERENTIAL SKELETAL MUSCLE PROTEOME IN HIGH AND LOW ACTIVE MICE....	47
3.1 Synopsis.....	47
3.2 Introduction.....	48
3.3 Methods.....	49
3.3.1 Experiment 1: Proteome Determination.....	50
3.3.2 Experiment 2: Role of Candidate Proteins in Physical Activity.....	54
3.3.3 Statistics.....	56
3.4 Results.....	57
3.4.1 Experiment 1: Proteome Determination.....	57
3.4.2 Experiment 2: Role of Candidate Proteins in Physical Activity.....	58
3.5 Discussion.....	59
3.5.1 High-active Animals.....	61
3.5.2 Low-active Animals.....	66
IV LESSONS LEARNED FROM VIVO-MORPHOLINOS: HOW TO AVOID VIVO-MORPHOLINO TOXICITY.....	70
4.1 Synopsis.....	70
4.2 Introduction.....	71
4.3 Observation of the Problem.....	72
4.4 Potential Solutions to the Problem Provided by GeneTools.....	74
4.5 Investigation into the Cause of Death	74
4.6 Suggested Mechanism for Blood Clot Formation and Cardiac Death.....	76
4.7 Solution to Fatal Vivo-morpholinos	78
V CONCLUSIONS.....	79
REFERENCES.....	81
APPENDIX A: FIGURES.....	105
APPENDIX B: TABLES.....	127

APPENDIX C: PROTEIN ASSAY TECHNIQUES.....	134
APPENDIX D: VIVO-MORPHOLINO DOSE CALCULATOR.....	145

CHAPTER I

INTRODUCTION AND LITERATURE REVIEW

Behavior traits, such as voluntary physical activity, are generally accepted to be a result of environmental and genetic/biological factors. A large amount of literature¹⁻⁴ has examined the environmental influence on physical activity. While the literature has focused on environmental factors such as culture, peer influence, and the “built environment” (i.e. access to sidewalks)²⁻⁴, it has been shown that the main effects contributing to the control of voluntary physical activity are genetic and biological influence⁵. Voluntary physical activity is an important trait to study because it has been positively correlated with decreases in cardiovascular disease, obesity, type II diabetes and some types of cancer⁵. With only 3.5% of adults meeting the recommended physical activity guidelines⁶, physical inactivity is the second actual leading cause of death (~250,000 cases/year) in the United States⁷, with an estimated \$507 billion a year in health care costs⁸. Thus, the identification of mechanisms that regulate voluntary physical activity could improve the quality of life of individuals and potentially reduce health care costs. Despite promising research on the genetic regulation of physical activity, there has been limited information on mechanisms that regulate physical activity.

While the literature has not provided specific mechanisms for the regulation of physical activity, the literature has provided models by which to study physical activity that could be used to identify mechanisms associated with voluntary physical activity. Two of the most widely used models for voluntary physical activity regulation are humans^{9,10} and mice¹¹⁻¹⁷. Human studies require a large number of subjects in order to achieve statistical power to

human genome¹⁰. A method to reduce the heterozygous nature of the human genome is the use of identical twins as subjects¹⁰. This technique has been employed with some success in the physical activity literature, which has shown genetic influence accounting for 48-71% of the effect on physical activity level¹⁰. However, a limitation on virtually all of the human activity literature is that the method used was a survey, where subjects were asked to recall their past physical activity levels¹⁰. While a popular tool, the use of recall surveys could skew the results due to the subjective nature of data collection⁵; for example, recall surveys have estimated that the number of Americans that meet the physical activity requirements for health benefits ranges from 7-70% which is widely variant from the 3.5% measurement derived from objective measurements¹⁸. The discrepancy in the survey data is a result of the type of questions used to classify physical activity, with most agreeing that in order to assess physical activity level, questions must address physical activity intensity, frequency, and duration¹⁸. Physical activity intensity is objectively measured by the amount of energy expended during a bout of activity (expressed as kilojoules); however, most questionnaires do not reliably address physical activity intensity due to the fact that most often the questions are presented in a way where the subject must provide a subjective rating ranging from “easy” to “hard”¹⁸. Frequency is the number of activity bouts a subject partakes in during a defined time span and often frequency is over estimated by recall surveys especially if the survey requires the subject to recall a time period longer than three months¹⁸. Alternately, short term surveys have not been found to be more reliable than long term surveys due to the fact that surveys that measure only one week often do not distinguish between weekday and weekend, which depending on the subject’s occupation can reflect drastically different physical activity levels¹⁸. Lastly, the evaluation of duration (time spent doing activity) is problematic for recall surveys in that subjects report the

time allotted for physical activity and not the amount of time engaged in physical activity¹⁸.

This phenomenon is often observed in children's gymnasium classes where physical activity is reported on a survey as the duration of the class period but in fact the majority of that time the child is listening to the instructor or waiting his/her turn to engage in physical activity¹⁸. Thus, physical activity level is over estimated by surveys and can potentially skew results associated with the phenotype.

Another approach to examining genetic mechanisms of physical activity is to use animal models, which have several benefits over the human model. Specifically, mice can be bred to limit heterozygosity of the population, environmental factors can be controlled by the investigator, and the short life span of the animal provides the opportunity to measure physical activity across multiple generations⁵. Inbred mice are produced using at least 20 consecutive generations of parent x offspring or sister x brother mating, allowing for mice to be genetically homozygous at all loci¹². Thus, the use of inbred mice allow for the rigorous control of heterozygosity of the genome and the environment allowing for controlled investigation into the genetic regulation of physical activity. Furthermore, the mouse is an excellent model of the human genome given that there is approximately 75% homology between the mouse and human genome¹⁹. While there is some discrepancy in homology between mice and humans, this difference appears to be a result of differences in non-coding regions of the genome¹⁹. Thus, the demonstrated human-mouse genomic homology increases the probability that results from genetic studies using the mouse model can be directly translated to humans.

To evaluate voluntary physical activity in the mouse model several methods have been utilized. The most frequently used methods in the literature have been wheel running, home

cage activity, and maze activity. However, it has been suggested that studies using home cage activity and/or maze activity evaluate both physical activity level and fear/ anxiety level²⁰. Therefore, results from cage and maze activity studies may provide ambiguous results since this methodology characterizes both physical activity level and fear/anxiety. Therefore, in the mouse model, the method most often used to assess voluntary physical activity level is wheel running¹². Wheel running as a measure of physical activity has a similar physiological response as does partaking in physical activity by humans, such as self-selection of intensity, heart rate response, and neurological changes. Specifically it has been shown that humans self select an average running intensity of 70%²¹. Interestingly it has been shown that mice self select a wheel running intensity of 65-70%²². The self-selection of physical activity level results in similar cardiovascular and neurological adaptations between mice and humans. Adlam *et al*²³ showed that during wheel running there was a significant increase in heart rate and blood pressure, however following five weeks of wheel running there was a decrease in resting heart rate and blood pressure²³. Similarly, the human literature has shown that regular bouts of moderate intensity exercise (60-70% max heart rate) result in a decrease of resting heart rate and systolic blood pressure^{24,25}. Additionally, mouse wheel running and human physical activity engagement result in similar neurological responses. Dishman *et al*²⁶ characterized the norepinephrine, 5-hydroxytryptamine, dopamine, and gamma aminobutyric acid responses to wheel running and showed that there was an increase in norepinephrine and dopamine following mouse wheel running which led the authors to conclude that physical activity had a protective effect on brain monoamine depletion and thus an antidepressant affect²⁶. The human literature has documented similar findings of antidepressant effects following bouts of physical activity²⁷. However, due to the nature of the study, brain monoamines could not be

directly measured in humans²⁶ for comparison to the mouse model. Given the similarities between human and mouse physiological parameters during voluntary exercise and voluntary wheel running, the use of the mouse wheel running model is appropriate to determine the regulation of physical activity level with the use of genetic linkage, transcriptome, and proteome analyses.

1.1 Genomic Regions Associated with the Regulation of Voluntary Physical Activity

As noted earlier, it has been shown that in the mouse and human model an individual's genome influences physical activity level^{5,13}. Most often, the genetic influence on a trait is characterized as heritability (i.e. how much parental lineage affects behavior of the individual). Heritability is most often expressed as a percentage of the total phenotype²⁸. The human literature has shown that genetic regulation accounts for 20-92% of the influence on voluntary physical activity level^{5,9,10}. The large range in genetic influence could be due to the methodology used to evaluate the physical activity phenotype. When using accelerometers Joosen *et al*⁹ found genetic influence accounted for 92% of physical activity regulation⁹. However, Stubbe *et al*¹⁰ used 37,051 twin pairs and observed that the genetic influence on physical activity level ranged from 48-71% with nationality being one of the largest factors accounting for the variance¹⁰. The Stubbe study used self-reported surveys on leisure time activity to assess physical activity level¹⁰. The different methodologies from the Joosen (accelerometer) and Stubbe (survey) studies could account for the difference in heritability, in that it has been shown that recall surveys do not correlate with actual physical activity level¹⁸. As to the 'nationality' component in the Stubbe study it was demonstrated that cultural background also influenced heritability, specifically subjects from Australia, the Netherlands,

and Norway had higher heritability associated with physical activity as opposed to subjects from Sweden and Denmark¹⁰; this is not surprising in that it has been shown that cold weather climates decrease the physical activity response due to individuals remaining indoors¹⁸. The fact that Norway and the Netherlands (both cold weather climates) had higher heritability associated with physical activity is a result their culture endorsing outdoor activity¹⁰. Thus, the influence of the environment on activity lends support for the mouse model because the investigator can directly and robustly control the environmental influence⁵. In the adult mouse model directly measuring wheel running resulted in a heritable range of 50-80% for the regulation of physical activity level²⁹. Thus, heritability studies using both the human and mouse model have shown a heritable range of 20-92%, with the majority of work centering on 50-70% influence on physical activity. Building on the results of the heritability studies, research has focused on identifying genetic mechanisms associated with physical activity.

Studies seeking to understand the genetic architecture of high and low active subjects have used a variety of approaches, with most employing either a positional cloning or linkage analysis approach³⁰. In either approach, one of the early steps is to determine quantitative trait loci (QTL) which identifies regions of the genome that are correlated to voluntary physical activity. Lightfoot *et al*¹³ was the first to determine QTL for mouse wheel running and used time spent on the wheel (duration), distance run on the wheel and the speed that the mouse ran on the wheel as the three phenotypes¹³. In order to accomplish this, the authors crossed high active inbred C57L/J mice with low active inbred C3H/HeJ mice and bred these mice to the F₂ generation. The authors showed that an area on chromosome 13 was associated with

increased wheel running time, distance, and speed. Additionally a region on chromosome 9 was associated with wheel running speed¹³.

From these results, Yang *et al*¹⁷ aimed to explore the role of chromosome 13 on voluntary physical activity using a chromosome substitution mouse model whereby chromosome 13 from the low active A/J mice was substituted into the high active C57Bl/6J (B6) mouse. The results showed that the B6 group had a significantly higher physical activity level than both the low-active A/J mice and the B6 mice with chromosome 13 from the low active A/J mice¹⁷. As a follow-up, Yang *et al*¹⁶ backcrossed the chromosome 13 substitution mice with the high active B6 mice to provide high resolution mapping for voluntary physical activity. Yang *et al*¹⁶ selected 15 single nucleotide polymorphism (SNP) markers on chromosome 13 for analysis in an attempt to identify genes associated with physical activity¹⁶. The results showed that two genes, dopamine receptor 1 (*Drd1*) and transcription factor AP-2 alpha (*tcfap2a*), were associated with voluntary physical activity level. Additionally, the finding by Yang *et al*¹⁶ of *tcfap2a* involvement further supports the role of *Drd1* because *tcfap2a* is a transcription factor for *Drd1* and can increase *Drd1* expression¹⁶. Thus, Yang and colleagues' data, even though correlative, suggested that dopamine acted to influence motivation and reward driven behavior, which in the case of physical activity, can "drive" the voluntary physical activity response.

While the work by Yang and Lightfoot is promising, the basis of the experimental design to examine chromosome 13 was centered on the comparison of only two inbred mouse strains (C57L/J and C3H/HeJ) from Lightfoot *et al*¹³. To further elucidate the genetic regions associated with physical activity, Lightfoot *et al*¹² increased the number of inbred mouse strains analyzed from two to 41 strains. In these 41 strains, the authors also included wild type strains to help

offset the “bind spots” of identical genomic regions from descent of inbred mouse strains¹². Not only did these results characterize the wheel running phenotype for these strains but identified several additional genomic regions associated with physical activity as well as the influence of sex on activity. Specifically, distance run was associated with genomic regions on chromosome 12, 18, and 19; however, when only analyzing males, distance run was associated with regions on chromosome 5, 6, 8, and 13. The females had regions associated with distance run on chromosome 8 and 11. Additionally when excluding the wild type mice there was a region on chromosome X associated with time spent running by the females¹².

Another approach to determining the genetics of physical activity is through selective breeding of mice that are high active, i.e. the generation of an inbred strain whose primary characteristic is high activity. Garland’s lab selected mice that displayed high wheel running (9,000 revolutions per day) and have bred the mice to the 65th generation^{14 31}. One of a number of interesting observations in these mice displayed the “mini-muscle” phenotype³². The mini muscle is primarily characterized by a reduction in size of the triceps surae muscle of high active mice. Interestingly this phenotype has been associated with increased aerobic capacity, muscle contractile performance, size of heart ventricles, size of liver, and size of spleen¹⁴. In 2008, Hartmann *et al*¹⁴ mapped the mini muscle phenotype to chromosome 11 within the 2.6335 Mbp region¹⁴. However, this region of chromosome 11 contains 102 genes¹⁴. Thus, the high number of genes located in the region on chromosome 11 prevents the determination of the genetic mechanisms associated with the mini muscle and the regulation of voluntary physical activity.

In an effort to understand which regions were associated with voluntary physical activity aside from just the mini-muscle phenotype, Nehrenberg *et al* 2010³³ QTL mapped the selective-bred high active mice for the phenotypic components of physical activity (e.g. daily distance run, etc.). The results showed that the regions associated with average speed of wheel running were located on chromosome 7, max speed of wheel running was located on chromosomes 6 and 7, ventricle size was located on chromosome 3, and spleen size was located on chromosome 6, 9 and 13³³. Interestingly the authors found that average speed and max speed were associated with the tyrosinase gene³³ (a precursor to dopamine) which was associated with physical activity as shown by Yang *et al*'s QTL study¹⁶. However, and perhaps due to different founder animals for the selective breeding as compared to previous QTL studies, none of the QTL identified by Nehrenberg, *et al.* co-localized with QTL identified by Lightfoot, *et al*^{12,13}.

In an effort to develop a finer mapping analysis of the mini muscle and physical activity phenotype, especially in regards to the role of tyrosinase and dopamine, Kelly *et al* 2010³⁴ crossed the "mini-muscle" mice with the B6 mouse³⁴. The authors supported the earlier study by Hartmann *et al*¹⁴ that found that the mini muscle was associated with chromosome 11 and tyrosinase. However, Kelly and colleagues also found that the QTL for running distance appeared to change across time and was affected by exposure of the mouse to the running wheel³⁴. The finding that the QTL associated with activity changed on a daily basis was subsequently supported by Leamy *et al*³⁵ using the earlier data from Lightfoot *et al*¹².

The fact that the QTL for wheel running distance might change on a daily basis highlights a significant limitation of QTL analysis, as well as both positional cloning and linkage

analysis techniques: they do not provide mechanistic pathways for the regulation of the desired phenotype, merely correlative evidence. If the phenotype slightly changes – as was the case in both Kelly *et al*³⁴ and Leamy *et al*³⁵, the correlations are altered, thus pointing to different genomic areas. Therefore, in order to understand the biological regulation of physical activity, other portions of central genetic pathways, such as the transcriptome and the proteome, must be analyzed.

While both the transcriptome and the proteome can be determined, the need to preferentially analyze the proteome arises from observations that transcript data (mRNA) does not always correlate to protein function and end phenotype³⁶⁻³⁸. Using liver cells, Anderson and Seilhamer found a positive, yet weak, correlation ($R^2 = 0.48$) between mRNA and protein levels³⁸. Furthermore Gygi *et al*³⁶ using a yeast model found a 20-fold difference between mRNA levels and the corresponding protein levels³⁶. In fact, Greenbaum *et al*³⁷ used RNA sequencing and 2D-DIGE to correlate RNA expression to protein expression. The authors showed a correlation of $r=0.66$ for nuclear RNA to protein expression and a correlation of $r=0.42$ for mitochondrial RNA to protein expression³⁹. Furthermore using the inbred mouse model Ghazalpour *et al*⁴⁰ demonstrated a correlation of $r=0.27$ between mRNA and protein levels⁴⁰. Ghazalpour *et al*⁴⁰ hypothesize that the weak correlation could be a result of alternative splicing of the mRNA⁴⁰. Thus, while both transcriptome and proteome data would augment the existing QTL data regarding the genetic mechanisms regulating physical activity, determining the differential proteomic signatures of high- and low-active animals would provide a description of the molecular processes closest to the determination of the

phenotype. However, if the proteome is pursued, the first concern is the site of regulation so that the proteome can be determined in the appropriate physiological location.

The physiological site of activity regulation is an evolving question. It has been proposed by Kelly *et al*³⁴ that the genetic control of voluntary physical activity is a result of both central drive and peripheral capability³⁴. Central drive is the result of mechanisms in the brain that influence the “drive” to be active while the “capability” to be active is a result of peripheral factors that reduce pain/fatigue allowing for more sustained physical activity level⁴¹. As indicated by earlier discussion, a logical starting point to address differences in mechanisms associated with central drive and peripheral capability is with the candidate genes identified by QTL analysis, specifically the role of dopamine as a means of central drive and motivation to be active.

1.2 Central Drive and Reward Driven Behavior Regulate Voluntary Physical Activity

There have been several candidate genes suggested to be involved in the central drive to be active which include *Insig2*, *BC014805*, *Socs2*, *Mod1*, *IL-15a*, *Prpcp*, *Arrdc4*, and *DBY*¹⁵. However, the literature has suggested that the strongest candidate genes are those in the Dopamine system⁵. Dopamine is responsible for reward driven behavior and as stated previously, has been suggested by Yang *et al*¹⁶ to affect the “drive” to be physically active^{16,42,43}. Knab *et al*⁴³ showed that high active mice under expressed dopamine receptor 1 (*Drd1*) and tyrosine hydroxylase (*TH*)⁴³. Knab’s work correlates to work by Mathes *et al*⁴² who effectively showed that high active mice had a decrease in dopamine receptors but an increase in dopamine level⁴², indicating high active mice have a decreased dopamine turnover rate⁴². Additionally, Mathes *et al*⁴² found that dopamine turnover was independent of wheel running,

which suggests that dopamine levels are inherent traits that could regulate physical activity⁴². The involvement of dopamine in the regulation of physical activity was also supported through pharmacological studies. Knab *et al*⁴⁴ was able to decrease wheel running of high active mice with a D1 type receptor agonist and increase activity of the low active mice with a dopamine transporter inhibitor⁴⁴, thus effectively demonstrating that modulation of the dopamine system affects reward driven behavior and is a regulator of voluntary physical activity.

An additional component of the dopamine system that may also be involved in the regulation of physical activity is Vesicular monoamine transporter 2 (*Vmat2*). *Vmat2* stores dopamine in synaptic vesicles prior to the release of dopamine into the synaptic cleft and alterations to *Vmat2* have been shown to lead to Parkinson's Disease⁴⁵. Taylor *et al*⁴⁵ has proposed two mechanisms by which a higher expression of *Vmat2* is associated with higher activity levels^{45,46}. The first mechanism by which higher expression of *Vmat2* increase physical activity is that an increased level of *Vmat2* decreases free dopamine⁴⁵. Free circulating dopamine has been shown to have toxic effects and could reduce the effects of dopamine on reward driven behavior⁴⁵. The second mechanism by which *Vmat2* may increase activity is that the higher abundance of *Vmat2* allows for greater release of dopamine, which has been shown, by Knab and Mathes to increase physical activity^{42,43,45}. These findings suggest that alterations in dopamine levels mediated by *Vmat2* contribute to the reward driven behavior that leads to changes in physical activity.

Recent literature has also suggested that the reward driven behavior of the dopamine system is influenced by the cannabinoid system and specifically, the cannabinoid receptor^{47,48}. This hypothesis supports and augments previous work investigating the dopamine system.

Specifically, it has been suggested that as the cannabinoid receptor is activated, dopamine release is stimulated⁴⁷. Current literature⁴⁷ has suggested that this response is the physiological mechanism for “the runners high.” Raichlen *et al*⁴⁷ investigated this mechanism by exposing humans, dogs, and ferrets to moderate and high intensity exercise on treadmills and then collected blood samples to analyze the cannabinoid receptors’ endogenous ligands response⁴⁷. The results showed that thirty minutes of high intensity exercise led to an increase in the ligands for the cannabinoid receptors and suggested the presence of the runners high⁴⁷.

Raichlen *et al*⁴⁷ defined the runners high as a sensation of pleasure with a coincident reduction in pain⁴⁷. Thus, it is possible that subjects that express a higher number of cannabinoid receptors could participate in longer physical activity bouts because of the reduction in pain and increased sense of euphoria. This hypothesis was tested by Dubreucq *et al*⁴⁸ by measuring wheel running in cannabinoid receptor 1 (CB1) knockout mice and control mice. The results showed that the CB1 knockout mice ran significantly less than the control animals⁴⁸.

In conclusion, it has been hypothesized that there are central pathways that influence physical activity and current literature^{5,16,43,44,49} suggest that dopaminergic systems and/or endocannabinoid systems play a role in the drive to be active. Most prominently, these systems are thought to play a role in producing increased physical activity through either activity-induced euphoria and/or an inhibition of pain. While the dopaminergic and endocannabinoid systems are centrally located, their effects can be peripherally related since pain associated with activity has been correlated to skeletal muscle fatigue⁵⁰. Thus, it is

possible that the fatigability of skeletal muscle – a peripheral factor influencing capability - could also influence physical activity level.

1.3 Peripheral Factors Affecting the Capability to be Physically Active

As noted earlier, Kelly, *et al*³⁴ suggested that there are both central (drive) and peripheral (capability) mechanisms involved in regulating activity. As shown above, there are a growing number of studies that have investigated potential central mechanisms. However, there is limited literature addressing the role of potential peripheral “capability to be active” factors in regulating physical activity. The available studies in this area have focused on skeletal muscle with potential peripheral factors that may be associated with physical activity regulation being components of substrate utilization and skeletal muscle contraction.

1.3.1 Substrate Utilization Influences Physical Activity

Tsao *et al*⁵¹ showed that an over expression of glucose transport 4 (*Glut4*) in skeletal muscle led to a fourfold increase in wheel running as compared to control animals⁵¹. The methodology used by Tsao *et al*⁵² utilized an over expression of *Glut4* in the 129/SV mouse strain⁵². Specifically, the MLC1 promoter was spliced upstream of the *Glut4* gene allowing for an over expression of *Glut4* in muscle and heart tissue⁵². Tsao *et al*⁵¹ examined glucose and fat metabolism with *Glut4* over expression and interestingly, the authors observed a 45% increased in food intake and a fourfold increase in wheel running as compared to the control mice (~1 km ran for control mice and ~4 km ran for *Glut4* over expressed mice)⁵¹. The authors hypothesized that glucose transport was the rate-limiting step in skeletal muscle glucose

uptake. Therefore, an increase in glucose transporters could increase glucose uptake allowing for an increased physical activity response⁵¹.

In addition to *Glut4*, there have been several studies that have shown nutritional factors may alter physical activity through alteration of substrate utilization. Researchers from the Garland lab have shown that mice bred for high activity for over 60 generations – mice whose activity had plateaued at \approx generation 25 - when treated with a high fat diet, significantly increased their daily wheel running by 160%⁵³. To date, this is the only treatment that Garland's research group has used that has increased physical activity level of their high active mice^{53,54}. The fact that an increase in fat in the diet would lead to an increased activity is supported by the literature because high endurance athletes utilize lipids as their primary fuel source during activity due to the increased source of calories that fat represents⁵³. Therefore, Meek *et al*⁵³ has suggested that treatment of a high fat diet allowed for increased fat utilization as a primary fuel source allowing for an increased capability resulting in a higher physical activity level in these mice whose activity had previously plateaued⁵³.

1.3.2 Skeletal Muscle Force of Contraction and Muscle Fatigue Influences Physical Activity

The ability of skeletal muscle to produce force and recover from fatigue is another component that may affect physical activity. Reichart *et al*⁵⁵ demonstrated that an over expression of *Drd1* in skeletal muscle increased the second messenger cAMP and increased skeletal muscle force production and prevented muscle atrophy⁵⁵. Thus, the ability of skeletal muscle to produce increased force may lead to an increased physical activity level through an increased capability.

Calcium is a key regulator in muscle contraction⁵⁶. During muscle contraction, the axon terminal of a motor neuron releases a neurotransmitter into the synaptic cleft. The neurotransmitters bind to receptors on the sarcolemma, which transmit an action potential to the Transverse tubule (T tubule) of the sarcolemma. Once the action potential reaches the T tubule, there is a release of calcium (Ca^{2+}) from the sarcoplasmic reticulum (SR). Ca^{2+} binds to troponin C which causes a conformational change in tropomyosin thereby exposing actin binding sites allowing for binding of the myosin head²⁵. It is the binding of actin and myosin that causes skeletal muscle contraction²⁵. As Ca^{2+} is a regulator of skeletal muscle contraction it is foreseeable that regulators of Ca^{2+} homeostasis could be involved in the regulation of voluntary physical activity. While there are multiple potential calcium regulator proteins that could be involved in physical activity regulation, because of their unique properties, we have chosen to concentrate on Annexin A6 and Calsequestrin 1.

The Annexin family of proteins, which consists of 17 different proteins in animals, is involved primarily in Ca^{2+} homeostasis⁵⁷. Annexins are expressed in all tissues and share structural and functional similarities with other members of the Annexin family, with the exception of Annexin A6 which contains a repeat sequence resulting in eight domains as opposed to the standard four⁵⁸. The combination of the similarities in structure and the expression in various tissues has led to difficulty in identifying the functions of individual members of the Annexin family⁵⁹. In fact, functions of Annexin A6 have been hypothesized to include inhibition of blood coagulation, inhibition of protein kinase C, intracellular trafficking of endosomal vesicles, regulation of voltage gated calcium channels, structural modification of actin, and organization of lipid components of cell membranes^{57,59,60}. The function of Annexin

A6 in muscle is still ambiguous partly because the role of Annexin A6 varies depending on the type of muscle. What is known is that Annexin A6 binds acidic phospholipids of membranes in a Ca^{2+} dependent manner⁵⁷⁻⁶⁷. Thus, the more calcium that is present the more binding there is of Annexin A6 to lipid membranes.

The function of Annexin A6 in smooth muscle is clearly understood thanks to the work of Babiychuk and colleagues⁶¹⁻⁶³. Smooth muscle contracts in a segmental pattern unlike skeletal and cardiac muscle and is most prominent in the gut and vasculature system where the muscle surrounds a lumen and is used to propel substances along the length of the lumen²⁵. Babiychuk *et al*⁶² hypothesized that during smooth muscle contraction there would be stress placed on the cell membrane of the smooth muscle and that this stress could disrupt structures present in the membrane⁶¹⁻⁶³. Babiychuk *et al*⁶² showed that during relaxation Annexin A6 was located in the cytosol and at the initial phase of contraction, Ca^{2+} rose to a concentration of 700 nM causing Annexin 2 to link micro domains of the cell membrane and sarcolemma. This linking caused a further release of Ca^{2+} and raised Ca^{2+} concentration to 800 nM, which caused Annexin A6 to link to the sarcolemma. The linking of Annexin A6 to the sarcolemma allowed for the maintenance of force transduction while preventing cell structure damage from muscle contraction⁶¹⁻⁶³.

In cardiac and skeletal muscle, Annexin A6 is located around the myofibril and is associated with the sarcoplasmic reticulum (SR)^{60,64}. Song *et al*⁶⁷ observed that in patients with end stage heart failure Annexin A6 was down regulated as compared to healthy age matched controls^{57,67} leading to an initial thought that the loss of Annexin A6 is what led to end stage heart failure. However, Kaetzel *et al*⁵⁸ observed that when Annexin A6 is removed from cardiac

muscle there is an increase in free Ca^{2+} which leads to an increase in the inotropic state of the heart thereby allowing for a mechanism to compensate for the increased work load associated with end stage heart failure⁵⁸. However, this does not mean that over expressing Annexin A6 will result in a healthy heart. Gunteski-Hamblin *et al*⁶⁴ over expressed Annexin A6 tenfold in mice and observed myocyte necrosis, inflammation, and cardiac death⁶⁴, which was possibly due to two factors: 1) a tenfold over expression of Annexin A6 is considered supraphysiological and not to be relevant to normal physiological function; and 2) potential confounding with the method in which Annexin A6 over expression was generated. Using cloned cDNA, Annexin A6 was spliced into the promoter region. However, this region also contained the promoter for myosin heavy chain and the authors acknowledged that this over expression methodology could have disrupted the myosin heavy chain promoter causing the observed cardiac death⁶⁴.

The function of Annexin A6 in skeletal muscle is less studied as compared to cardiac and smooth muscle. Initially it was shown by Diaz-Munoz *et al*⁶⁰ that Annexin A6 bound calcium channels allowing for an increase in Ca^{2+} release⁶⁰. Additionally, Hazarika *et al*⁶⁸ demonstrated that in skeletal muscle Annexin A6 is associated with the SR and that during the initial phase of muscle contraction with the release of Ca^{2+} from channels of the sarcolemma, Annexin A6 binds to the T tubule and propagates the further release of Ca^{2+} ⁶⁸. Thus, Hazarika *et al*⁶⁸ proposed that Annexin A6 acts to stimulate more Ca^{2+} release from the SR hence increasing force of contraction⁶⁸. Similar to Reichart *et al*⁵⁵'s study examining *Drd1* expression in skeletal muscle, an increase in force production can lead to an increase in physical activity level⁵⁵. Therefore, Annexin A6 levels are an attractive potential mechanism for the regulation of voluntary physical activity level.

Another regulator of calcium homeostasis in skeletal muscle that may be involved in regulation of physical activity is Calsequestrin 1 (Casq1). Unlike Annexin A6, Casq1 has been widely investigated for its function in skeletal muscle^{56,69}. Casq1 is a Ca²⁺ buffer that helps to regulate the release of and reuptake of Ca²⁺ in skeletal muscle⁷⁰. Casq1 has a highly acidic C-terminal tail with a high binding affinity for Ca²⁺. As Ca²⁺ binds to Casq1 a conformational change in the structure occurs allowing for increased Ca²⁺ binding⁵⁶. It was initially thought that Casq1's only function was to remove Ca²⁺ from the myoplasm following muscle contraction; however, recent evidence has shown that Casq1 functions in the release of Ca²⁺ from the Ryanodine Receptor (RyR)⁷⁰. It has been suggested that Casq1 acts on the RyR to inhibit Ca²⁺ release through triadin and junction⁵⁶. As a result of these functions, Casq1 acts as a Ca²⁺ sensor ensuring that Ca²⁺ levels are appropriately maintained in the muscle cell. Interestingly it has been noted that Casq1 knockout mice can still maintain normal muscle contraction in spite of their lack of Casq1. However, the Casq1 knockout mice have increased lethargy, atrophy, and a decreased life span as compared to wild-type mice⁷⁰.

There have been no studies looking at Casq1 and its relation to voluntary physical activity level. However, there have been several studies that evaluated Casq1 expression following regular bouts of exercise⁷¹⁻⁷³. The studies by Jiao *et al*⁷¹ and Sugizaki *et al*⁷³ were conducted in cardiac tissue and showed that with an increase in endurance training there was an increase in Casq1 expression^{71,73} suggesting that Casq1 may play a role in the increased endurance. Kinnunen *et al*⁷² examined Casq1 expression in various skeletal muscle tissues following endurance or sprint training in a mouse model⁷². Interestingly, the authors observed that depending on the muscle fiber composition and the type of training there was a

differential expression of Casq1⁷². Specifically it was observed that following endurance training there was a decrease in Casq1 in the soleus (slow twitch fiber) while there was an increase in Casq1 in the EDL (fast twitch fiber)⁷². Following sprint training, Casq1 was increased in the gastrocnemius (mixed muscle fiber) and the EDL, with no change in the soleus⁷². The authors note that in fast fiber type muscle the Ca²⁺ storage capacity is 3-4 times higher and the release of and uptake of Ca²⁺ is more efficient compared to slow twitch fibers⁷². Thus, the authors propose that modulation to Casq1 following training allows for skeletal muscle to have increased capability to engage in the trained activity⁷². Thereby, Casq1 would be an attractive potential mechanism to regulate physical activity through its influence on Ca²⁺ homeostasis.

Combined, the above referenced studies have provided tentative evidence that substrate utilization and skeletal muscle contractile performance may be peripheral factors that directly affect the capability to be active. However, as was the case with the QTL findings, these conclusions have been primarily based on correlative results highlighting the need for cause-effect research designs to provide mechanisms of activity regulation. Further, as noted earlier, in order to understand the regulation of physical activity level an initial step would be to determine the proteome associated with physical activity level.

1.4 Methods to Elucidate the Proteome that is Associated with Voluntary Physical Activity

There are several methods to measure protein differences. The most well established method is by using western blots, which can provide semi-quantitative measurements of a known protein. However, identification of differential expression of multiple unknown proteins requires methodologies other than western blotting. Currently, it is thought that two dimensional differential gel electrophoresis (2D-DIGE) has the highest sensitivity,

reproducibility, and reliability⁷⁴ in identifying proteomic differences between various samples. Because of their widespread use, 2D-DIGE methods are well established⁷⁵⁻⁸⁷. Briefly, as the name implies, 2D-DIGE uses two dimensions to separate the proteins in a sample; the first dimension separates proteins based on their individual isoelectric point, and the second dimension separates the proteins based on their molecular weight. The first step in modern 2D-DIGE methodology is labeling the proteins with a fluorescent tag, then isoelectrically focusing the proteins on a pH gradient strip, followed by electrophoresis to separate the proteins by their molecular weight using polyacrylamide gels. The resulting gels are then imaged using the fluorescent tags to identify differences between two samples. The proteins appear as spots and significantly, different spots are removed from the gel and identified by mass spectroscopy. As a result, proteins that are differentially expressed between conditions are identified through this process, providing a listing of differentially expressed proteins that can be used for further study.

To date, there are no studies using 2D-DIGE to investigate voluntary physical activity. While an earlier study by Kromer *et al*⁸⁸ investigated locomotor activity as it related to trait anxiety⁸⁸, the tests used in that study were aimed at identifying anxiety and fear and therefore did not provide a protein-signature associated with the regulation of voluntary physical activity.

While there have been no 2D-DIGE studies on voluntary physical activity, there have been six studies regarding proteomic differences associated with exercise training^{74,89-93}. While these studies do not provide information on the inherent proteomic differences of low and high active subjects, the studies do highlight the effectiveness of the 2D-DIGE model. Goto *et al*⁹² examined the kidney and Diffie *et al*⁹¹ analyzed cardiomyocytes while four separate studies

investigated skeletal muscle^{74,89,90,93} responses to exercise. The work by Goto *et al*⁹² on the kidney identified proteins associated with aging, specifically carbonylated proteins⁹². The authors hypothesized that the presence of carbonylated proteins led to oxidative stress that was in turn an indicator of aging⁹². Adding to this literature, Diffie *et al*⁹¹ examined rat cardiomyocytes following treadmill running⁹¹. The results showed that following treadmill running there was an increase in calcium sensitivity and contractile function of the myocardium⁹¹. However, a limitation of this study was that the researchers focused on the proteome associated with myosin light chain (MLC) as opposed to the whole myocardial proteome. While not a flaw in the experimental design, this limitation was a result of the available technology. 2D-DIGE can be conducted in two ways; the classical method, used by Diffie *et al*⁹¹, involved staining the proteins on the gel with silver, then qualitatively visually inspecting for differences between samples. However, new advancements in technology have allowed proteins to be fluorescently labeled which results in a more sensitive identification of proteomic differences and the ability to quantitatively determine proteomic differences^{74,89}.

The four studies using 2D-DIGE in skeletal muscle used the fluorescent labeling technique and provided evidence for how exercise training can improve skeletal muscle contractile function. Egan *et al*⁸⁹ analyzed mitochondrial proteins before and after 14 days of endurance training in the vastus lateralis of college-aged males⁸⁹. The results showed several metabolic adaptations to training, including increases in proteins associated with enhanced flux of electrons through the electron transport chain (NADH dehydrogenase, cytochrome c oxidase, F type ATP Synthase). Additionally there was an increase in proteins of the Krebs cycle (fumarate and pyruvate dehydrogenase). The authors concluded that through the increase

in proteins of the Krebs's cycle there was an enhanced capacity for substrate utilization through improved use of pyruvate leading to increased cofactors (NADH and FADH₂)⁸⁹. Thus with an increase in cofactors there was a greater ability to generate ATP in the electron transport chain.

Additionally, Egan *et al*⁸⁹ identified proteins that are involved in the antioxidant defense and contractile force generation of skeletal muscle. The antioxidant protein identified was Manganese Superoxide Dismutase (Mn-SOD), which removes superoxide radicals following the electron transport chain (ETC)⁸⁹. The contractile proteins identified were Serca1, myosin regulator light chain 2, and tripartite motif 72⁸⁹. These proteins appear to influence calcium flux in skeletal muscle allowing for a more efficient contraction⁸⁹. These results indicated that in order to have a higher exercise capacity there was a need to meet the metabolic demand of the muscle and increase the efficiency of the contraction, which was obtained through increased calcium sensitivity⁸⁹.

Interestingly, Gelfi *et al*⁷⁴ also identified proteins associated with skeletal muscle contractile properties⁷⁴. The authors aimed to examine vastus lateralis changes in human skeletal muscle of both young and old subjects who participated in exercise⁷⁴. Their results showed that the young subjects had an over expression of tropomyosin and myosin heavy chain as compared to the elderly and further suggested that in order to maintain force production and decrease fatigue there was an increase in calcium flux and calcium sensitivity⁷⁴. In a study by Hody *et al*⁹³, an increase in troponin protein was observed in the rectus femorus following high intensity eccentric exercise in college-aged males⁹³. Yamaguchi *et al*⁹⁰ performed repeated swim tests in rats and compared proteomic changes of the epitrochlearis muscle before and after training. The results showed that following training there was an

increase in electron transport chain proteins (ATP Synthase, NADH dehydrogenase, oxoglutare dehydrogenase) and an increase in contractile proteins such as myosin light chain and parvalbumin⁹⁰. Thus, the evidence suggests that in order to have a higher exercise capacity there needs to be an increase in calcium handling and substrate utilization.

These results highlight the utility of using 2D-DIGE to understand the proteomic changes following exercise training that allow subjects to have the increased capability to perform at higher intensity levels. However, as with earlier approaches (e.g. QTL, transcriptome) the results from these studies do not directly provide mechanistic explanations for a particular phenotype. However, while correlative, the benefit of using 2D-DIGE is that it provides targets that are more precise than either QTL analysis or transcriptome expression. These proteome-derived targets can then be used in cause-effect based experiments to determine functional relevance of these targets.

1.5 Confirming Candidate Genes' Involvement in Physical Activity

While correlation is often the first step in an investigation, cause and effect cannot be established using associative research designs. Thus, it is critical for research designs to test the effects of a particular gene on physical activity level. To provide these causal genetic relationships, it is necessary to directly investigate the effect of a specific gene on physical activity. There are a variety of methods that could be used in these types of investigations, including the development of transgenic animals, or the use of gene-silencing technology.

The most common approach used in these types of studies has either been to develop transgenic animals with genes deleted (i.e. knocked-out) or increased (i.e. over expressed).

Wankhade *et al*⁹⁴ used *Nhlh2* knockout mouse to investigate the mechanisms associated with obesity⁹⁴. *Nhlh2* knockout mice display higher percent body fat, leptin levels, and body temperatures with a decreased physical activity level⁹⁴. Additionally, Pistilli *et al*⁹⁵ used knockout animals to investigate the role of IL-15 receptor alpha on skeletal muscle physiology⁹⁵. IL-15 receptor alpha is a plasma membrane receptor, that when knocked out results in a fiber shift from fast twitch to fatigue resistant which results in IL-15 receptor alpha knockout mice running longer than their control counterparts do. Unfortunately, the use of knockout mice in these studies also highlight several limitations, including the ability to investigate only a limited number of genes at once, developmental issues, and the potential loss of regulatory regions⁹⁶. An example of the limitations with transgenic animals was exhibited by Manzl *et al*⁹⁷ with the knockout of caspases and Beta cell lymphoma-2 family proteins evident during apoptosis⁹⁷. The authors stated that the technique, which utilized the cross of the C57Bl/6 mouse strain with the 129/SvJ mouse strain, led to developmental issues for the animal, such as ocular problems, kidney disease and inflammation of the urogenital tract⁹⁷. Thus, at least in this case, the generation of this knockout animal prevented the desired investigation into programmed cell death. Additionally with a knockout animal it is difficult to knockout multiple genes at once, which is a limiting factor in that it has been shown that the regulation of voluntary physical activity probably includes multiple genes/proteins as well as epistatic relationships between multiple genes¹².

Given the complications of developing and using transgenic animals, there has been a search for *in vivo* techniques that could transiently silence genes in healthy animals. This search has resulted in numerous promising tools identified including antisense

oligonucleotides, small interfering RNA (siRNA), phosphorodiamidate morpholino oligomers (PMO), and Vivo-morpholinos. Antisense oligonucleotides and siRNA have been shown to be effective at gene silencing yet are highly unstable in body fluids and are rapidly degraded⁹⁸. The decreased stability is due to the fact that oligonucleotides alone are not rapidly up taken into the cell, allowing for nucleases to break down the oligonucleotides⁹⁹. To alleviate this problem, researchers experimented with modifying the oligo's structure. The initial type of modified oligonucleotides were the PMOs⁹⁸. Initial results with PMOs showed an increase resistance to degradation by nucleases. However, *in vivo* experiments were associated with increased toxicity⁹⁹, thus, decreasing the enthusiasm for their usage.

Vivo-morpholinos were developed by Morcos and colleagues¹⁰⁰ and represent a potential *in vivo* method for transiently silencing specific genes. Morpholinos are anti-sense oligonucleotide (oligo) analogs that bind to complementary RNA sequences and inhibit processing of mRNA by blocking translation or splicing of pre-mRNA^{100,101}. Marcos and colleagues¹⁰⁰ altered the delivery moiety of morpholinos by using eight guanidinium head groups of arginine-rich peptides attached to the anti-sense oligo. The resulting oligo analog, named "Vivo-morpholinos," is transported into the cell by endocytosis and is protected from proteases and nucleases for a length of time (7-14 days) that is dependent upon the gene-turnover rate¹⁰⁰. In effect, the Vivo-morpholinos provide a method to transiently silence specific genes to determine cause-effect relationships. To date there are only twenty-seven studies using Vivo-morpholinos¹⁰⁰⁻¹²⁶ and all have reported at least 50% knockdown of the target with no adverse side effects. Fourteen of these studies used a mouse model^{100,101,103,110,112,114,119,121-127} with the remaining studies using rats¹¹⁵⁻¹¹⁷, newts¹²⁰, chicken

embryos¹⁰⁶, zebrafish^{102,104,105} and amphibians^{107,109,118}. In the mouse model, it has been shown that Vivo-morpholinos were equally efficacious with intravenous (IV) or intraperitoneal (IP) administration, and recent studies have shown success with direct injection in target tissue¹¹⁵⁻¹¹⁷.

The novelty of Vivo-morpholinos has resulted in limited literature on appropriate methods regarding Vivo-morpholinos. For example, the literature has presented studies with appropriate dosage ranges from 6 mg/kg to 17 mg/kg, with once a day treatments to a maximum of three consecutive days of treatment^{122,123}. Initially, it was suggested that in order to get longer-term knockdown of targeted proteins, Vivo-morpholino administration had to be at the higher dosages¹²². However, few studies have employed this route with the majority focusing on lower doses and evaluating protein knockdown only 24-48 hours post treatment^{123,124}.

The majority of Vivo-morpholino mammal studies have delivered Vivo-morpholinos via IV. This method of delivery has been shown to be efficacious in knocking down proteins in various tissues¹⁰⁰. However, this method of delivery has not been effective at knocking down proteins in the brain or cardiovascular system¹⁰⁰. Morcos *et al*¹⁰⁰ has suggested that these tissues see a reduced Vivo-morpholino delivery because of a limited ability of Vivo-morpholinos to cross membranes in the blood vessels and the heart¹⁰⁰. Additionally it has been shown that Vivo-morpholinos cannot pass the blood brain barrier due to the fact that Vivo-morpholinos are ~10,000 Daltons in size¹⁰⁰ and the blood brain barrier only allows substances less than 400 Daltons to freely pass¹²⁸, limiting the application of Vivo-morpholinos to genes in tissues outside the brain. Three studies using rats have used direct tissue injection to deliver Vivo-

morpholinos to the brain¹¹⁵⁻¹¹⁷ by using intracranial cannula implantation to direct Vivo-morpholinos to various brain regions. The results have shown success with protein knockdown in the desired brain region using directly injected Vivo-morpholinos. However, it is noted that protein knockdown only occurred in the targeted brain region and not surrounding regions^{116,117}. If total brain protein knockdown is desired, other strategies involving IV administration should be employed, such as using a pharmacological aid to increase blood brain barrier permeability¹²⁸ allowing Vivo-morpholino penetration. Thus, Vivo-morpholinos are a unique tool that will transiently silence genes; however, there are numerous methodological questions that need to be resolved so that Vivo-morpholinos can be employed in an optimal fashion.

1.6 Summary

Regular physical activity is associated with reductions in rates of several diseases and chronic conditions. Current research has shown that physical activity level is a result of genetic influence but the existing data on the genetic regulation of physical activity has focused on QTL and gene expression studies. These studies do not provide mechanistic explanations for the genetic regulation of physical activity. In order to elucidate mechanisms that could influence physical activity level, a whole systems proteomic approach to identify protein differences between high and low active mice combined with a gene-silencing approach to transiently knockdown and confirm identified proteins must be employed.

CHAPTER II

VIVO-MORPHOLINOS INDUCED TRANSIENT KNOCKDOWN OF PHYSICAL ACTIVITY RELATED PROTEINS*

2.1 Synopsis

Physical activity is associated with disease prevention and overall wellbeing. Additionally there has been evidence that physical activity level is a result of genetic influence. However, there has not been a reliable method to silence candidate genes *in vivo* to determine causal mechanisms of physical activity regulation. Vivo-morpholinos are a potential method to transiently silence specific genes. Thus, the aim of this study was to validate the use of Vivo-morpholinos in a mouse model for voluntary physical activity with several sub-objectives. We observed that Vivo-morpholinos achieved between 60 – 97% knockdown of Drd1-, Vmat2-, and Glut4-protein in skeletal muscle, the delivery moiety of Vivo-morpholinos (scramble) did not influence physical activity and that a cocktail of multiple Vivo-morpholinos can be given in a single treatment to achieve protein knockdown of two different targeted proteins in skeletal muscle simultaneously. Knocking down Drd1, Vmat2, or Glut4 protein in skeletal muscle did not affect physical activity. Vivo-morpholinos injected intravenously alone did not significantly knockdown Vmat2-protein expression in the brain ($p=0.28$). However, the use of a bradykinin analog to increase blood-brain-barrier permeability in conjunction with the Vivo-morpholinos significantly ($p=0.0001$) decreased Vmat2-protein in the brain with a corresponding later over expression of Vmat2 coincident with a significant ($p=0.0016$) increase in physical activity. We conclude that Vivo-morpholinos can be a valuable tool in determining causal gene-phenotype relationships in whole animal models.

*Reprinted with permission from “Vivo-Morpholinos Induced Transient Knockdown of Physical Activity Related Proteins” by Ferguson DP, Schmitt EE, Lightfoot JT, 2013. PLoS ONE 8(4): e61472. doi:10.1371/journal.pone.0061472

2.2 Introduction

Physical inactivity has been correlated with cardiovascular disease, obesity, type II diabetes and some types of cancers⁵. With only 3.5% of adults meeting the recommended physical activity guidelines⁶, physical inactivity is the second leading actual cause of death (~250,000 cases/year) in the United States⁷ with an estimated \$507 billion a year in health care costs⁵. Several potential candidate genes associated with the genetic influence on voluntary physical activity have been identified^{5,20,43,46,51,55,117,129,130} with potential regulatory effects both in the brain and skeletal muscle.

Of the candidate genes identified, Dopamine Receptor 1 (*Drd1*)^{5,20,43,55,117}, Glucose Transporter 4 (*Glut4*, aka: *Slc2a4*)⁵¹, and Vesicular Monoamine Transporter 2 (*Vmat2*)^{45,46,129,131}, have been the most widely studied in association with voluntary physical activity. *Vmat2* is expressed in the brain and skeletal muscle. Studies examining the nucleus accumbens of the brain have shown that *Vmat2* stores dopamine in synaptic vesicles^{45,46,129,131}. A loss of *Vmat2* has been associated with a decrease in physical activity and development of Parkinson's disease^{45,46}. Another central factor contributing the regulation of physical activity is *Drd1*; high active mice have an under expression of *Drd1* which results in a decrease in dopamine turnover in the nucleus accumbens⁴³ and a suggested increase in reward driven behavior and voluntary physical activity^{20,43}. It has recently been proposed that *Drd1* expression in skeletal muscle could have similar effects on physical activity with an increase in D1 receptors (*Drd1* and *Drd5*) in skeletal muscle being associated with an increase in muscle force production and prevention of atrophy⁵⁵. An additional mechanism by which peripheral factors could regulate physical activity is through *Glut4*. *Glut4* transports glucose into skeletal muscle¹³² and it has been

shown that an over expression of *Glut4* is associated with a fourfold increase in voluntary physical activity⁵¹.

Quantitative genetics rarely identify a mechanistic link relating a potential candidate gene to the regulation of a phenotype. To prove causal relationship, transgenic animals with targeted genes knocked-out can be employed. However, a transgenic approach can be confounded by the loss of regulatory regions in the genome as well as developmental issues for the animal⁹⁶. A tool that could transiently silence a specific gene *in vivo* without confounding effects would be ideal in identifying genes that regulate voluntary physical activity and other phenotypes.

Morpholinos are anti-sense oligonucleotide analogs that bind to complementary RNA sequences and inhibit processing of mRNA by blocking translation or splicing of pre-mRNA¹⁰⁰. While early versions of morpholinos have been in use for over fifteen years with *in vitro* applications, these early morpholino designs presented several problems that prevented use in an *in vivo* model, including rapid degradation by proteases/nucleases¹²³ and the inability of the morpholino to cross membranes¹¹⁰. These problems were solved when Marcos and colleagues¹⁰⁰ altered the delivery moiety of morpholinos by using eight guanidinium head groups of arginine-rich peptides. The resulting oligonucleotide analog, termed “Vivo-morpholinos,” are transported into the cell by endocytosis and protected from proteases and nucleases¹⁰⁰. Recently there has been evidence suggesting protein knockdown can be achieved equally with intravenous (IV), intraperitoneal (IP), or direct injection into targeted tissue^{100,110,115,123}.

To date there are only twenty-seven studies using Vivo-morpholinos¹⁰⁰⁻¹²⁶ and all have reported at least 50% knockdown of the target with no adverse side effects. Fourteen of these studies used a mouse model^{100,101,103,110,112,114,119,121-127} with the remaining studies using rats¹¹⁵⁻¹¹⁷, newts¹²⁰, chicken embryos¹⁰⁶, zebrafish^{102,104,105} and amphibians^{107,109,118}. In the mouse models, it has been shown that Vivo-morpholinos were equally efficacious with IV or IP, and recent studies have shown success with direct injection in target tissue^{115,116}. While these studies have established the use of Vivo-morpholinos, they were limited in the application parameters used. One of the major limitations of the initial validation studies was the short-term nature of the studies (e.g. 24-48 hours post treatment) even though it has been suggested¹⁰⁰ that gene silencing with Vivo-morpholinos will theoretically last much longer (e.g. 7 days). Further, the existing Vivo-morpholino studies have only evaluated effects of a single Vivo-morpholino without indication of whether multiple genes can be silenced simultaneously. Additionally, there has been little success in applying Vivo-morpholinos to the mouse brain¹⁰⁰.

The purpose of this study was to validate the use of Vivo-morpholinos in silencing targeted genes in a mouse model of voluntary physical activity. This study included evaluation of the appropriate control, the effectiveness of transporting a Vivo-morpholino across the blood brain barrier (BBB) with a pharmacological aid, the ability to combine multiple Vivo-morpholinos in a “cocktail” to silence multiple genes simultaneously, and whether daily physical activity altered the washout time course of an intravenous injected Vivo-morpholino.

2.3 Methods

Three separate experiments were used to fulfill the purposes of this project. All experiments were approved by the Texas A&M Institutional Animal Care and Use Committee (Animal use protocols 2010-256, 2010-187, 2011-140, and 2011-147) and all animals were housed in an AAALAC certified vivarium on a 12-hour light/dark cycle with *ad libitum* access to standard chow and water. Animals were monitored and efforts were taken to ameliorate any animal suffering. All experiments used Vivo-morpholinos ordered in the 400-nmol batch.

2.3.1 Experiment 1: Evaluation of Vivo-morpholinos' Gene Silencing in Mouse Activity Model

This experiment evaluated the effectiveness of silencing genes in a physical activity model using Vivo-morpholinos, a method of Vivo-morpholino delivery across the BBB, as well as the appropriate control vehicle. Eighteen male C57Bl/6J mice (Jackson Labs, Bar Harbor, ME) were randomly assigned to one of three treatment groups:

Group 1) intravenously injected a translation-blocking Vivo-morpholino (11mg/kg)¹⁰⁰; Gene Tools LLC, Philomath, OR) targeting *Vmat2* (**Vmat2** group, n=6);

Group 2) Intravenously injected a Vivo-morpholino scramble control (11mg/kg) which consisted of vehicle plus an oligonucleotide target (5'-CCTCTTACCTCAGTTACAATTTATA-3') that did not correspond to murine mRNA (**Scramble** group, n=6); and

Group 3) An intravenously injected control group that received an equal volume (110ul) of physiological saline (**Saline** group, n=6).

Preliminary experiments determined that systemically delivered Vivo-morpholinos did not knockdown brain proteins¹³³. Thus, to facilitate Vivo-morpholino transport across the BBB, all treatment groups received the bradykinin analog RMP-7 (6.5µg/kg; Bachem, Prussia, PA)¹²⁸. Pharmacological studies have shown that using endogenous analogs of bradykinin¹³⁴ increase permeability of the BBB while maintaining physiological function of the animal¹²⁸. Bradykinin activates β 2 receptors on endothelial cells of cerebral capillaries thereby disengaging tight junctions and causing an increase in permeability of cerebral blood vessels^{128,134}. RMP-7 is a bradykinin analog that has several benefits over bradykinin; specifically RMP-7 resists degradation, has little to no toxicity to the brain, can be administered intravenously, and is fast acting producing a result within 60 seconds of administration¹³⁴. RMP-7 was initially developed as a delivery method for chemotherapeutics in brain glioma patients with studies showing a linear dose response between RMP-7 and BBB permeability in conjunction with a variety of chemotherapeutics¹²⁸.

At eight weeks of age mice were individually housed with running wheels equipped with computers (Sigma Sport, St. Charles, IL) to measure average daily distance run¹², and beginning at nine weeks of age, completed a week of baseline wheel running. At ten weeks of age, mice were randomly assigned to one of the three treatment groups and received a tail vein injection of the specific treatment for three consecutive days. At 11 weeks of age (4 days post the last injection) half the cohort was sacrificed (n=3 per treatment group). The activity of the remaining mice was monitored for an additional week (recovery) and the mice were then sacrificed.

At sacrifice, mice were anesthetized using vaporized isoflurane followed by cervical dislocation. The soleus (peripheral slow twitch muscle) and nucleus accumbens (reward center of the brain) were removed and flash-frozen for later analysis. Gene silencing was evaluated by determining protein knockdown using standard SDS-Page and Western blotting techniques. Briefly, proteins were extracted by placing the tissue in lysis buffer and homogenizing the tissue with a motor and pestle. Protein concentration was determined by Bradford assay to ensure equal amount of protein loading per sample on the gel. The proteins were separated by SDS-Page, and then transferred to a nitrocellulose membrane with transfer confirmed by *Ponceau S* stain. Membranes were incubated overnight in 1:1000 ratio of primary antibody recognizing Vmat2 (Cell Applications, San Diego, CA) and blocking buffer (5% Nonfat Dried Milk, 0.5% Tween 20). Membranes were then incubated in the secondary horseradish peroxidase antibody (Cell Signaling Technology, Beverly, MA). Chemiluminescence was imaged with a Flurochem analyzer (Derbyshire, UK) and the blot was analyzed using the individual protein band's optical density that allowed for a semi-quantitative estimate of protein knockdown.

The Western blot optical densities were analyzed using one-way ANOVA to compare Vmat2 protein expression between the treatments with an *a priori* alpha level of 0.05. Activity data was analyzed using a 3x3 ANOVA with the main effects being treatment group (i.e. **Vmat2**, **Saline**, or **Scramble**) and week of treatment (i.e. baseline, injection, or recovery). If there was a significant main-effect, a Tukey's HSD *post hoc* ($p < 0.05$) test was employed. All statistical tests were carried out using GraphPad Prism 5 (GraphPad Software Inc, La Jolla, CA).

2.3.2 Experiment 2: Determination of Vivo-morpholino Washout Period

To evaluate if physical activity altered the efficacy of the Vivo-morpholino, 24 eight week old C57Bl/6J male mice (Jackson Labs, Bar Harbor, ME) were individually housed and randomly assigned to either a running wheel group (n=12; unlocked wheels) or a fixed wheel group (n=12; locked wheels). The running wheel group had free moving wheels attached to a computer as described in Experiment 1. Each mouse in the fixed running wheel group had a running wheel that was secured to prevent wheel movement. Beginning at nine weeks of age, daily distance was measured in the running wheel group using methods from Experiment 1. At ten weeks of age one mouse from each group was sacrificed to establish a baseline level of *Vmat2* protein expression, while the remaining mice received a concurrent tail vein injection of RMP-7 (6.5ug/Kg)¹²⁸ and a Vivo-morpholino targeting *Vmat2* (11mg/Kg)¹⁰⁰ for three consecutive days. Each day thereafter, one mouse was sacrificed from each group to determine the washout of the Vivo-morpholino and whether exposure to activity affected protein knockdown.

On the day of sacrifice, mice were euthanized using vaporized isoflurane and cervical dislocation, with subsequent harvesting of the soleus and nucleus accumbens. Afterwards, proteins were extracted from each sample and *Vmat2* expression, as well as α -synuclein (Cell Signaling, Danvers, MA), which has been shown to be an indicator of *Vmat2* transcription¹³⁵, were determined using Western Blot techniques described in Experiment 1. The washout data was then analyzed for linearity and if nonlinear, nonlinear regression approaches were used to obtain R^2 values for the washout curves. The nonlinear data was then log transformed to meet the parameters of a linear regression, which allowed the comparison of the regression parameters between the locked and unlocked running wheel groups. A p value of 0.05 was set

a priori to determine if the slopes and y intercepts were different from each other. If there were no differences between the locked and unlocked wheel groups, the data points were pooled. To facilitate the comparison of baseline physical activity across the treatment protocol, average daily distance measurements were pooled in animals sacrificed in days 1-5 and days 6-11 of the protocol and compared using a one-way ANOVA (*a priori* alpha value = 0.05).

2.3.3 Experiment 3: Utilization of a Vivo-morpholino Cocktail

Twelve, eight-week old male C57Bl/6J mice (Jackson Labs, Bar Harbor, ME) were individually housed with running wheels as described in Experiment 1 to measure average daily distance run. At nine weeks of age mice completed a week of baseline wheel running and then at ten weeks of age, randomly received a tail vein injection of either the Vivo-morpholino cocktail (n=6) containing a Vivo-morpholino targeting *Drd1* (11mg/kg)¹⁰⁰ and another Vivo-morpholino targeting *Glut4* (11mg/kg)¹⁰⁰ or physiological saline (n=6) for three consecutive days. Physiological saline was used as a control since Experiment 1 showed no difference in the activity response of physiological saline and Vivo-morpholino scrambled control (see Results). At 11 weeks of age (four days post-last injection), half the cohort was sacrificed to evaluate the initial protein knockdown efficacy of the Vivo-morpholino cocktail. The remaining mice ran for one week and were then sacrificed. Upon sacrifice, the soleus was harvested and protein expression of *Drd1* (Cell Applications, San Diego, CA) and *Glut4* (Cell Applications, San Diego, CA) as well as the potential compensatory proteins dopamine receptor 5 (*Drd5*, Proteintech Group Inc, Chicago, IL) and glucose transporter 1 (*Glut1*, Cell Applications, San Diego, CA) were determined using standard Western blotting techniques, as described in Experiment 1. Similar statistical analysis was used as in Experiment 1 with the exception of a 2x3 ANOVA with the

main effects being treatment (Saline or Vivo-morpholino cocktail) and treatment week (Baseline, Injection, or Recovery).

2.4 Results

2.4.1 Experiment 1: Evaluation of Vivo-morpholinos in Activity Model

In the brain, treatment with a Vivo-morpholino targeting *Vmat2* did not result in a significant knockdown of *Vmat2* expression in the nucleus accumbens of the brain four days after the last Vivo-morpholino injection as compared to saline or scramble treatment (Figure 2.1, Panel A). However, there was a 79% knockdown ($p=0.04$) of *Vmat2* in the soleus four days post-injection as compared to both saline and scramble (Figure 2.2, Panel A). Surprisingly, during the recovery week (11 days post treatment) *Vmat2* protein level had a significant 354% over expression in the soleus of the **Vmat2**-Vivo-morpholino group compared to the saline and scramble treatment (Figure 2.2, Panel B, $p=0.03$). In the nucleus accumbens (Figure 2.1) and the soleus (Figure 2.2) there was no difference in *Vmat2* expression between saline and scramble treatments.

The initial reduction of *Vmat2* in the soleus did not affect daily physical activity (Figure 2.3). However, the **Vmat2** group had a significant 139% increase in activity during the recovery week as compared to the baseline and injection week (Figure 2.3, $p=0.001$), which corresponded to the *Vmat2* over expression observed in the soleus eleven days post-injection (Figure 2.2, Panel B).

2.4.2 Experiment 2: Determination of Vivo-morpholino Washout Period

The evaluation of the washout time course of Vivo-morpholinos targeting *Vmat2* showed there was a significant ($p=0.001$) 55% knockdown of *Vmat2* in the soleus on Days 2-6 (Figure 2.4 Panels A and C) with a significant 129% over expression observed on Day 9 ($p=0.001$). There was no difference ($p=0.74$) between the washout curves for the animals who had access to a running wheel ($R^2=0.65$) compared to those that had a locked running wheel ($R^2=0.55$) (Figure 2.4 Panel B).

In the nucleus accumbens, there were similar observations as in the soleus. There was a significant 74% knockdown in *Vmat2* (Figure 2.4 Panels D and F) on Days 5-6 ($p=0.001$) with a 988% over expression on Day 11 ($p=0.001$). Additionally there was no difference in the washout curves ($p=0.66$) for animals on wheels ($R^2=0.99$) or locked wheels ($R^2=0.99$) (Figure 2.4 Panel E).

To confirm the over expression of *Vmat2*, western blot analysis was performed probing for α -synuclein, which is an indicator of *Vmat2* transcription¹³⁵. The results showed that in the brain on Days 2 and 7 there was a 275% increase α -synuclein protein level (Figure 2.5).

There was no difference ($p>0.05$) in physical activity level of the running wheel group between the baseline week and days 1-5 post-injection (Figure 2.6). During days 6-11 of the washout protocol there was a significant 164% increase in physical activity ($p=0.0016$) versus baseline and days 1-5, corresponding to the increase in *Vmat2* expression during the same time period (Figure 2.4).

2.4.3 Experiment 3: Utilization of a Vivo-morpholino Cocktail

Western blot analysis showed that there was significant knockdown in Drd1 (97%) protein (Figure 2.7, Panel A, $p=0.01$) and Glut4 (60%) protein (Figure 2.7, Panel A, $p=0.042$) in the soleus four days after the last injection. Expression of both Drd1 and Glut4 returned to control levels during the recovery week (11 days post injection, Figure 2.7, Panel B). With the Vivo-morpholino cocktail treatment (*Drd1* and *Glut4*) there was no change in physical activity at any time period (Figure 2.8, $p=0.15$).

To evaluate potential compensation for the decreases in Drd1 and Glut4, Drd5 and Glut1 were probed by western blotting (Figure 2.9). There was no difference in Drd5 protein levels between control and treatment at four days post treatment ($p=0.22$) or eleven days post treatment ($p=0.93$). There was also no difference in Glut1 protein levels between control and treatment at four days post treatment ($p=0.56$) or eleven days post treatment ($p=0.36$).

2.5 Discussion

A molecular biology tool that can transiently silence genes in a whole-animal model will significantly advance the capability to determine cause-effect relationships between specific genes and targeted phenotypes. We have found that the use of Vivo-morpholinos targeting *Vmat2*, *Drd1*, and *Glut4* resulted in transient protein knock-down in the skeletal muscle up to four days after the last application. While the use of a pharmacological agent to facilitate Vivo-morpholino delivery across the blood brain barrier seemed promising, our results indicate marginal knockdown in the brain as compared to the soleus when using RMP-7. Further, we observed that concurrent physical activity did not influence the action of Vivo-morpholinos on

Vmat2 protein expression. Maybe most importantly, we also observed that the use of multiple Vivo-morpholinos in a cocktail would knock down more than one protein at a time in skeletal muscle. Interestingly, while initial knockdown of these proteins did not affect physical activity, we observed an increased physical activity coincident with post-washout over expression of Vmat2.

The search for an *in vivo* technique to transiently silence genes has been pursued for several decades with numerous promising tools identified including antisense oligonucleotides, small interfering RNA (siRNA), and phosphorodiamidate morpholino oligomers (PMO). Antisense oligonucleotides are effective at gene silencing yet are highly unstable in body fluids and are rapidly degraded¹²³. Initially, siRNA promised to transiently silence genes but presented difficulty with *in vivo* applications¹²⁵, which has limited siRNA's usefulness in integrative physiology. PMOs resist degradation *in vivo* yet have been associated with increased toxicity¹²³. Morpholinos, which are a form of antisense oligonucleotides, have had several modifications to their structure to limit toxicity and improve gene silencing which led to the development of the more stable Vivo-morpholino¹⁰⁰. Additionally, the fact that we observed no change in daily physical activity with the vivo-morpholino delivery vehicle (scramble) makes the Vivo-morpholino ideal for the investigation of candidate genes associated with physical activity.

Our results showed that *Drd1*-, *Glut4*-, and *Vmat2*-targeted Vivo-morpholinos significantly knocked down *Drd1*, *Glut4*, and *Vmat2* protein expression in skeletal muscle by an average 97%, 60%, and 79%, respectively. Furthermore, the use of the Vivo-morpholino cocktail showed that simultaneous protein knockdown was possible. Previous studies have

shown that treatment with Vivo-morpholinos at a similar dosage as used in this study (i.e. 11mg/kg) resulted in 50-70% knockdown^{105,136} similar to the knockdown amounts we observed. Recent literature¹²² suggests that to obtain 100% protein knockdown, the Vivo-morpholino dosage must be 160% greater than the amount prescribed by the manufacturer (i.e. 17.6 mg/kg) or the Vivo-morpholino injections must be given regularly over the course of the study^{123,124}. The fact that there were differences in the magnitude of Drd1 and Glut4 knockdown suggests that the nature of the target gene also may play a role in the magnitude of gene silencing. Genes coding for proteins that exhibit faster turnover rates in skeletal muscle may require the higher Vivo-morpholino dose. Therefore, protein turnover characteristics should be considered as a design parameter in Vivo-morpholino protocols.

Our initial results with Vivo-morpholinos in brain tissue were not promising due to a potential lack of BBB penetration¹³³. Vivo-morpholinos are ~10,000 Daltons in size and the BBB prevents substances greater than 400 Daltons from reaching the brain¹²⁸, thus we utilized RMP-7 as means to facilitate Vivo-morpholino delivery across the BBB. Unfortunately, in spite of the potential benefits of using RMP-7, Experiment 1 did not show significant knockdown in the nucleus accumbens of Vmat2 protein when using RMP-7 on day four after the injection. Interestingly, we did observe Vmat2 knockdown in the nucleus accumbens in Experiment 2 on Days 5 and 6 after the last injection, which was outside of our measurement range in Experiment 1. We suspect that due to the high activity of the dopamine system in the brain¹³⁷⁻¹³⁹, there may be a decreased protein turnover rate of Vmat2 in the brain as compared to skeletal muscle^{137,140-142} resulting in a slower protein turnover rate leading to a slower knockdown time course of Vmat2 in the brain. Thus, while the use of RMP-7 appears to have

facilitated some knockdown of Vmat2 in the brain, knockdown of brain genes using Vivo-morpholinos needs to be carefully designed to optimize both knock-down magnitude and time-course.

Surprisingly, in both Experiments 1 and 2, we observed a rebound over expression of Vmat2 protein compared to baseline during the recovery week in both skeletal muscle and nucleus accumbens. To our knowledge, this rebound phenomena has not been reported in the Vivo-morpholino literature. We would suggest that this rebound over expression was actually the result of the feedback loop that controls Vmat2¹⁴². Speculatively, with the blocking of *Vmat2* mRNA and a reduction of Vmat2 protein concentration, the cell would have been stimulated to transcribe more *Vmat2*. With subsequent Vmat2 production being blocked by the Vivo-morpholino, the stimulus to produce more *Vmat2* mRNA would become further elevated compared to the initial days of treatment. Once the Vivo-morpholino was degraded and removed, the elevated signal to produce Vmat2 would result in an increased translation of *Vmat2* mRNA¹⁴² and over expression of Vmat2 protein. This hypothesis is supported by our observation of a significant increase in α -synuclein in the nucleus accumbens on Day 2, with a continued increased signaling from Day 7 and peaking on Day 10 (Figure 2.5). Whereas α -synuclein has been observed to be an indicator of the cell's stimulus to transcribe *Vmat2*¹³⁵, it appears that once Vmat2 was knocked down there was an increase in the stimulus to transcribe *Vmat2* which resulted in the over expression of Vmat2 in the recovery week. While we did not observe a rebound over expression with either of the other genes we investigated (Drd1 and Glut4), the possibility of such a rebound effect occurring with other genes is

potentially an intriguing way to use Vivo-morpholinos to explore consequences of both gene under expression and over expression in the same model.

It has been previously suggested that *Drd1*, *Glut4*, and *Vmat2* are potential candidate genes for the regulation of physical activity^{20,43,45,46,55} with *Glut4* in particular, showing a direct effect on activity when over expressed⁵¹. Thus, we were somewhat surprised that knockdown of both *Drd1* and *Glut4* simultaneously in soleus (Experiment 3) did not affect activity levels. However, our observed lack of effect of *Glut4* and *Drd1* knockdown on physical activity in spite of an observed 60% and 97% protein reduction, respectively, could have reflected a general redundancy in these physiological systems. For example, it has been shown that with a 50% reduction in *Glut4* there is no apparent change in muscle physiology because of a compensatory *Glut1* over-expression for the loss of *Glut4*^{143,144}. Therefore, we evaluated possible compensation in these two systems by analyzing *Drd5* and *Glut1* protein levels. We observed no differences in *Drd5* or *Glut1* levels between control and treatment groups suggesting that compensation for the knock down of *Glut4* or *Drd1* did not occur and therefore, neither *Glut4* nor *Drd1* are primary peripheral regulating genes in voluntary activity. However, in spite of these results, it is clear that future studies can take advantage of the use of vivo-morpholino cocktails to silence multiple genes at once to consider their phenotypic effects.

Vmat2 was an attractive knockdown target for the regulation of physical activity given its proven role in the development of Parkinson disease⁴⁶. However, we observed no change in activity with a decrease in peripheral *Vmat2* in Experiments 1 and 2. However, the rebound of *Vmat2* observed in the soleus (Experiment 1 and 2) and nucleus accumbens (Experiment 2) along with the associated increase in physical activity could provide a potential explanation for

the regulation of voluntary physical activity. It has been shown that the dopamine system in skeletal muscle affects muscle force production⁵⁵ and in the brain affects reward driven behavior⁴³. When mice are given, artificial dopamine there is an associated hyperactivity response^{137,138,140,145}. We would suggest that as the effects of the Vivo-morpholinos wore off and *Vmat2* expression returned and surpassed baseline, there was an increase in extracellular dopamine that elicited the hyperactive effects similar to artificially administering dopamine. Further, this extracellular dopamine would have increased skeletal muscle tone and force production^{55,146} as well as reward driven behavior⁴³, which would have further increased physical activity.

The purpose of these experiments was to evaluate the efficacy of a potential transient gene-silencing tool, the Vivo-morpholino, when used in a physical activity model for an extended period of time. We observed that Vivo-morpholinos that targeted *Vmat2*, *Drd1* or *Glut4* significantly reduced associated protein expression in skeletal muscle up to four days after treatment with a subsequent recovery to baseline levels in *Drd1* and *Glut4* and with an over expression in *Vmat2*. Physical activity during the treatment did not affect the time course of protein knockdown. The delivery vehicle used (scramble Vivo-morpholino) did not affect protein knockdown or physical activity. Further, we found that multiple Vivo-morpholinos given in a cocktail knocked down multiple proteins simultaneously. While knocking-down any of the targeted genes did not result in hypothesized reductions in physical activity, a rebound of *Vmat2* protein was associated with an increase in physical activity during the same time as the rebound. We conclude that the use of Vivo-morpholinos can be a powerful tool to transiently silence specific genes and determine whether those genes are causally related to a phenotype

of interest, especially when the targeted gene's protein characteristics, such as turnover rate and location, are used to strengthen the research design.

CHAPTER III

THE DIFFERENTIAL SKELETAL MUSCLE PROTEOME IN HIGH AND LOW ACTIVE MICE

3.1 Synopsis

Physical inactivity contributes to cardiovascular disease, type II diabetes, obesity and some types of cancer with an estimated \$507 billion per year in related health care costs. While the literature is clear that there is genetic regulation of physical activity with existing gene knockout data suggesting that skeletal muscle mechanisms contribute to the regulation of activity, actual differences in end-protein expression between high- and low-active mice have not been investigated. This study used two-dimensional differential gel electrophoresis coupled with mass spectrometry to evaluate the proteomic differences between high active (C57L/J) and low-active mice (C3H/HeJ) in the soleus and extensor digitorum longus (EDL). Furthermore, Vivo-morpholinos were used to transiently knockdown candidate proteins to confirm their involvement in physical activity regulation. The high-active mice over expressed 21 proteins in the soleus and 3 in the EDL compared to the low-active mice. The low-active mice over expressed 21 proteins in the soleus and 5 in the EDL compared to the high-active mice. Primarily, proteins with higher expression patterns generally fell into the calcium-regulating and Krebs's (TCA) cycle pathways in the high-active mice (e.g. Annexin A6 $p=0.0031$; Calsequestrin 1 $p=0.000025$), while the over expressed proteins in the low-active mice generally fell into electron transport chain related pathways (e.g. ATPase, $p=0.031$; NADH dehydrogenase, $p=0.027$). Transient knockdown of Annexin A6 and Calsequestrin 1 protein in skeletal muscle of high active mice with Vivo-morpholinos resulted in decreased physical activity levels ($p=0.001$). These data suggest that high- and low-active mice have unique

protein expression patterns and that each pattern contributes to the peripheral capability to be either high- or low-active, suggesting that different specific mechanisms regulate activity leading to the high- or low-activity status of the animal.

3.2 Introduction

Regular physical activity prevents cardiovascular disease, obesity, and type II diabetes⁵. However, when objectively measured, only 3.5% of adults meet the recommended daily physical activity guidelines⁷. Recent data has shown that physical activity levels are a result of genetic influence^{5,11,14,29,30,35,147}; however, the identity of the genetic mechanisms involved remain unclear in spite of efforts to determine genomic variance and transcripts associated with activity levels. Genetic variance and transcript data only illustrate a portion of the potential regulatory mechanisms for voluntary physical activity and neither avenue of investigation accurately predict the final protein products that are associated with the phenotype^{36,148,149}.

Two dimensional differential gel electrophoresis (2D-DIGE) is an accurate and reliable method to identify proteomic differences in skeletal muscle^{74,89,90}; however, 2D-DIGE has not been used in the physical activity literature, but rather in literature focusing on proteomic changes following sprint or endurance exercise training^{74,89,90,93}. While, adaptation to exercise is an important field of study for physiology, these studies do not provide information on the inherent protein expression differences between high and low active individuals.

While 2D-DIGE paired with mass spectroscopy provides protein identification, the results are correlative with end phenotype. In order to determine causal mechanisms 2D-DIGE

results must be confirmed with an *in vivo* method to knockdown identified proteins in order to determine the proteins' role in the phenotype of interest. Vivo-morpholinos are a novel tool developed by Morcos and colleagues¹⁰⁰ that allows for transient knockdown of a targeted protein. Our lab has evaluated Vivo-morpholino effectiveness in the physical activity model in terms of delivery to brain and skeletal muscle tissue, washout time courses of Vivo-morpholinos, as well as appropriate Vivo-morpholino dosages and controls¹⁵⁰. Our results show that Vivo-morpholinos are an ideal tool to be paired with 2D-DIGE and mass spectroscopy in order to identify mechanisms associated with the physical activity phenotype¹⁵⁰.

Kelly *et al*¹⁵ has hypothesized that the biological regulation of activity that arises through genetic control mechanisms has both central (brain) and peripheral (skeletal muscle) components. Indeed, several studies have shown that alteration of skeletal muscle gene expression (e.g. *Glut4*⁵¹; *IL-15R α* ¹⁵¹) without alteration in central brain gene expression can markedly change voluntary physical activity. Thus, the purpose of this study was to identify proteomic differences between high- and low-active mice in slow and fast twitch skeletal muscle, followed by causal determination of the role of strong candidate proteins in regulating physical activity.

3.3 Methods

This study was conducted in two phases: the first was a proteome determination phase where differential proteins were identified from the inherent skeletal muscle proteome of high- and low-active mice. The second phase was to determine whether highly significant proteins determined in phase one were causally linked to physical activity using transient gene-silencing techniques. The Institutional Animal Care and Use Committee at Texas A&M

University approved all procedures in this study.

3.3.1 Experiment 1: Proteome Determination

Twelve, eight week old C3H/HeJ mice (6 male and 6 female) and 12, eight-week-old C57L/J mice (6 male and 6 female) were obtained from The Jackson Laboratory (Bar Harbor, ME). Previous extensive work from our lab has shown that the C3H/HeJ mice have a lower physical activity level (1.2 ± 1.7 km run per day) as compared to the C57L/J (10.7 ± 2.7 km run per day) mice^{11-13,30,35,43,44,152}. Our standard operating procedure has been to monitor physical activity in each mouse for at least seven days. Where at eight weeks of age mice are individually housed with running wheels equipped with computers (Sigma Sport, St. Charles, IL) to measure average daily distance run¹². However, due to our concern that wheel running would alter protein expression in the skeletal muscle¹⁵³, the mice, after one week of acclimation, were individually housed with locked running wheels for one week. Locked running wheels were used to simulate the environment of previous physical activity studies from this lab¹² while preventing wheel running. All animals were housed in an AAALAC certified vivarium maintained at 18–21°C and 20–40% humidity with 12:12-h light dark cycles that initiated at 6:00 AM. Food (Harland Teklad 8604 Rodent Diet, Madison, WI) and water were provided *ad libitum*. Body masses (to the nearest 0.1 g) were collected once per week throughout the study and body composition was determined prior to sacrifice using a GE Lunar Piximus dual X-ray absorptiometer (GE Healthcare Waukesha, WI).

At 10 weeks of age, mice were anesthetized using vaporized isoflurane followed by cervical dislocation. The soleus (peripheral slow twitch skeletal muscle) and extensor digitorum longus (EDL, peripheral fast twitch skeletal muscle)¹⁵⁴ were removed and flash frozen for later

analysis. Subsequently, for protein extraction, tissues were placed in Tris/CHAPs Lysis buffer and homogenized. Protein concentration was determined by Bradford assay. Due to differential protein concentrations in the soleus and EDL and in order to obtain optimal results, the soleus samples were isoelectric focused on 13 cm immobilized pH gradient (IPG) strips while the EDL samples were run on a 24 cm IPG strips.

Two-dimensional differential in-gel electrophoresis (2-D DIGE) and protein identification was initiated using techniques previously published^{155,156}. In brief, protein was precipitated with chloroform/methanol and dissolved in DIGE labeling buffer (7 M urea, 2 M thiourea, 4% CHAPS, 30 mM Tris, pH 8.5). Samples were fluorescently labeled by combining either 50 µg of EDL protein or 45 µg of soleus protein with 200 pmol CyDye DIGE Fluors (GE Healthcare). One sample was labeled with Cy3 while the other was labeled with Cy5 to allow for preferential labeling. A pooled sample containing equal amounts of each sample was labeled with Cy2. The labeling reactions were quenched with 10 mM lysine. The samples were randomly mixed so that one Cy3 and one Cy5-labeled sample were loaded on a single gel, along with the Cy2-labeled pooled sample, which was used as an internal standard and allowed for each resolved protein to be semi-quantitatively assessed relative to the standard within and between all gels, thereby minimizing gel-to-gel variation. Unlabeled protein samples were added to the labeled proteins (800 µg total protein for EDL and 328.5 µg total protein for soleus) and used to rehydrate the IPG strips (either 24 cm, pH 4-7, Immobiline™ DryStrip for EDL or 13 cm, pH 4-7, Immobiline™ DryStrip for soleus, GE Healthcare) by passive diffusion. Isoelectric focusing was performed on an IPGPhor (GE Healthcare) with a program of 500 volts for one hour followed by 1000 volts for one hour followed by a linear gradient to 8000 volts

until approximately 60,000 Vhr for EDL or 40,000 Vhr for soleus was achieved. The focused strips were equilibrated in two steps: 15 minutes in SDS equilibration buffer I (6M urea, 2% SDS, 30% glycerol, 50 mM Tris, pH 8.8, 0.01% bromophenol blue, and 10 mg/ml DTT) followed by 15 minutes with equilibration buffer II in which the DTT was replaced by 25 mg/ml iodoacetamide. The equilibrated IPG strips were placed directly on top of polymerized 12% SDS gels and covered with low-melt agarose. Gels were run in cooled tanks at 1 watt per gel until the dye front was at the bottom of the gel.

Gel images were obtained using a Typhoon™ Trio, Variable Mode Imager (GE Healthcare). DeCyder software (GE Healthcare, version 6.5) was used to detect spots, subtract background, and to normalize spots against the pooled standard. Further, DeCyder was used to match spots between gels and determine significant changes in protein expression ($p < 0.05$) and the average ratio. Average ratio was derived from the normalized spot volume standardized against the intra-gel standard thus providing a measure of the magnitude of expression differences between identified proteins. Spot detection and matching were verified visually. Gels to be used for spot picking were fixed in 10% methanol and 7.5% acetic acid overnight, and post-stained with Deep Purple™ Total Protein Stain (GE Healthcare) and imaged on the Typhoon. The post-stained spots were matched to the CyDye gel images using DeCyder software. Picking and digestion were performed using Ettan robotic components (GE Healthcare).

Spots that showed significant ($p < 0.05$) differences in abundance between low active (C3H/HeJ) and high active (C57L/J) mice were robotically picked, washed, and digested (GE Healthcare, Ettan system) with recombinant porcine trypsin (Promega, Madison, WI) as

described elsewhere⁸³. Extracted tryptic peptides were concentrated by SpeedVac and analyzed by nano-electrospray ionization/ion trap mass spectrometry (LC/MS/MS with an LTQ XL linear; ThermoFinnigan, San Jose, CA). Subsequently, peptides from the MS were identified using the MASCOT search engine. The MASCOT program (v2.2) searched the mouse genome using the following parameters for protein identification: 1) one missed cleavage by trypsin; 2) monoisotopic peptide masses; 3) peptide mass tolerance of 1.2 Da; and 4) fragment mass tolerance of 0.8 Da. Further, oxidation of methionine and carbamidomethylation of cysteine were taken into consideration by MASCOT in the protein identification. By meeting these parameters, the peptides were matched to proteins at a significance level of $p < 0.05$. Protein identifications were verified by Scaffold (Proteome Software, Portland, OR). Proteins were then categorized based on their function using String 9.0¹⁵⁷.

From the 2D-DIGE results, two highly significantly expressed ($p < 0.001$) proteins (Annexin A6 – Anxa6, and Calsequestrin 1 – Casq1, see results) were validated using standard western blot techniques. Briefly, proteins from three randomly chosen samples of each strain were separated by SDS-Page, and then transferred to a nitrocellulose membrane with transfer confirmed by *Ponceau S* stain. Membranes were incubated overnight in 1:1000 ratio of primary antibody recognizing Anxa6 (Biorbyt, San Francisco CA) or Casq1 (GeneTex, Irvine, CA) and blocking buffer (5% Nonfat Dried Milk, 0.5% Tween 20). Membranes were then incubated in the secondary horseradish peroxidase antibody (Cell Signaling Technology, Beverly, MA). Chemiluninescence was imaged and all analysis was performed with a Flurochem analyzer (Derbyshire, UK). Additionally GAPDH (GeneTex) was analyzed as a loading control. Western

blots were analyzed using the individual protein band's optical density that allowed for a semi-quantitative estimate of protein level.

In an effort to elucidate potential protein networks associated with the highly significantly expressed candidate proteins, we conducted co-immunoprecipitation (CoIP) experiments using the Pierce Crosslink IP Kit (Thermo Scientific, Rockford, IL). Briefly, the CoIP antibody (Anxa6 or Casq1) was bound to Protein A/G Agarose resin. A non-specific control was used (no antibody) in order to establish a "background" effect. The antibody resin was then incubated with the whole sample extract that contained the protein antigen of interest, allowing the antibody:antigen complex to form. After washing to remove non-bound components of the sample, the antigen was recovered by dissociation from the antibody with elution buffer¹⁵⁸. The eluted sample was then run on an SDS page. As the sample entered the 10% running gel, the electrophoresis was stopped, proteins were stained with Coomassie blue, and the bands were cut from the gel, digested, and subjected to mass spectroscopy for identification as described previously.

3.3.2 Experiment 2: Role of Candidate Proteins in Physical Activity

The 2D-DIGE results showed that Anxa6 and Casq1 were highly significantly over expressed ($p < 0.001$) in high active mice. Given that both proteins are involved in calcium homeostasis of skeletal muscle^{60,69}, Anxa6 and Casq1 were determined to be strong candidates for the peripheral regulation of physical activity and selected for further evaluation using transient gene silencing Vivo-morpholinos. Forty-two high-active C57L/J male mice were obtained from The Jackson Laboratory. Male mice were chosen since there was no difference in protein expression between males and females (see 2D-DIGE results) and to prevent any

effects of the estrous cycle of female mice on physical activity response¹⁵⁹. The mice were randomly divided into three treatment groups: 1) Control mice (n=15) that were treated with physiological saline; 2) Anxa6-targeted mice (n=15); and 3) Casq1-targeted mice (n=12). Previous results from our lab have shown that physiological saline is an appropriate control as compared to Vivo-morpholino scramble in terms of physical activity response, and expression of targeted protein¹⁵⁰.

At eight weeks of age, mice were individually housed on running wheels with *ad libitum* access to food and water for three days to establish baseline wheel running. Following baseline wheel running the running wheel was locked for four days in order to mirror the settings of the 2D-DIGE study (described previously) and prevent the expression of proteins because of a training effect. At the end of the first week (three days running, four days locked wheel), three mice were euthanized as described above and the soleus and EDL were extracted to determine baseline levels of Anxa6 and Casq1 expression using western blotting techniques described earlier. During the subsequent treatment week, mice were administered either Vivo-morpholinos targeting Anxa6 or Casq1 (11mg/kg, GeneTools, LLC, Philomath, OR) or equal volume physiological saline (~56 ul) via tail vein injection on treatment weekdays 1, 3, 5, and 7. After the Vivo-morpholino-treatment week, mice were allowed to recover for one week (Days 8-15). Throughout both the treatment and recovery weeks, the wheels were unlocked and activity was measured using the previously described methods.

To establish the protein expression pattern during the treatment (Days 1-7) and recovery weeks (Days 8 -15) a cohort (n=3) of mice were euthanized at intervals throughout the protocol. Control mice soleus and EDL were analyzed on Days 2, 4, 8, and 15, the Anxa6 Vivo-

morpholino group's tissue was analyzed on Days 2, 3, 4, and 15, and the Casq1 group's tissue was analyzed on Days 2, 3, and 15. Initially, tissues from the Vivo-morpholino groups were to be analyzed on a similar pattern, as was the Control group; however, due to Vivo-morpholino production issues, several mice had to be excluded from analysis. Protein knockdown was measured by western blot as described above. Additionally, to provide a comparison to the low active C3H/HeJ mice Anxa6 and Casq1 expression in soleus from the Vivo-morpholino treated animals (treatment day three) and C3H/HeJ mice were analyzed using western blots.

3.3.3 Statistics

Physical characteristics were analyzed with an ANOVA to compare strain (C57L/J and C3H/HeJ), sex (male and female), weight and percent body fat. An alpha level of 0.05 was set *a priori* and if a significant main effect was found, a Tukey's HSD *post hoc* test was used. 2D-DIGE results were analyzed using ANOVA, with significantly differentially expressed protein spot determination with an *a priori* alpha value of 0.05, with subsequent protein identification (mass spectroscopy identification) using an *a priori* alpha value of 0.05. The conformational western blot optical densities (Experiment 1) were analyzed using a Student's t test (GraphPad Software Inc, La Jolla, CA) to compare protein levels between high active and low-active mice with an alpha level of 0.05 set *a priori*. For the western blot used to analyze Vivo-morpholino results (Experiment Two) a 2x2 ANOVA was used to compare day of treatment and treatment group with an alpha level of 0.05 set *a priori* and a Tukey's HSD *post hoc* test if main effects were significant. Further comparisons of wheel running with Vivo-morpholino-treatment were analyzed using a 3 x 3 ANOVA with week (baseline, treatment, and recovery) and treatment group (control, Anxa6 Vivo-Morpholino, and Casq1 Vivo-morpholino) as the main effects. An

alpha level of 0.05 was set *a priori*. If a main effect was found significant, a Tukey's HSD *post hoc* test was used.

3.4 Results

3.4.1 Experiment 1: Proteome Determination

At the time of sacrifice, the male mice in both strains were significantly ($p=0.001$) heavier than the females (C3H/HeJ males 21.25 ± 1.60 g; C3H/HeJ females 18.91 ± 1.06 g; C57L/J males 22.21 ± 1.16 g; C57L/J females 17.21 ± 0.92 g). However, there was no difference ($p=0.0501$) in the percent body fat of the mice between or within strains (C3H/HeJ males $16.54 \pm 3.75\%$; C3H/HeJ females $14.64 \pm 1.64\%$; C57L/J males $13.23 \pm 1.92\%$; C57L/J females $12.62 \pm 1.75\%$).

Representative 2D-DIGE gels are depicted in Figure 3.1 and Figure 3.2 for soleus and EDL, respectively. There were 42 differentially expressed proteins identified in the soleus (Table 1), with 21 proteins over expressed in high-active animals and 21 over expressed in low-active animals. We observed eight differentially expressed proteins in the EDL (Table 2) with three proteins over expressed in high-active animals and five over expressed in low-active animals. Of the differentially expressed soleus proteins, the coding genes for 11 are located in known physical activity quantitative trait loci (QTL – Table 1) while the coding genes for three EDL proteins are located in QTL for physical activity (Table 2). Table 3 lists the identified proteins by their functional relation to muscle contraction. In general, when examining protein differences based on their function, the low active mice exhibited an over expression of proteins associated with the electron transport chain and cytoskeletal structure while the high

active animals over expressed proteins associated with the Krebs's (TCA) cycle and calcium regulation.

Anxa6 ($p=0.00031$) and Casq1 ($p=0.000025$) were differentially expressed in a highly significant manner between the high and low active mice and were categorized as strong potential candidates for the peripheral regulation of physical activity due to their role in skeletal muscle calcium regulation and thus their expression levels were confirmed by Western blot. Anxa6 was confirmed as significantly over expressed ($p=0.01$) in both the soleus and EDL of the C57L/J mice (Figure 3.3). Similarly, Casq1 in the soleus of high active mice was confirmed as being significantly more highly expressed ($p=0.0024$) (Figure 3.4).

Co-immunoprecipitation experiments (Table 4) identified one protein associated with Anxa6 in both soleus and EDL (alpha S1 casein) of the high-active mice. Two proteins associated with Anxa6 were identified, one in the low-active mice soleus (beta-lactoglobulin) and one in the EDL (actin, alpha 1). Five proteins were associated with Casq1 in the soleus of high active mice, including alpha S1 casein (in common with Anxa6). Three of the Casq1-associated proteins in high-active mice (creatine kinase M-type, LIM domain binding 3, troponin T3) were also associated with Casq1 in the soleus of low-active mice.

3.4.2 Experiment 2: Role of Candidate Proteins in Physical Activity

The Vivo-morpholino treatments were successful in transiently knocking down the expression of both Anxa6 and Casq1. Specifically, in the soleus, both Anxa6 ($p=0.0048$, Figure 3.5A) and Casq1 ($p=0.0152$, Figure 3.5B) were significantly knocked down from baseline. Interestingly the control samples over expressed both Anxa6 and Casq1 compared to baseline

values during the treatment and recovery weeks. In the EDL Anxa6 was significantly ($p=0.0019$) knocked down from baseline (Figure 3.6). However, unlike the soleus there was no difference in expression between control baseline protein levels and protein levels during treatment or recovery. EDL Casq1 expression was not analyzed since Casq1 was not expressed differently in that tissue between high- and low-active animals (Table 2).

When comparing soleus Vivo-morpholino treated samples from Day 3 of treatment to C3H/HeJ samples there was no difference in Anxa6 protein expression (Figure 3.7A; $p=0.14$), i.e. the high-active animals had a similar Anxa6 level as the low-active animals when the gene was transiently silenced. However, while Vivo-morpholino did decrease Casq1 levels in the high-active animals (80% knockdown from baseline), the low-active C3H/HeJ animals had a lower expression of Casq1 (Figure 3.7B, $p=0.002$).

The Vivo-morpholino results showed that as expected, there was no difference in physical activity response between the treatment groups during the baseline wheel exposures (Figure 3.8). However, during the treatment week, the Anxa6 and Casq1 Vivo-morpholino groups ran significantly less than the control group ($p=0.001$). At the end of the recovery week, activity was similar between all groups. Interestingly the control group during the treatment week and all groups during the recovery week ran significantly ($p=0.01$) further than the corresponding groups during the baseline week (Figure 3.8).

3.5 Discussion

The aim of this study was to utilize proteomic and gene-silencing techniques to identify skeletal muscle proteins that may be involved in the regulation of physical activity utilizing a

high-active versus low-active mouse model. We observed different protein signature patterns in the high- and low-active mice, with the differentially expressed proteins falling into specific physiological-function groups depending on the mouse strain. In general, the high active mice over expressed proteins associated with the Krebs' (TCA) cycle and proteins involved in calcium regulation while the low active mice over expressed proteins in the electron transport chain and cytoskeletal proteins that influence cell motility and force transduction, suggesting that peripheral mechanisms contributing to low-activity and those contributing to high-activity are distinct. Further, when we transiently silenced two of the most differentially expressed proteins found in the high-active mice (*Anxa6* and *Casq1*), we observed significant decreases in physical activity suggesting that these proteins are involved in regulating physical activity levels.

While it has been clearly shown that there is a significant genetic influence on physical activity regulation⁵, the site of regulation as well as the specific mechanisms regulating physical activity are still ambiguous. Kelly³⁴ has suggested that both peripheral and central mechanisms may be involved in activity regulation; indeed, several studies have considered central brain mechanisms focused around the reward pathways, dopaminergic mechanisms⁴⁴ and endocannabinoid mechanisms¹⁶⁰. These central mechanisms have been suggested to provide the 'drive' to be active. However, other studies have suggested that without the 'capability' to be active, an organism will not exhibit high levels of physical activity. Indeed, Tsao, *et al*⁵¹ showed that a transgenic over expression of *Glut4* in skeletal muscle induced a four-fold increase in daily activity and Pistilli, *et al*¹⁵¹ showed that knocking-out *IL-15R α* in skeletal muscle also increased wheel running activity. These data, along with Meek, *et al*'s⁵³ results showing that feeding of a higher-fat diet caused selectively-bred high active mice to run further on a

daily basis, strongly suggest that skeletal muscle mechanisms can markedly influence the amount of physical activity completed, irrespective of central drive. Thus, this study focused on skeletal muscle proteomic differences between high- and low-physically active mice to provide foundational targets for further mechanistic studies as well as potential interventions to influence physical activity level.

3.5.1 High-active Animals

Overall, our results indicated a greater number of differentially expressed proteins in the soleus (n=42), as compared to the number of proteins expressed differentially in the EDL (n=8) which was not surprising given the markedly greater duration of daily activity that C57L/J mice exhibit (avg±SD 351.1±61.6 mins/day) compared to the C3H/HeJ mice (75.6±99.0 mins/day;¹². In that regard, several protein expression patterns emerged from this study. In particular, the high active C57L/J mice generally over expressed calcium regulatory proteins, including *Casq1* and *Anxa6*. From these results, we would suggest that the high active C57L/J mice have an increased capability to be active because their skeletal muscles can more efficiently release and take up calcium due to the relative over expression of these calcium regulatory proteins. *Casq1* is a calcium binding protein located in the sarcoplasmic reticulum (SR)⁶⁹ while *Anxa6* influences calcium release from the SR⁵⁷ by increasing the open probability time of the calcium channel^{60,161}. While *Casq1* is located in the SR, *Anxa6* is localized around individual myofibrils and is associated with the terminal cisternae of the SR membrane⁵⁷. Further, the *Anxa6* gene is located in a previously identified QTL for the “mini muscle” phenotype, which leads to an increased force production from the triceps surae of mice selectively bred for high physical activity¹⁴. Thus, the over expression of both *Casq1* and *Anxa6*,

in conjunction with their biological roles, could form a potential mechanism by which high-active mice exhibit decreased fatigability of skeletal muscle and an increase in force production resulting in an increased capability to do physical activity (Figure 3.9).

It has been shown that there is an inverse relationship between skeletal muscle force production and skeletal muscle fatigue resistance¹⁶² due in large part to calcium concentration during excitation coupling^{162,163}. A higher level of Anxa6 in the high-active animals would result in a higher concentration of calcium released from the SR, which would cause greater force production¹⁶⁴. However, this higher myoplasmic calcium concentration following contraction would actually increase the fatigability of skeletal muscle^{162,164}. Offsetting this potential increase in fatigability with Anxa6, Casq1's calcium-binding properties in the SR⁶⁹, would lead to an increased binding of calcium following the Anxa6-induced increased release of calcium from the SR. Thus, Casq1 would act to decrease myoplasmic calcium levels and thereby reduce fatigability. In fact, the lower the myoplasmic calcium level following contraction results in a fatigue resistant phenotype of skeletal muscle¹⁶⁵. The interplay between increased levels of Anxa6 and Casq1 would theoretically lead to both an increase in force production and a decreased fatigability of the skeletal muscle, especially in the slow-twitch fiber dominated soleus tissue¹⁵⁴. A decreased fatigability – especially of slow-twitch fibers - could conceptually increase duration of activity, while an increased force production in both slow- and fast-twitch fibers would increase speed of activity. Supporting this hypothesis is previous work from our lab has shown that the high-active C57L/J – which we used in this study - run significantly farther (892%), longer (464%) and faster (228%) than the low-active C3H/HeJ on a daily basis¹². Additional support for the role of calcium regulation in increasing physical activity comes from

our observations of over expression in the high active mice of Annexin A4 and Sarcalumenin, which are involved in calcium regulation and force production.

As a means to confirm the hypothesis of Anxa6 and Casq1 influencing calcium homeostasis and resultant physical activity level, we used transient gene silencing to knockdown both proteins in high active C57L/J mice. Our hypothesis of the role of Anxa6 and Casq1 levels in regulating physical activity was supported by our observations that with knockdown of either Anxa6 or Casq1, there was a significant reduction in wheel running (Figure 3.8). Further, to confirm that calcium regulation in skeletal muscle was not impaired by knockout of Anxa6 or Casq1, we compared Anxa6 and Casq1 between Vivo-morpholino treated animals and the low-active C3H/HeJ animals. We observed that with knockdown, Anxa6 levels were similar between high- and low-active animals (Figure 3.7A). Casq1, while decreased from the normal state, was still higher in the treated animals versus the low-active animals (Figure 3.7B). Thus, while protein knock down decreased activity in the high-active mice - Anxa6 Vivo-morpholino mice ran a distance of 1.37 ± 0.85 km/day and the Casq1 Vivo-morpholino group ran 1.36 ± 0.02 km/day, from the control average of 10.01 ± 1.10 km/day - these distances were still higher than typical low-active C3H/HeJ male mice (0.6 ± 1.1 km)¹². Thus, the Vivo-morpholino treatments did not knock down Anxa6 and Casq1 completely below C3H/HeJ levels, but still significantly decreased protein expression and decreased physical activity.

Interestingly during the treatment week, the control animals exhibited a significant increase in physical activity compared to baseline (Figure 3.8). This increased activity corresponded to an increase in Anxa6 (Figure 3.5A) and Casq1 (Figure 3.5B) in the soleus. Yang *et al*¹⁷ observed that when a running wheel is returned after it has been removed – which was

the case in our study - there is an increase in physical activity level. Yang *et al*^{16,17} speculated that the increased activity after having no wheel was a result of increased action in the reward driven behavior system of the brain¹⁷. In fact we have shown in previous studies that an increase in expression of Vesicular monoamine transporter 2 (Vmat2) leads to an increase in wheel running¹⁵⁰. Vmat2 stores dopamine in synaptic vesicles and has been suggested to be associated with reward driven behavior⁴⁵. We would hypothesize that in addition to Yang's suggested mechanism and the action of Vmat2, the increase in physical activity could also be a result of our observation of the over expression of Anxa6 and Casq1 in the control animals' soleus. Additionally in the soleus, Anxa6 and Casq1 returned to baseline levels, which could have resulted in the increase in wheel running seen in the recovery week.

Results from the CoIP in the high active mouse tissues – especially the soleus - further support our hypothesis of an altered calcium-regulation affecting physical activity. Casq1 is permissive in a network formed by several proteins we identified in the CoIP (Troponin 3, desmin, creatine kinase M, and LIM domain binding 3) in both mice and humans¹⁵⁷. Thus, we would suggest that an increase in Casq1 would increase the activity of this network which would further increase muscle contractile state and contribute to the regulation of physical activity level in the high-active animals.

Potential functional roles for some of the proteins identified with the CoIP are not as clear. For example, both Anxa6 and Casq1 in the high active animals are associated with alpha S1 casein in both the soleus and EDL tissues. There is little information regarding the role of alpha S1 casein in skeletal muscle. However, alpha S1 casein does influence the transport of

calcium phosphate from the endoplasmic reticulum¹⁶⁶ suggesting a potential functional linkage with calcium-regulation and physical activity response.

In addition to calcium regulation, enhanced Krebs (TCA) Cycle activity could positively affect maintenance of high physical activity. The high active C57L/J animals over expressed several proteins associated with the Krebs's(TCA) cycle, with the most significant being an over expression of three proteins in the pyruvate dehydrogenase complex (i.e. pyruvate dehydrogenase protein X component, pyruvate dehydrogenase [acetyl-transferring]-phosphatase 1, and pyruvate dehydrogenase E1 component subunit beta). The over expression of the subunits of pyruvate dehydrogenase could conceptually lead to an increased capability to convert pyruvate to acetyl-CoA, with a potential subsequent increase in Krebs's (TCA) cycle activity and an increased NADH and FADH availability¹⁶⁷. This process would increase available ATP to meet the demands of an increased physical activity level.

In support of a potential increased Krebs's (TCA) cycle capability in the high-active mice, was an over expression of the key Krebs's (TCA) regulator dihydrolipoyllysine-residue succinyltransferase component of the 2-oxoglutarate dehydrogenase complex¹⁶⁸. The oxoglutarate dehydrogenase complex primarily controls the production of Succinyl-COA; an over expression of the dihydrolipoyllysine-residue succinyltransferase component would increase the capability to produce both succinyl-COA as well as increased levels of both NADH and FADH¹⁶⁸. Further, the coding gene for dihydrolipoyllysine-residue succinyltransferase component is located in identified QTL associated with both wheel running distance¹² and the mini muscle¹⁴. In addition to the hypothesis that increased Krebs's (TCA) cycle activity supports higher activity is that apolipoprotein A-1 (Apo1) was identified in the soleus and EDL of high

active mice. Apo1 is associated with cholesterol and fat storage, and in skeletal muscle, Apo1 could facilitate the use of fat as an additional substrate source for the Krebs's (TCA) cycle¹⁶⁹. This suggestion is supported by Meek *et al*⁵³ who showed that mice bred for high activity increase their activity level when fed a high fat diet. Thus, an over expression of Apo1 and proteins associated with the Krebs's (TCA) cycle could contribute to the high wheel running activity of the C57L/J mice by increasing NADH and FADH production, which would meet the energy demands for high physical activity. The higher efficiency of the TCA cycle combined with an increased usage of fat, decreased fatigability and increased force production due to the over expression of calcium-regulating proteins, would lead to the high-active animals having an increased capability of sustaining activity.

3.5.2 Low-active Animals

While we observed several protein expression patterns that would support high-activity in those mice that have inherently higher-activity patterns, there were also protein expression patterns in the low-active animals that could conceptually inhibit activity (Figure 3.10). The low active animals over expressed the enzyme 6-phosphofructo-2 kinase/fructose-2, 6-biphosphate 1 which decreases the activity of the primary regulator of glycolysis, phosphofructokinase 1¹⁷⁰. An over expression of 6-phosphofructo-2 kinase/fructose-2, 6-biphosphate 1 would lead to a higher level of degradation of 2,6-bisphosphate which would subsequently decrease glycolysis and increase gluconeogenesis¹⁷⁰. The decrease in glycolysis would decrease the generation of pyruvate and acetyl-CoA, thereby leading to a decrease in electron donors for the electron transport chain (ETC) and a potential decrease in available energy needed to support activity.

Interestingly, we also observed that the C3H/HeJ mice over expressed proteins associated with the ETC (e.g. electron transfer flavoprotein ubiquinone oxidoreductase, ATPase, and NADH dehydrogenase [ubiquinone]). The over expression of these proteins would generally lead to a more efficient generation of ATP via the electron transport chain¹⁷¹. We would speculate that in the low active animals a more efficient generation of ATP through the ETC could serve as a compensatory mechanism for the inhibited glycolytic production of electron donors as well as the relative under expression of proteins in the Krebs's (TCA) cycle as compared to the high-active animals.

In addition to the metabolic proteins, the C3H/HeJ animals over expressed proteins associated with cytoskeletal structure, specifically radixin, Lumican, tubulin beta 3, cofilin 2, alpha actinin 2, and tubulin 8. These proteins bind actin and microtubules to influence cell membrane/cytoskeletal organization¹⁷²⁻¹⁷⁵. The over expression of these proteins suggest that there is increased rigidity of the muscle cells resulting in an overall decreased motility of the C3H/HeJ skeletal muscle fiber as compared to the C57L/J mice¹⁷⁶. Peng, *et al*¹⁷⁶ suggested that the decreased motility of the cell can decrease force transduction and skeletal muscle force production. Thus, the over expression of these cytoskeletal structural proteins, as well as the observed over expression of the specific glycolytic and ETC proteins could theoretically hinder the capability for wheel running and physical activity. These proteins are attractive targets for further Vivo-morpholino studies investigating whether the knockdown of these proteins could increase the activity of the low-active animals.

While our results provide attractive potential peripheral mechanisms for further study, there is a limitation that should be considered. It is possible that not all proteins differentially

expressed between high- and low-active animals were detected in this study. However, this is the first study to investigate the peripheral proteomic regulation of physical activity and given that 2D-DIGE is currently considered one of the most sensitive methods for an initial global protein scan⁸⁹, it is probable that we detected the majority of differentially expressed proteins associated with the inherent high- and low-activity states in these mouse strains. As such, these results can be used as a foundation for future research using more specific protein methodologies to discover other proteins associated with activity level, as well as providing a target list for further gene-silencing studies.

In conclusion, our results support the hypothesis that peripheral, skeletal muscle factors that participate in the regulation of voluntary physical activity arise from multiple protein pathways. Specifically, there appears to be different mechanism regulating high versus low activity. High active animals over expressed proteins associated with the Krebs's (TCA) cycle and calcium regulation suggesting a decreased fatigability, increased force production, and increased capability of providing substrates for the electron transport chain. We confirmed the role of two calcium-handling proteins in regulating activity by transiently knocking down the proteins in healthy animals with a subsequent reduction in activity. Conversely, low-active animals over expressed structural proteins that could decrease muscle fiber motility, as well as over expressing proteins that would decrease glycolysis with a potential compensation through an increased efficiency of the electron transport chain. Future studies should focus on confirming these proteins' roles in the low-activity state. Maybe most importantly, given the potentially different peripheral regulating mechanisms in the high- and low-active mice,

conclusions regarding causal mechanisms of low-activity cannot be inferred from results on high-active animals and vice-versa.

CHAPTER IV

LESSONS LEARNED FROM VIVO-MORPHOLINOS: HOW TO AVOID VIVO-MORPHOLINO

TOXICITY

4.1 Synopsis

Vivo-morpholinos are oligonucleotide analogs that transiently silence genes by blocking translation or splicing of pre mRNA. Vivo-morpholinos are a promising tool in that there has been little to no toxicity reported with the treatment. However, in a recent study conducted in our lab, we observed that treatment with Vivo-morpholinos resulted in high mortality rates. Cause of death was the result of oligonucleotide hybridization resulting in clustering of the dendrimer delivery moiety of the Vivo-morpholino. The dendrimer clusters increased blood viscosity and caused cardiac arrest. Therefore, in order to achieve the gene silencing benefits of Vivo-morpholinos, the base pairing potential of the oligonucleotide analogs should be considered when designing experiments.

4.2 Introduction

The ability to silence genes *in vivo* provides the opportunity to identify gene function and could serve as a treatment for a variety of genetic disorders. Attempts to develop tools to silence genes *in vivo* have resulted in limited success. Initially, siRNA and phosphorodiamidate morpholino oligomers (PMOs) were thought to be potential methodologies for *in vivo* gene silencing; however, their use resulted in limited gene silencing and associated toxicity⁹⁹. Morcos *et al*¹⁰⁰ developed Vivo-morpholinos as an alternative to siRNA and PMOS. Vivo-morpholinos are anti-sense oligonucleotide analogs that bind to complementary RNA sequences and block translation of a targeted gene¹⁰⁰. Vivo-morpholinos are unique in that the delivery moiety consists of eight guanidinium head groups (dendrimer) of arginine-rich peptides, thus allowing for resistance to proteases and nucleases to prevent degradation and increase the efficiency of uptake into the cell by endocytosis¹⁰⁰.

To date there are twenty-eight studies using Vivo-morpholinos^{100-126,150} and all have reported at least 50% knockdown of the target gene with no adverse side effects. Fifteen of these studies used a mouse model^{100,101,103,110,112,114,119,121-127,150} with the remaining studies using rats¹¹⁵⁻¹¹⁷, newts¹²⁰, chicken embryos¹⁰⁶, zebrafish^{102,104,105} and amphibians^{107,109,118}. In the mouse model, it has been shown that Intravenous (IV) or intraperitoneal (IP) administration Vivo-morpholinos were equally efficacious, and recent studies have shown success with direct injection in target tissue¹¹⁵⁻¹¹⁷. To this point, no toxicity of Vivo-morpholinos has been reported.

Our lab has evaluated the gene silencing ability and washout effects of Vivo-morpholinos in various tissues¹⁵⁰. We have published the effects of three different Vivo-morpholinos in addition to a Vivo-morpholino cocktail (combination of two Vivo-morpholinos)

and achieved significant knockdown of the targeted proteins (Drd1, Glut4, Vmat2) and observed no adverse side effects even when using with the Vivo-morpholino cocktail¹⁵⁰.

Recently, we initiated a study with the goal of using Vivo-morpholinos to silence Annexin A6 (*Anxa6*) and Calsequestrin 1 (*Casq1*), both genes being involved in skeletal muscle calcium regulation, via IV injection in the mouse model. In addition to these single Vivo-morpholino treatments, we combined the *Anxa6* and *Casq1* Vivo-morpholinos in a cocktail in an attempt to silence both genes at the same time to determine the effect on physical activity. The initial results were disconcerting in that the treatments resulted in numerous fatalities. Thus, the purpose of this report is to characterize the cause of death, mechanism of action, and propose possible solutions to the toxicity we observed with Vivo-morpholinos in this model.

4.3 Observation of the Problem

Vivo-morpholinos were obtained from GeneTools LLC (Philomath, OR) targeting *Anxa6* and *Casq1* in 2000 nmol batches. GeneTools LLC provides a Vivo-morpholino design service whereby the investigator provides the gene of interest along with the NCBI accession number. GeneTools LLC then generates Vivo-morpholinos for the targeted genes. Previous work from our lab has utilized the 400 nmol batch of Vivo-morpholinos due to the smaller sample sizes of our studies¹⁵⁰. Given that our research focus is on the genetic mechanisms regulating daily physical activity, we used previously phenotyped high-active C57L/J mice¹² (The Jackson Laboratory, Bar Harbor, ME) and gave them a tail vein injection of Vivo-morpholinos (11mg/kg or ~56 ul of *Anxa6* or *Casq1* Vivo-morpholino) or a cocktail treatment (11mg/kg of each Vivo-morpholino or ~112 ul). These dosages have been recommended by GeneTools¹⁰⁰ and used in the literature¹³⁶ without toxicity. Following the injections, the mice appeared to recover and

were ambulatory within the cage for 1-2 minutes, followed by an immediate loss of consciousness, an increased breathing rate, and fluid leakage from the nose. Once mice displayed these signs of distress, mice were placed on heating pads (37° C) and given supplemental oxygen (via nose cone). Unfortunately, once the mouse lost consciousness, we observed in all cases that death occurred within five minutes. By the time the solution to the problem was determined (detailed below) and after using several potential solutions provided by the company, a total of 14 out of 17 (82%) animals receiving the Vivo-morpholino cocktail died, while 6 out of 9 (66%) of the *Casq1* Vivo-morpholino died and 2 out of 8 (25%) animals receiving the *Anxa6* Vivo-morpholino died. None of the 15 control animals (saline injection) had a fatality.

These observations were disconcerting for several reasons, including financial, logistical, scientific, but most importantly, the trauma placed on the animals. While all measures were taken to insure humane treatment of the animals (and all studies had been approved by our IACUC), the Vivo-morpholino treatment resulted in unnecessary stress placed on the mice prior to death. As noted earlier, there has been no previous evidence indicating the observed fatalities seen in our study. Thus, for further use as a laboratory tool and given that potential future applications for Vivo-morpholino may include both non-human primates¹¹⁵ and human clinical trials¹²³ it is critical that the cause of the Vivo-morpholino toxicity in this study be understood to prevent future fatalities associated with Vivo-morpholino treatment.

4.4 Potential Solutions to the Problem Provided by GeneTools

Following the fatalities associated with Vivo-morpholinos, GeneTools LLC, was consulted. GeneTools acknowledged that they were aware of similar fatalities associated with Vivo-morpholino treatment; however, GeneTools was unaware of the mechanism of action that caused the increased mortality rates. GeneTools hypothesized that the fatalities were a result of guanidinium toxicity and recommended treatment with lower dosages even though we had previously used the recommended dosages without incident¹⁵⁰. Therefore, we subsequently injected C57L/J mice with Vivo-morpholino treatment of *Casq1*, *Anxa6*, and cocktail at a dosage of 4mg/kg (reduced from normal dose of 11 mg/kg). This treatment resulted in 8 out of 8 (100%) fatalities in the cocktail group, along with 3 out of 7 (43%) fatalities in the *Casq1* group and 1 out of 6 (17%) fatalities in the *Anxa6* group. Thus, by markedly reducing the dose, we eliminated the possibility that guanidinium toxicity was the causal factor. Supporting this conclusion is much older literature that reports that the fatal dose of guanidinium is actually 30 times more than the amount the mice received with any of the Vivo-morpholino treatments¹⁷⁷. Further, as we have noted earlier, neither we nor others have observed fatalities with a Vivo-morpholino dosage of 11mg/kg^{122,136,150}. Thus, guanidinium toxicity was ruled out as the cause of death.

4.5 Investigation into the Cause of Death

In order to determine the cause of death, mice that died were immediately necropsied with brain, heart, lung, liver, spleen, large intestine, soleus, gastrocnemius, extensor digitorum longus, and kidneys removed. Two initial observations were made during necropsy that set these animals apart from normal anatomical findings during routine dissections: 1) the

deceased animals' eyes had a cloudy opaque appearance (Figure 4.1 Panel A); and 2) there was necrotic tissue in the left ventricle (Figure 4.1 Panel B) of the heart with an increased blood thickness in the vena cava and aorta. These observations were common across all animals that died after Vivo-morpholino treatment. These observations have not been previously documented nor have we observed these symptoms in our previous Vivo-morpholino studies. Interestingly, one of our previous studies¹³³ used the *Casq1* Vivo-morpholino (ordered 400 nmol batch) and did not result in increased mortality rates of the mice. Thus, we initially hypothesized that the mechanism of action for mortality was due to an unknown uniqueness of the synthesis of the 2000 nmol product.

Using standard techniques¹⁷⁸, we evaluated the *Casq1* Vivo-morpholino at 2000 and 400 nmol concentrations via Matrix Assisted laser desorption/ionization time of flight (MALDI-TOF) with sinapinic acid as the matrix in an effort to identify any potential contaminants in the 2000 nmol Vivo-morpholino. We observed no difference in the spectra between the 2000 or 400 nmol *Casq1* Vivo-morpholinos (Figure 4.2). Furthermore, the spectra were not different from the spectra provided by GeneTools in the quality control report.

With the potential of contamination eliminated, we revisited the necropsy results, especially the necrosis of the left ventricle and increased blood thickness in the vena cava and aorta. Given these observations, we hypothesized that Vivo-morpholinos caused significant blood clotting in the heart and vessels, resulting in markedly decreased oxygen delivery to the heart and subsequent myocardial infarction.

To initially evaluate this hypothesis, a test of the effects of Vivo-morpholinos on blood clotting was conducted. A C57L/J mouse that had not received Vivo-morpholinos was

anesthetized with isoflurane and blood was removed by cardiac puncture. The mouse was then euthanized using cervical dislocation. Three blood droplets consisting of 100 ul of whole blood were aliquoted on a microscope slide. Each blood droplet was mixed with either 10 ul of saline, 10 ul of *Casq1* Vivo-morpholino or 10 ul of the Vivo-morpholino cocktail. The blood droplets were then monitored using a dissecting microscope (Olympus, Center Valley Pennsylvania) with clotting time evaluated by the amount of time it took for a lattice-like structure to form around the outer ring of the blood droplet. To ensure objectivity, the technician performing the evaluation was blinded to the treatment groups. The results showed that treatment with the *Casq1* Vivo-morpholino decreased clotting time by 21% and treatment with the Vivo-morpholino cocktail further decreased clotting time by 59% as compared to the saline control (Figure 4.3). Thus, treatment with Vivo-morpholino caused significant clotting suggesting that Vivo-morpholino treatment (and especially the cocktail treatment) resulted in blood clot formation that resulted in cardiac death.

4.6 Suggested Mechanism for Blood Clot Formation and Cardiac Death

With our results of a reduced clotting time with Vivo-morpholino treatment and the increased blood viscosity observed in the Vivo-morpholino-treated animals, we hypothesized that the structure of the Vivo-morpholino was leading to a significantly enhanced blood clot formation. Due to the fact that the majority of the fatalities occurred in the cocktail treatment group, we examined the sequences of the *Casq1* and *Anxa6* Vivo-morpholino. As noted earlier, the sequences chosen for the oligo-portion of the Vivo-morpholino are generally chosen by GeneTools (as was the case in our previous studies), but there is an option for the client to provide the oligo-sequences. When examining the sequences of the supplied *Casq1* and *Anxa6*

Vivo-morpholino, we noted that there were nine nucleotide bases that could hybridize when the sequence was arranged by aligning the 3' and 5' ends (Figure 4.4). Furthermore, there were four potential nucleotide-hybridizing pairs in the *Casq1* Vivo-morpholino and three in the *Anxa6* Vivo-morpholino (Figure 4.4). In checking the previous Vivo-morpholino we had used in our non-fatal experiments¹⁵⁰, we found that the oligos we employed did not have 5' to 3' base pairing/hybridization. Thus, we would suggest that as the Vivo-morpholinos hybridized, especially in the cocktail treatments, this hybridization formed a complex consisting of the hybridized Vivo-morpholino as well as the delivery moiety (dendrimer). This dendrimer cluster probably was responsible for the observed increased blood viscosity¹⁷⁹ which likely led to an ischemia state of the heart with a resulting fatality¹⁸⁰.

The hypothesized mechanism by which the dendrimer cluster induced fatality is based on the work by Roberts *et al*¹⁸¹ who investigated the toxic effects associated with dendrimer administration *in vivo*. Specifically, Roberts *et al*¹⁸¹ examined the effects of dendrimer generations on *in vivo* function. The results showed that the higher generation of dendrimers (over 10,000 Daltons) had an effect on red blood cell aggregation¹⁸¹. The increased number of cationic dendrimer head groups associated with the higher generation level altered the surface charge density of the membranes of the red blood cells. This caused a conformational change in the membrane of the red blood cells resulting in sedimentation of the red blood cells^{181,182}. The sedimentation of red blood cells caused increased blood viscosity and blood clotting which led to myocardial infarction¹⁸⁰.

4.7 Solution to Fatal Vivo-morpholinos

The easiest solution to the toxicity issue appears to be care taken when designing the Vivo-morpholinos to insure little to no hybridization possibility. GeneTools allows customers to design their own oligos and we would recommend this option. However, there are situations such as ours, where targeted genes may have similar sequences. While we would recommend that wherever possible to use careful oligo design, one potential solution to alleviate the dendrimer clustering if the oligo shows a potential for hybridization is by adding an equal volume of physiological saline to the Vivo-morpholino injection and vortexing vigorously before injection. When we employed this simple procedure, we eliminated fatalities in the mice that received these treatments (n=6), yet still observed significant gene silencing. The addition of physiological saline is thought to prevent red blood cell aggregation by preserving the surface charge density of the red blood cells, which is accomplished by the Cl⁻ present in the physiological saline.

In conclusion, while Vivo-morpholinos are an ideal tool for transient gene silencing, caution should be taken in oligo design to avoid dendrimer cluster formation and resultant increased blood viscosity. In order to prevent fatalities it is recommended that the oligonucleotide analogs be analyzed for potential 3' to 5' base pair hybridization in order to prevent clustering of dendrimers.

CHAPTER V

CONCLUSIONS

Physical activity is correlated to decreased rates of cardiovascular disease, obesity, type II diabetes and some types of cancer. While there is strong evidence that genetic factors account for most of the influence on physical activity regulation, little is known about how these factors contribute to physical activity regulation. The studies in this dissertation aimed to evaluate the use of the novel gene silencing tool, Vivo-morpholinos in the physical activity mouse model, to identify proteomic differences between high and low physically active mice, and to use Vivo-morpholinos to transiently silence identified proteins.

The results showed that Vivo-morpholinos are an effective tool for gene silencing in skeletal muscle and that in order to achieve gene silencing in the brain, the bradykinin analog RMP-7 is required with treatment. However, caution should be taken when designing Vivo-morpholinos to avoid hybridization. It is further recommended that equal volume of physiological saline be mixed with Vivo-morpholinos in order to prevent the possibility of hybridization.

The identification of proteins associated with high physical activity were proteins associated with calcium regulation and Krebs's (TCA) cycle while there was an over expression in the low active mice of ETC and structural proteins. Annexin A6 and Calsequestrin 1, both over-expressed in high-active mice and were selected for further evaluation for their involvement in physical activity regulation. The results showed that with a transient knock down of Annexin A6 and Calsequestrin 1 there was a significant reduction in physical activity. Moreover, the over expression of both proteins led to an increase in physical activity level. The results of this

dissertation show that there are peripheral components regulating physical activity and that further investigations into the regulation of physical activity must include a gene silencing approach to evaluate cause and affect mechanisms.

REFERENCES

1. Heath GW, Troped PJ. The role of the built environment in shaping the health behaviors of physical activity and healthy eating for cardiovascular health. *Future Cardiology*. Sep 2012;8(5):677-679.
2. Troped PJ, Starnes HA, Puett RC, et al. Relationships between the built environment and walking and weight status among older women in three U.S. states. *Journal of aging and Physical Activity*. Mar 26 2013. E Pub Ahead of Print
3. Troped PJ, Tamura K, Whitcomb HA, Laden F. Perceived built environment and physical activity in U.S. women by sprawl and region. *American Journal of Preventive Medicine*. Nov 2011;41(5):473-479.
4. Troped PJ, Wilson JS, Matthews CE, Cromley EK, Melly SJ. The built environment and location-based physical activity. *American Journal of Preventive Medicine*. Apr 2010;38(4):429-438.
5. Lightfoot JT. Current understanding of the genetic basis for physical activity. *The Journal of Nutrition*. Mar 2011;141(3):526-530.
6. Troiano RP, Berrigan D, Dodd KW, Masse LC, Tilert T, McDowell M. Physical activity in the United States measured by accelerometer. *Medicine and Science in Sports and Exercise*. Jan 2008;40(1):181-188.
7. Mokdad AH, Marks JS, Stroup DF, Gerberding JL. Actual causes of death in the United States, 2000. *JAMA : the Journal of the American Medical Association*. Mar 10 2004;291(10):1238-1245.
8. D C, J. L. The economic cost of physical inactivity and excess weight in American adults. *J Phys Act Health* 2006;3:148-163.

9. Joosen AM, Gielen M, Vlietinck R, Westerterp KR. Genetic analysis of physical activity in twins. *The American Journal of Clinical Nutrition*. Dec 2005;82(6):1253-1259.
10. Stubbe JH, de Moor MH, Boomsma DI, de Geus EJ. The association between exercise participation and well-being: a co-twin study. *Preventive Medicine*. Feb 2007;44(2):148-152.
11. Leamy LJ, Pomp D, Lightfoot JT. An epistatic genetic basis for physical activity traits in mice. *The Journal of Heredity*. Nov-Dec 2008;99(6):639-646.
12. Lightfoot JT, Leamy L, Pomp D, et al. Strain screen and haplotype association mapping of wheel running in inbred mouse strains. *Journal of Applied Physiology*. Sep 2010;109(3):623-634.
13. Lightfoot JT, Turner MJ, Pomp D, Kleeberger SR, Leamy LJ. Quantitative trait loci for physical activity traits in mice. *Physiological Genomics*. Feb 19 2008;32(3):401-408.
14. Hartmann J, Garland T, Jr., Hannon RM, Kelly SA, Munoz G, Pomp D. Fine mapping of "mini-muscle," a recessive mutation causing reduced hindlimb muscle mass in mice. *The Journal of Heredity*. Nov-Dec 2008;99(6):679-687.
15. Kelly SA, Nehrenberg DL, Hua K, Garland T, Jr., Pomp D. Functional genomic architecture of predisposition to voluntary exercise in mice: expression QTL in the brain. *Genetics*. Jun 2012;191(2):643-654.
16. Yang HS, Shimomura K, Vitaterna MH, Turek FW. High-resolution mapping of a novel genetic locus regulating voluntary physical activity in mice. *Genes, Brain, and Behavior*. Feb 2012;11(1):113-124.

17. Yang HS, Vitaterna MH, Laposky AD, Shimomura K, Turek FW. Genetic analysis of daily physical activity using a mouse chromosome substitution strain. *Physiological Genomics*. Sep 9 2009;39(1):47-55.
18. Shephard RJ. Limits to the measurement of habitual physical activity by questionnaires. *British Journal of Sports Medicine*. Jun 2003;37(3):197-206; discussion 206.
19. Ponting CP, Goodstadt L. Separating derived from ancestral features of mouse and human genomes. *Biochemical Society Transactions*. Aug 2009;37(Pt 4):734-739.
20. Knab AM, Lightfoot JT. Does the difference between physically active and couch potato lie in the dopamine system? *International Journal of Biological Sciences*. 2010;6(2):133-150.
21. Ekkekakis P. Let them roam free? Physiological and psychological evidence for the potential of self-selected exercise intensity in public health. *Sports Medicine*. 2009;39(10):857-888.
22. Rezende EL, Chappell MA, Gomes FR, Malisch JL, Garland T, Jr. Maximal metabolic rates during voluntary exercise, forced exercise, and cold exposure in house mice selectively bred for high wheel-running. *The Journal of Experimental Biology*. Jun 2005;208(Pt 12):2447-2458.
23. Adlam D, De Bono JP, Danson EJ, et al. Telemetric analysis of haemodynamic regulation during voluntary exercise training in mouse models. *Experimental Physiology*. Nov 2011;96(11):1118-1128.
24. Middleton N, Shave R, George K, et al. Impact of repeated prolonged exercise bouts on cardiac function and biomarkers. *Medicine and Science in Sports and Exercise*. Jan 2007;39(1):83-90.

25. Powers SK, Howley ET. *Exercise Physiology. Theory and Application to Fitness and Performance* 5ed. New York: McGraw Hill; 2004.
26. Dishman RK. Brain monoamines, exercise, and behavioral stress: animal models. *Medicine and Science in Sports and Exercise*. Jan 1997;29(1):63-74.
27. Eikelboom R. Human parallel to voluntary wheel running: exercise. *Animal Behaviour*. Mar 1999;57(3):F11-F12.
28. Smith C, Falconer DS, Duncan LJ. A statistical and genetical study of diabetes. II. Heritability of liability. *Annals of Human Genetics*. Mar 1972;35(3):281-299.
29. Turner MJ, Kleeberger SR, Lightfoot JT. Influence of genetic background on daily running-wheel activity differs with aging. *Physiological Genomics*. Jun 16 2005;22(1):76-85.
30. Lightfoot JT, Turner MJ, Daves M, Vordermark A, Kleeberger SR. Genetic influence on daily wheel running activity level. *Physiological Genomics*. Nov 17 2004;19(3):270-276.
31. Meek TH, Lonquich BP, Hannon RM, Garland T, Jr. Endurance capacity of mice selectively bred for high voluntary wheel running. *The Journal of Experimental Biology*. Sep 15 2009;212(18):2908-2917.
32. Houle-Leroy P, Guderley H, Swallow JG, Garland T, Jr. Artificial selection for high activity favors mighty mini-muscles in house mice. *American Journal of Physiology. Regulatory, integrative and comparative physiology*. Feb 2003;284(2):R433-443.
33. Nehrenberg DL, Wang S, Hannon RM, Garland T, Jr., Pomp D. QTL underlying voluntary exercise in mice: interactions with the "mini muscle" locus and sex. *The Journal of Heredity*. Jan-Feb 2010;101(1):42-53.

34. Kelly SA, Nehrenberg DL, Peirce JL, et al. Genetic architecture of voluntary exercise in an advanced intercross line of mice. *Physiological Genomics*. Jul 7 2010;42(2):190-200.
35. Leamy LJ, Pomp D, Lightfoot JT. A search for quantitative trait loci controlling within-individual variation of physical activity traits in mice. *BMC Genetics*. 2010;11:83.
36. Gygi SP, Rochon Y, Franza BR, Aebersold R. Correlation between protein and mRNA abundance in yeast. *Molecular and Cellular Biology*. Mar 1999;19(3):1720-1730.
37. Greenbaum D, Colangelo C, Williams K, Gerstein M. Comparing protein abundance and mRNA expression levels on a genomic scale. *Genome Biology*. 2003;4(9):117.
38. Anderson L, Seilhamer J. A comparison of selected mRNA and protein abundances in human liver. *Electrophoresis*. Mar-Apr 1997;18(3-4):533-537.
39. Greenbaum D, Jansen R, Gerstein M. Analysis of mRNA expression and protein abundance data: an approach for the comparison of the enrichment of features in the cellular population of proteins and transcripts. *Bioinformatics*. Apr 2002;18(4):585-596.
40. Ghazalpour A, Bennett B, Petyuk VA, et al. Comparative analysis of proteome and transcriptome variation in mouse. *PLoS Genetics*. Jun 2011;7(6):e1001393.
41. Moore-Harrison T, Lightfoot JT. Driven to be inactive? The genetics of physical activity. *Progress in Molecular Biology and Translational Science*. 2010;94:271-290.
42. Mathes WF, Nehrenberg DL, Gordon R, Hua K, Garland T, Jr., Pomp D. Dopaminergic dysregulation in mice selectively bred for excessive exercise or obesity. *Behavioural Brain Research*. Jul 11 2010;210(2):155-163.
43. Knab AM, Bowen RS, Hamilton AT, Gullledge AA, Lightfoot JT. Altered dopaminergic profiles: implications for the regulation of voluntary physical activity. *Behavioural Brain Research*. Dec 1 2009;204(1):147-152.

44. Knab AM, Bowen RS, Hamilton AT, Lightfoot JT. Pharmacological manipulation of the dopaminergic system affects wheel-running activity in differentially active mice. *Journal of Biological Regulators and Homeostatic Agents*. Jan-Mar 2012;26(1):119-129.
45. Taylor TN, Caudle WM, Miller GW. VMAT2-Deficient Mice Display Nigral and Extranigral Pathology and Motor and Nonmotor Symptoms of Parkinson's Disease. *Parkinson's Disease*. 2011;2011:124165.
46. Taylor TN, Caudle WM, Shepherd KR, et al. Nonmotor symptoms of Parkinson's disease revealed in an animal model with reduced monoamine storage capacity. *The Journal of Neuroscience : the Official Journal of the Society for Neuroscience*. Jun 24 2009;29(25):8103-8113.
47. Raichlen DA, Foster AD, Gerdeman GL, Seillier A, Giuffrida A. Wired to run: exercise-induced endocannabinoid signaling in humans and cursorial mammals with implications for the 'runner's high'. *The Journal of Experimental Biology*. Apr 15 2012;215(Pt 8):1331-1336.
48. Dubreucq S, Koehl M, Abrous DN, Marsicano G, Chaouloff F. CB1 receptor deficiency decreases wheel-running activity: consequences on emotional behaviours and hippocampal neurogenesis. *Experimental Neurology*. Jul 2010;224(1):106-113.
49. Dubreucq S, Kambire S, Conforzi M, et al. Cannabinoid type 1 receptors located on single-minded 1-expressing neurons control emotional behaviors. *Neuroscience*. Mar 1 2012;204:230-244.
50. Ge HY, Arendt-Nielsen L, Madeleine P. Accelerated muscle fatigability of latent myofascial trigger points in humans. *Pain Medicine*. Jul 2012;13(7):957-964.

51. Tsao TS, Li J, Chang KS, et al. Metabolic adaptations in skeletal muscle overexpressing GLUT4: effects on muscle and physical activity. *FASEB journal : Official Publication of the Federation of American Societies for Experimental Biology*. Apr 2001;15(6):958-969.
52. Tsao TS, Burcelin R, Katz EB, Huang L, Charron MJ. Enhanced insulin action due to targeted GLUT4 overexpression exclusively in muscle. *Diabetes*. Jan 1996;45(1):28-36.
53. Meek TH, Eisenmann JC, Garland T, Jr. Western diet increases wheel running in mice selectively bred for high voluntary wheel running. *International Journal of Obesity*. Jun 2010;34(6):960-969.
54. Keeney BK, Meek TH, Middleton KM, Holness LF, Garland T, Jr. Sex differences in cannabinoid receptor-1 (CB1) pharmacology in mice selectively bred for high voluntary wheel-running behavior. *Pharmacology, Biochemistry, and Behavior*. Jun 2012;101(4):528-537.
55. Reichart DL, Hinkle RT, Lefever FR, et al. Activation of the dopamine 1 and dopamine 5 receptors increase skeletal muscle mass and force production under non-atrophying and atrophying conditions. *BMC Musculoskeletal Disorders*. 2011;12:27.
56. Beard NA, Wei L, Dulhunty AF. Ca(2+) signaling in striated muscle: the elusive roles of triadin, junctin, and calsequestrin. *European Biophysics Journal : EBJ*. Dec 2009;39(1):27-36.
57. Song G, Harding SE, Duchon MR, et al. Altered mechanical properties and intracellular calcium signaling in cardiomyocytes from annexin 6 null-mutant mice. *FASEB Journal: Official Publication of the Federation of American Societies for Experimental Biology*. Apr 2002;16(6):622-624.

58. Kaetzel MA, Dedman JR. Annexin VI regulation of cardiac function. *Biochemical and Biophysical Research Communications*. Oct 1 2004;322(4):1171-1177.
59. Enrich C, Rentero C, de Muga SV, et al. Annexin A6-Linking Ca²⁺ signaling with cholesterol transport. *Biochimica et Biophysica Acta*. May 2011;1813(5):935-947.
60. Diaz-Munoz M, Hamilton SL, Kaetzel MA, Hazarika P, Dedman JR. Modulation of Ca²⁺ release channel activity from sarcoplasmic reticulum by annexin VI (67-kDa calcimedlin). *The Journal of Biological Chemistry*. Sep 15 1990;265(26):15894-15899.
61. Babiychuk EB, Draeger A. Annexins in cell membrane dynamics. Ca²⁺-regulated association of lipid microdomains. *The Journal of Cell Biology*. Sep 4 2000;150(5):1113-1124.
62. Babiychuk EB, Palstra RJ, Schaller J, Kampfer U, Draeger A. Annexin VI participates in the formation of a reversible, membrane-cytoskeleton complex in smooth muscle cells. *The Journal of Biological Chemistry*. Dec 3 1999;274(49):35191-35195.
63. Babiychuk VS, Draeger A, Babiychuk EB. Smooth muscle actomyosin promotes Ca²⁺-dependent interactions between annexin VI and detergent-insoluble glycosphingolipid-enriched membrane domains. *Acta Biochimica Polonica*. 2000;47(3):579-589.
64. Guntjeski-Hamblin AM, Song G, Walsh RA, et al. Annexin VI overexpression targeted to heart alters cardiomyocyte function in transgenic mice. *The American Journal of Physiology*. Mar 1996;270(3 Pt 2):H1091-1100.
65. Hayes MJ, Rescher U, Gerke V, Moss SE. Annexin-actin interactions. *Traffic*. Aug 2004;5(8):571-576.

66. Schulzki HD, Kramer B, Fleischhauer J, Mercola DA, Wollmer A. Calcium-dependent distance changes in binary and ternary complexes of troponin. *European Journal of Biochemistry / FEBS*. May 20 1990;189(3):683-692.
67. Song G, Campos B, Wagoner LE, Dedman JR, Walsh RA. Altered cardiac annexin mRNA and protein levels in the left ventricle of patients with end-stage heart failure. *Journal of Molecular and Cellular Cardiology*. Mar 1998;30(3):443-451.
68. Hazarika P, Kaetzel MA, Sheldon A, et al. Annexin VI is associated with calcium-sequestering organelles. *Journal of Cellular Biochemistry*. May 1991;46(1):78-85.
69. Rossi AE, Dirksen RT. Sarcoplasmic reticulum: the dynamic calcium governor of muscle. *Muscle & Nerve*. Jun 2006;33(6):715-731.
70. Protasi F, Paolini C, Canato M, Reggiani C, Quarta M. Lessons from calsequestrin-1 ablation in vivo: much more than a Ca(2+) buffer after all. *Journal of Muscle Research and Cell Motility*. Dec 2011;32(4-5):257-270.
71. Jiao Q, Bai Y, Akaike T, Takeshima H, Ishikawa Y, Minamisawa S. Sarcalumenin is essential for maintaining cardiac function during endurance exercise training. *American Journal of Physiology. Heart and Circulatory Physiology*. Aug 2009;297(2):H576-582.
72. Kinnunen S, Manttari S. Specific effects of endurance and sprint training on protein expression of calsequestrin and SERCA in mouse skeletal muscle. *Journal of Muscle Research and Cell Motility*. Jun 2012;33(2):123-130.
73. Sugizaki MM, Leopoldo AP, Conde SJ, et al. Upregulation of mRNA myocardium calcium handling in rats submitted to exercise and food restriction. *Arquivos Brasileiros de Cardiologia*. Jul 2011;97(1):46-52.

- 74.** Gelfi C, Vigano A, Ripamonti M, et al. The human muscle proteome in aging. *Journal of Proteome Research*. Jun 2006;5(6):1344-1353.
- 75.** Buensanteai N, Mukherjee PK, Horwitz BA, Cheng C, Dangott LJ, Kenerley CM. Expression and purification of biologically active *Trichoderma virens* proteinaceous elicitor Sm1 in *Pichia pastoris*. *Protein Expression and Purification*. Jul 2010;72(1):131-138.
- 76.** Chaput CD, Dangott LJ, Rahm MD, Hitt KD, Stewart DS, Wayne Sampson H. A proteomic study of protein variation between osteopenic and age-matched control bone tissue. *Experimental Biology and Medicine*. May 1 2012;237(5):491-498.
- 77.** Chiara DC, Dangott LJ, Eckenhoff RG, Cohen JB. Identification of nicotinic acetylcholine receptor amino acids photolabeled by the volatile anesthetic halothane. *Biochemistry*. Nov 25 2003;42(46):13457-13467.
- 78.** Djonovic S, Pozo MJ, Dangott LJ, Howell CR, Kenerley CM. Sm1, a proteinaceous elicitor secreted by the biocontrol fungus *Trichoderma virens* induces plant defense responses and systemic resistance. *Molecular Plant-microbe Interactions : MPMI*. Aug 2006;19(8):838-853.
- 79.** Han BK, Bogomolnaya LM, Totten JM, Blank HM, Dangott LJ, Polymenis M. Bem1p, a scaffold signaling protein, mediates cyclin-dependent control of vacuolar homeostasis in *Saccharomyces cerevisiae*. *Genes & Development*. Nov 1 2005;19(21):2606-2618.
- 80.** Jordan MC, Harrington JR, Cohen ND, et al. Effects of iron modulation on growth and viability of *Rhodococcus equi* and expression of virulence-associated protein A. *American Journal of Veterinary Research*. Nov 2003;64(11):1337-1346.

81. Li J, Dangott LJ, Fitzpatrick PF. Regulation of phenylalanine hydroxylase: conformational changes upon phenylalanine binding detected by hydrogen/deuterium exchange and mass spectrometry. *Biochemistry*. Apr 20 2010;49(15):3327-3335.
82. Lim SM, Trzeciakowski JP, Sreenivasappa H, Dangott LJ, Trache A. RhoA-induced cytoskeletal tension controls adaptive cellular remodeling to mechanical signaling. *Integrative Biology: Quantitative Biosciences from Nano to Macro*. Jun 2012;4(6):615-627.
83. Nability MB, Lees GE, Dangott LJ, Cianciolo R, Suchodolski JS, Steiner JM. Proteomic analysis of urine from male dogs during early stages of tubulointerstitial injury in a canine model of progressive glomerular disease. *Veterinary Clinical Pathology / American Society for Veterinary Clinical Pathology*. Jun 2011;40(2):222-236.
84. Sacharidou A, Cifuentes-Rojas C, Halbig K, et al. RNA editing complex interactions with a site for full-round U deletion in *Trypanosoma brucei*. *Rna*. Jul 2006;12(7):1219-1228.
85. Wang J, Chen L, Li D, et al. Intrauterine growth restriction affects the proteomes of the small intestine, liver, and skeletal muscle in newborn pigs. *The Journal of Nutrition*. Jan 2008;138(1):60-66.
86. Wang J, Li D, Dangott LJ, Wu G. Proteomics and its role in nutrition research. *The Journal of Nutrition*. Jul 2006;136(7):1759-1762.
87. Wang XX, Dangott LJ, Pfenninger KH. The heterogeneous growth cone glycoprotein gp93 is identical to the signal regulatory protein SIRPalpha/SHPS-1/BIT. *Journal of Neurochemistry*. Jul 2003;86(1):55-60.

88. Kromer SA, Kessler MS, Milfay D, et al. Identification of glyoxalase-I as a protein marker in a mouse model of extremes in trait anxiety. *The Journal of Neuroscience : the Official Journal of the Society for Neuroscience*. Apr 27 2005;25(17):4375-4384.
89. Egan B, Dowling P, O'Connor PL, et al. 2-D DIGE analysis of the mitochondrial proteome from human skeletal muscle reveals time course-dependent remodelling in response to 14 consecutive days of endurance exercise training. *Proteomics*. Apr 2011;11(8):1413-1428.
90. Yamaguchi W, Fujimoto E, Higuchi M, Tabata I. A DIGE proteomic analysis for high-intensity exercise-trained rat skeletal muscle. *Journal of Biochemistry*. Sep 2010;148(3):327-333.
91. Diffie GM, Nagle DF. Regional differences in effects of exercise training on contractile and biochemical properties of rat cardiac myocytes. *Journal of Applied Physiology*. Jul 2003;95(1):35-42.
92. Goto S, Nakamura A, Radak Z, et al. Carbonylated proteins in aging and exercise: immunoblot approaches. *Mechanisms of Ageing and Development*. Mar 15 1999;107(3):245-253.
93. Hody S, Leprince P, Sergeant K, et al. Human muscle proteome modifications after acute or repeated eccentric exercises. *Medicine and Science in Sports and Exercise*. Dec 2011;43(12):2281-2296.
94. Wankhade UD, Vella KR, Fox DL, Good DJ. Deletion of Nhlh2 results in a defective torpor response and reduced Beta adrenergic receptor expression in adipose tissue. *PLoS One*. 2010;5(8):e12324.

95. Pistilli EE, Bogdanovich S, Garton F, et al. Loss of IL-15 receptor alpha alters the endurance, fatigability, and metabolic characteristics of mouse fast skeletal muscles. *The Journal of Clinical Investigation*. Aug 2011;121(8):3120-3132.
96. Osokine I, Hsu R, Loeb GB, McManus MT. Unintentional miRNA ablation is a risk factor in gene knockout studies: a short report. *PLoS Genetics*. Feb 2008;4(2):e34.
97. Manzl C, Baumgartner F, Peintner L, Schuler F, Villunger A. Possible pitfalls investigating cell death responses in genetically engineered mouse models and derived cell lines. *Methods*. Feb 27 2013. E Pub Ahead of Print
98. Warfield KL, Panchal RG, Aman MJ, Bavari S. Antisense treatments for biothreat agents. *Current Opinion in Molecular Therapeutics*. Apr 2006;8(2):93-103.
99. Stein DA. Inhibition of RNA virus infections with peptide-conjugated morpholino oligomers. *Current Pharmaceutical Design*. 2008;14(25):2619-2634.
100. Morcos PA, Li Y, Jiang S. Vivo-Morpholinos: a non-peptide transporter delivers Morpholinos into a wide array of mouse tissues. *BioTechniques*. Dec 2008;45(6):613-614, 616, 618 passim.
101. Osorio FG, Navarro CL, Cadinanos J, et al. Splicing-directed therapy in a new mouse model of human accelerated aging. *Science Translational Medicine*. Oct 26 2011;3(106):106ra107.
102. Guo Y, Ma L, Cristofanilli M, Hart RP, Hao A, Schachner M. Transcription factor Sox11b is involved in spinal cord regeneration in adult zebrafish. *Neuroscience*. Jan 13 2011;172:329-341.
103. Kang JK, Malerba A, Popplewell L, Foster K, Dickson G. Antisense-induced myostatin exon skipping leads to muscle hypertrophy in mice following octa-guanidine

- morpholino oligomer treatment. *Molecular therapy : the Journal of the American Society of Gene Therapy*. Jan 2011;19(1):159-164.
- 104.** Kim S, Radhakrishnan UP, Rajpurohit SK, Kulkarni V, Jagadeeswaran P. Vivo-Morpholino knockdown of α IIb: A novel approach to inhibit thrombocyte function in adult zebrafish. *Blood Cells, Molecules & Diseases*. Mar 15 2010;44(3):169-174.
- 105.** Kizil C, Brand M. Cerebroventricular microinjection (CVMI) into adult zebrafish brain is an efficient misexpression method for forebrain ventricular cells. *PLoS One*. 2011;6(11):e27395.
- 106.** Kowalik L, Hudspeth AJ. A search for factors specifying tonotopy implicates DNER in hair-cell development in the chick's cochlea. *Developmental Biology*. Jun 15 2011;354(2):221-231.
- 107.** Liu Y, Yu H, Deaton SK, Szaro BG. Heterogeneous nuclear ribonucleoprotein K, an RNA-binding protein, is required for optic axon regeneration in *Xenopus laevis*. *The Journal of Neuroscience : the Official Journal of the Society for Neuroscience*. Mar 7 2012;32(10):3563-3574.
- 108.** Maki N, Suetsugu-Maki R, Sano S, et al. Oocyte-type linker histone B4 is required for transdifferentiation of somatic cells in vivo. *FASEB Journal : Official Publication of the Federation of American Societies for Experimental Biology*. Sep 2010;24(9):3462-3467.
- 109.** Matsuda H, Shi YB. An essential and evolutionarily conserved role of protein arginine methyltransferase 1 for adult intestinal stem cells during postembryonic development. *Stem Cells*. Nov 2010;28(11):2073-2083.

110. Nazmi A, Dutta K, Basu A. Antiviral and neuroprotective role of octaguanidinium dendrimer-conjugated morpholino oligomers in Japanese encephalitis. *PLoS Neglected Tropical Diseases*. 2010;4(11):e892.
111. Nazmi A, Mukhopadhyay R, Dutta K, Basu A. STING Mediates Neuronal Innate Immune Response Following Japanese Encephalitis Virus Infection. *Scientific Reports*. 2012;2:347.
112. Owen LA, Uehara H, Cahoon J, Huang W, Simonis J, Ambati BK. Morpholino-mediated increase in soluble Flt-1 expression results in decreased ocular and tumor neovascularization. *PloS One*. 2012;7(3):e33576.
113. Parra MK, Gallagher TL, Amacher SL, Mohandas N, Conboy JG. Deep intron elements mediate nested splicing events at consecutive AG dinucleotides to regulate alternative 3' splice site choice in vertebrate 4.1 genes. *Molecular and Cellular Biology*. Jun 2012;32(11):2044-2053.
114. Parra MK, Gee S, Mohandas N, Conboy JG. Efficient in vivo manipulation of alternative pre-mRNA splicing events using antisense morpholinos in mice. *The Journal of Biological Chemistry*. Feb 25 2011;286(8):6033-6039.
115. Quinn M, Ueno Y, Pae HY, et al. Suppression of the HPA axis during extrahepatic biliary obstruction induces cholangiocyte proliferation in the rat. *American Journal of Physiology. Gastrointestinal and Liver Physiology*. Jan 1 2012;302(1):G182-193.
116. Reissner KJ, Sartor GC, Vazey EM, Dunn TE, Aston-Jones G, Kalivas PW. Use of vivo-morpholinos for control of protein expression in the adult rat brain. *Journal of Neuroscience Methods*. Jan 30 2012;203(2):354-360.

117. Sartor GC, Aston-Jones GS. A septal-hypothalamic pathway drives orexin neurons, which is necessary for conditioned cocaine preference. *The Journal of Neuroscience : the Official Journal of the Society for Neuroscience*. Mar 28 2012;32(13):4623-4631.
118. Shi YB, Hasebe T, Fu L, Fujimoto K, Ishizuya-Oka A. The development of the adult intestinal stem cells: Insights from studies on thyroid hormone-dependent amphibian metamorphosis. *Cell & Bioscience*. 2011;1(1):30.
119. Taniguchi-Ikeda M, Kobayashi K, Kanagawa M, et al. Pathogenic exon-trapping by SVA retrotransposon and rescue in Fukuyama muscular dystrophy. *Nature*. Oct 6 2011;478(7367):127-131.
120. Tsonis PA, Haynes T, Maki N, et al. Controlling gene loss of function in newts with emphasis on lens regeneration. *Nature Protocols*. May 2011;6(5):593-599.
121. Vera T, Stec DE. Moderate hyperbilirubinemia improves renal hemodynamics in ANG II-dependent hypertension. *American journal of physiology. Regulatory, Integrative and Comparative Physiology*. Oct 2010;299(4):R1044-1049.
122. Widrick JJ, Jiang S, Choi SJ, Knuth ST, Morcos PA. An octaguanidine-morpholino oligo conjugate improves muscle function of mdx mice. *Muscle & Nerve*. Oct 2011;44(4):563-570.
123. Wu B, Benrashid E, Lu P, et al. Targeted skipping of human dystrophin exons in transgenic mouse model systemically for antisense drug development. *PLoS One*. 2011;6(5):e19906.
124. Wu B, Li Y, Morcos PA, Doran TJ, Lu P, Lu QL. Octa-guanidine morpholino restores dystrophin expression in cardiac and skeletal muscles and ameliorates pathology in

- dystrophic mdx mice. *Molecular Therapy : The Journal of the American Society of Gene Therapy*. May 2009;17(5):864-871.
- 125.** Zammarchi F, de Stanchina E, Bournazou E, et al. Antitumorigenic potential of STAT3 alternative splicing modulation. *Proceedings of the National Academy of Sciences of the United States of America*. Oct 25 2011;108(43):17779-17784.
- 126.** Azoitei N, Pusapati GV, Kleger A, et al. Protein kinase D2 is a crucial regulator of tumour cell-endothelial cell communication in gastrointestinal tumours. *Gut*. Oct 2010;59(10):1316-1330.
- 127.** Wu B, Lu P, Benrashid E, et al. Dose-dependent restoration of dystrophin expression in cardiac muscle of dystrophic mice by systemically delivered morpholino. *Gene Therapy*. Jan 2010;17(1):132-140.
- 128.** Emerich DF, Dean RL, Osborn C, Bartus RT. The development of the bradykinin agonist labradimil as a means to increase the permeability of the blood-brain barrier: from concept to clinical evaluation. *Clinical Pharmacokinetics*. 2001;40(2):105-123.
- 129.** Boger HA, Mannangatti P, Samuvel DJ, et al. Effects of brain-derived neurotrophic factor on dopaminergic function and motor behavior during aging. *Genes, Brain, and Behavior*. Mar 2011;10(2):186-198.
- 130.** Egana LA, Cuevas RA, Baust TB, et al. Physical and functional interaction between the dopamine transporter and the synaptic vesicle protein synaptogyrin-3. *The Journal of Neuroscience : the Official Journal of the Society for Neuroscience*. Apr 8 2009;29(14):4592-4604.
- 131.** Russell VA, Sagvolden T, Johansen EB. Animal models of attention-deficit hyperactivity disorder. *Behavioral and Brain Functions : BBF*. Jul 15 2005;1:9.

- 132.** Bienso RS, Ringholm S, Kiilerich K, et al. GLUT4 and glycogen synthase are key players in bed rest-induced insulin resistance. *Diabetes*. May 2012;61(5):1090-1099.
- 133.** Ferguson DP, Schmitte EE, Lightfoot JT. The Effect of Vivo-morpholinos on Dopamine Receptor 1 (*Drd1*) and Physical Activity in mice. *Abstract Presentation at Experimental Biology, Washington DC*. 2011.
- 134.** Doctrow SR, Abelleira SM, Curry LA, et al. The bradykinin analog RMP-7 increases intracellular free calcium levels in rat brain microvascular endothelial cells. *The Journal of Pharmacology and Experimental Therapeutics*. Oct 1994;271(1):229-237.
- 135.** Zhou Z, Kim J, Insolera R, Peng X, Fink DJ, Mata M. Rho GTPase regulation of alpha-synuclein and VMAT2: implications for pathogenesis of Parkinson's disease. *Molecular and Cellular Neurosciences*. Sep 2011;48(1):29-37.
- 136.** Notch EG, Shaw JR, Coutermarsh BA, Dzioba M, Stanton BA. Morpholino gene knockdown in adult *Fundulus heteroclitus*: role of SGK1 in seawater acclimation. *PLoS One*. 2011;6(12):e29462.
- 137.** Colebrooke RE, Humby T, Lynch PJ, McGowan DP, Xia J, Emson PC. Age-related decline in striatal dopamine content and motor performance occurs in the absence of nigral cell loss in a genetic mouse model of Parkinson's disease. *The European Journal of Neuroscience*. Nov 2006;24(9):2622-2630.
- 138.** Mason SS, Baker KB, Davis KW, et al. Differential sensitivity to SSRI and tricyclic antidepressants in juvenile and adult mice of three strains. *European Journal of Pharmacology*. Jan 14 2009;602(2-3):306-315.
- 139.** Xiong N, Xiong J, Khare G, et al. Edaravone guards dopamine neurons in a rotenone model for Parkinson's disease. *PLoS One*. 2011;6(6):e20677.

140. Colebrooke RE, Chan PM, Lynch PJ, Mooslehner K, Emson PC. Differential gene expression in the striatum of mice with very low expression of the vesicular monoamine transporter type 2 gene. *Brain Research*. Jun 4 2007;1152:10-16.
141. Biolo G, Maggi SP, Williams BD, Tipton KD, Wolfe RR. Increased rates of muscle protein turnover and amino acid transport after resistance exercise in humans. *The American Journal of Physiology*. Mar 1995;268(3 Pt 1):E514-520.
142. Guillot TS, Richardson JR, Wang MZ, et al. PACAP38 increases vesicular monoamine transporter 2 (VMAT2) expression and attenuates methamphetamine toxicity. *Neuropeptides*. Aug 2008;42(4):423-434.
143. Fueger PT, Li CY, Ayala JE, et al. Glucose kinetics and exercise tolerance in mice lacking the GLUT4 glucose transporter. *The Journal of Physiology*. Jul 15 2007;582(Pt 2):801-812.
144. Wasserman DH, Kang L, Ayala JE, Fueger PT, Lee-Young RS. The physiological regulation of glucose flux into muscle in vivo. *The Journal of Experimental Biology*. Jan 15 2011;214(Pt 2):254-262.
145. Fukushima S, Shen H, Hata H, et al. Methamphetamine-induced locomotor activity and sensitization in dopamine transporter and vesicular monoamine transporter 2 double mutant mice. *Psychopharmacology*. Jul 2007;193(1):55-62.
146. Hood DA. Invited Review: contractile activity-induced mitochondrial biogenesis in skeletal muscle. *Journal of Applied Physiology*. Mar 2001;90(3):1137-1157.
147. Jonas I, Vaanholt LM, Doornbos M, et al. Effects of selective breeding for increased wheel-running behavior on circadian timing of substrate oxidation and ingestive behavior. *Physiology & Behavior*. Apr 19 2010;99(5):549-554.

148. DiPetrillo K, Wang X, Stylianou IM, Paigen B. Bioinformatics toolbox for narrowing rodent quantitative trait loci. *Trends in Genetics : TIG*. Dec 2005;21(12):683-692.
149. Flint J, Valdar W, Shifman S, Mott R. Strategies for mapping and cloning quantitative trait genes in rodents. *Nature reviews. Genetics*. Apr 2005;6(4):271-286.
150. Ferguson D, Schmitt E, Liightfoot J. Vivo-Morpholinos Induced Transient Knockdown of Physical Activity Related Proteins. *PLoS One*. 2013;8(4).
151. Pistilli EE, Siu PM, Alway SE. Interleukin-15 responses to aging and unloading-induced skeletal muscle atrophy. *American Journal of Physiology. Cell physiology*. Apr 2007;292(4):C1298-1304.
152. Knab AM, Bowen RS, Moore-Harrison T, Hamilton AT, Turner MJ, Lightfoot JT. Repeatability of exercise behaviors in mice. *Physiology & Behavior*. Oct 19 2009;98(4):433-440.
153. Czarkowska-Paczek B, Zenzian-Piotrowska M, Bartłomiejczyk I, Przybylski J, Gorski J. The effect of acute and prolonged endurance exercise on transforming growth factor-beta1 generation in rat skeletal and heart muscle. *Journal of Physiology and Pharmacology : an Official Journal of the Polish Physiological Society*. Dec 2009;60(4):157-162.
154. Barclay CJ, Constable JK, Gibbs CL. Energetics of fast- and slow-twitch muscles of the mouse. *The Journal of Physiology*. Dec 1993;472:61-80.
155. Karp NA, Lilley KS. Maximising sensitivity for detecting changes in protein expression: experimental design using minimal CyDyes. *Proteomics*. Aug 2005;5(12):3105-3115.

- 156.** Karp NA, McCormick PS, Russell MR, Lilley KS. Experimental and statistical considerations to avoid false conclusions in proteomics studies using differential in-gel electrophoresis. *Molecular & Cellular Proteomics : MCP*. Aug 2007;6(8):1354-1364.
- 157.** Szklarczyk D, Franceschini A, Kuhn M, et al. The STRING database in 2011: functional interaction networks of proteins, globally integrated and scored. *Nucleic Acids Research*. Jan 2011;39(Database issue):D561-568.
- 158.** Rubenstein RC, Lockwood SR, Lide E, Bauer R, Suaud L, Grumbach Y. Regulation of endogenous ENaC functional expression by CFTR and DeltaF508-CFTR in airway epithelial cells. *American Journal of Physiology. Lung Cellular and Molecular Physiology*. Jan 2011;300(1):L88-L101.
- 159.** Gorzek JF, Hendrickson KC, Forstner JP, Rixen JL, Moran AL, Lowe DA. Estradiol and tamoxifen reverse ovariectomy-induced physical inactivity in mice. *Medicine and Science in Sports and Exercise*. Feb 2007;39(2):248-256.
- 160.** Dubreucq S, Durand A, Matias I, et al. Ventral Tegmental Area Cannabinoid Type-1 Receptors Control Voluntary Exercise Performance. *Biological Psychiatry*. Dec 10 2012.
- 161.** Barrientos G, Hidalgo C. Annexin VI is attached to transverse-tubule membranes in isolated skeletal muscle triads. *The Journal of Membrane Biology*. Jul 15 2002;188(2):163-173.
- 162.** James RS, Walter I, Seebacher F. Variation in expression of calcium-handling proteins is associated with inter-individual differences in mechanical performance of rat (*Rattus norvegicus*) skeletal muscle. *The Journal of Experimental Biology*. Nov 1 2011;214(Pt 21):3542-3548.

- 163.** MacIntosh BR, Holash RJ, Renaud JM. Skeletal muscle fatigue--regulation of excitation-contraction coupling to avoid metabolic catastrophe. *Journal of Cell Science*. May 1 2012;125(Pt 9):2105-2114.
- 164.** Summermatter S, Thurnheer R, Santos G, et al. Remodeling of calcium handling in skeletal muscle through PGC-1alpha: impact on force, fatigability, and fiber type. *American Journal of Physiology. Cell physiology*. Jan 1 2012;302(1):C88-99.
- 165.** Rouviere C, Corona BT, Ingalls CP. Oxidative capacity and fatigability in run-trained malignant hyperthermia-susceptible mice. *Muscle & Nerve*. Apr 2012;45(4):586-596.
- 166.** Chanat E, Martin P, Ollivier-Bousquet M. Alpha(S1)-casein is required for the efficient transport of beta- and kappa-casein from the endoplasmic reticulum to the Golgi apparatus of mammary epithelial cells. *Journal of Cell Science*. Oct 1999;112 (Pt 19):3399-3412.
- 167.** Horecker BL. The biochemistry of sugars. *Internationale Zeitschrift fur Vitamin- und Ernährungsforschung. Beiheft*. 1976;15:1-21.
- 168.** Tylicki A, Bunik VI, Strumilo S. [2-Oxoglutarate dehydrogenase complex and its multipoint control]. *Postepy Biochemii*. 2011;57(3):304-313.
- 169.** Zhang H, Wang Y, Li J, et al. Proteome of skeletal muscle lipid droplet reveals association with mitochondria and apolipoprotein a-I. *Journal of Proteome Research*. Oct 7 2011;10(10):4757-4768.
- 170.** Hue L, Rider MH. Role of fructose 2,6-bisphosphate in the control of glycolysis in mammalian tissues. *The Biochemical Journal*. Jul 15 1987;245(2):313-324.

171. Yagi T, Seo BB, Di Bernardo S, Nakamaru-Ogiso E, Kao MC, Matsuno-Yagi A. NADH dehydrogenases: from basic science to biomedicine. *Journal of Bioenergetics and Biomembranes*. Jun 2001;33(3):233-242.
172. Ivetic A, Ridley AJ. Ezrin/radixin/moesin proteins and Rho GTPase signalling in leucocytes. *Immunology*. Jun 2004;112(2):165-176.
173. Howard J. The movement of kinesin along microtubules. *Annual Review of Physiology*. 1996;58:703-729.
174. Tischfield MA, Engle EC. Distinct alpha- and beta-tubulin isotypes are required for the positioning, differentiation and survival of neurons: new support for the 'multi-tubulin' hypothesis. *Bioscience Reports*. Oct 2010;30(5):319-330.
175. Lek M, Quinlan KG, North KN. The evolution of skeletal muscle performance: gene duplication and divergence of human sarcomeric alpha-actinins. *BioEssays : News and Reviews in Molecular, Cellular and Developmental Biology*. Jan 2010;32(1):17-25.
176. Peng X, Nelson ES, Maiers JL, DeMali KA. New insights into vinculin function and regulation. *International Review of Cell and Molecular Biology*. 2011;287:191-231.
177. National Institute for Occupational Safety and Health., Tracor Jitco Inc., Advanced Engineering & Planning Corp. Registry of toxic effects of chemical substances. 1977-19 : *DHEW Publication No (NIOSH)*. Microfiche ed. Cincinnati, Ohio Washington, D.C.: U.S. Dept. of Health, Education, and Welfare, Public Health Service, Center for Disease Control Supt. of Docs., U.S. G.P.O.:microfiches.
178. Fagerquist CK, Garbus BR, Williams KE, Bates AH, Harden LA. Covalent attachment and dissociative loss of sinapinic acid to/from cysteine-containing proteins from bacterial

- cell lysates analyzed by MALDI-TOF-TOF mass spectrometry. *Journal of the American Society for Mass Spectrometry*. May 2010;21(5):819-832.
- 179.** Tande B, Wagner N, Youg H. Influence of End Groups on Dendrimer Rheology and Conformation. *Macromolecules* 2003;36(12):4619-4623.
- 180.** Gordon RJ, Snyder GK, Tritel H, Taylor WJ. Potential significance of plasma viscosity and hematocrit variations in myocardial ischemia. *American Heart Journal*. Feb 1974;87(2):175-182.
- 181.** Roberts JC, Bhalgat MK, Zera RT. Preliminary biological evaluation of polyamidoamine (PAMAM) Starburst dendrimers. *Journal of Biomedical Materials Research*. Jan 1996;30(1):53-65.
- 182.** Klajnert B, Bryszewska M. Dendrimers: properties and applications. *Acta Biochimica Polonica*. 2001;48(1):199-208.
- 183.** Nehrenberg DL, Hua K, Estrada-Smith D, Garland T, Jr., Pomp D. Voluntary exercise and its effects on body composition depend on genetic selection history. *Obesity*. Jul 2009;17(7):1402-1409.

APPENDIX A:

FIGURES

II *Vivo*-morpholinos induced transient knockdown of physical activity related proteins

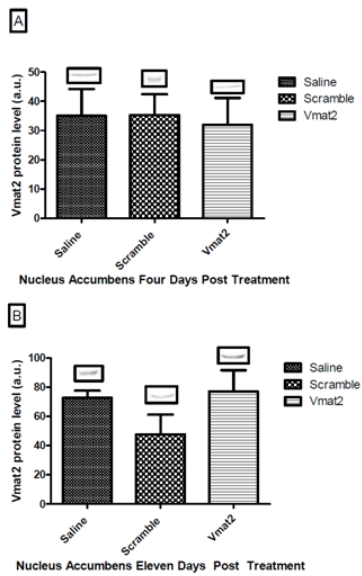


Figure 2.1: Experiment 1, Vmat2 protein level in the nucleus accumbens.

Mean \pm standard deviation of western blot optical band density and a representative western blot comparing Saline, Scramble, and *Vivo*-morpholino treated animals for Vmat2 protein expression in the nucleus accumbens of the brain. There was no difference between the treatment groups at four ($p=0.87$, Panel A) or eleven ($p=0.14$, Panel B) days post treatment.

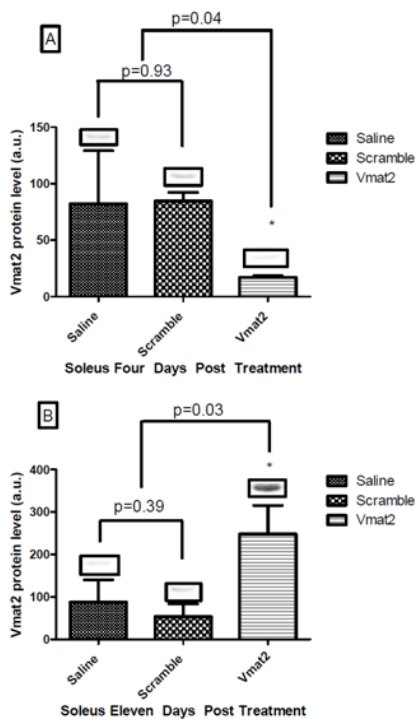


Figure 2.2: Experiment 1, Vmat2 protein level in the soleus.

Mean \pm standard deviation of western blot optical band density and a representative western blot comparing Saline, Scramble, and Vivo-morpholino treated animals for Vmat2 protein expression in the soleus. Panel A shows Vmat2 expression at four days post-last injection. There was a significant decrease ($p=0.04$) in Vivo-morpholino treated animals compared to Saline and Scramble treated animals in Vmat2 expression at four days post injection. Panel B shows Vmat2 expression at eleven days post-last injection. There was a significant increase ($p=0.03$) in Vivo-morpholino treated animals compared to Saline and Scramble treated animals in Vmat2 expression at eleven days post injection.

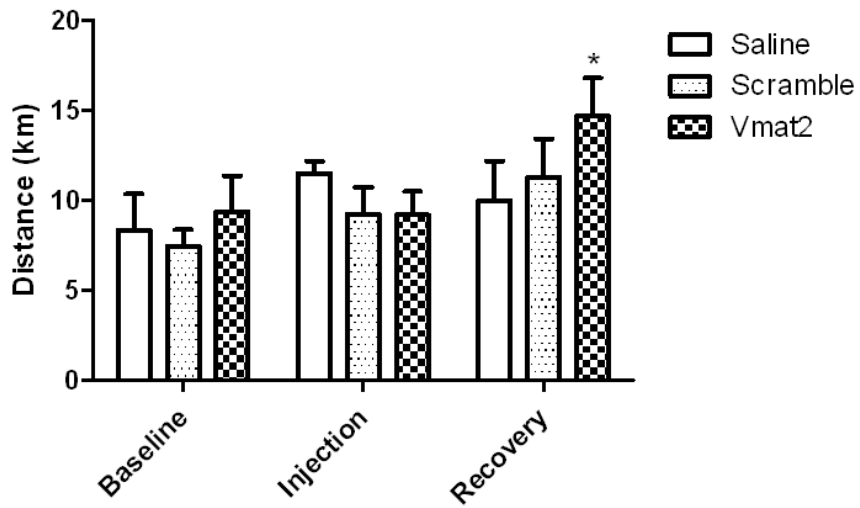


Figure 2.3: Experiment 1, mouse wheel running.

Average daily distance ran for the baseline, injection, and recovery week for animals treated with saline, Vivo-morpholino vehicle only (scramble) and the Vivo-morpholino targeting *Vmat2* (*Vmat2*). *Vmat2* group significantly (* $p=0.001$) increased activity in the recovery week compared to the baseline and injection week. There was no difference in physical activity ($p>0.05$) in the scramble or saline treated animals for baseline, injection, and recovery weeks.

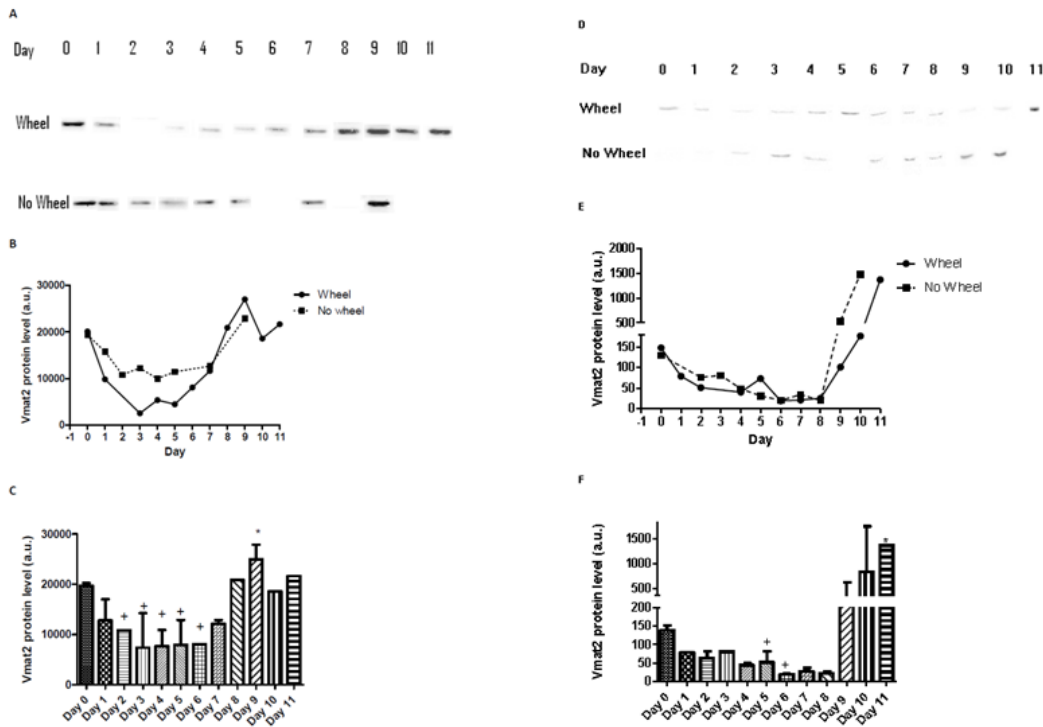


Figure 2.4: Experiment 2, Evaluation of the washout time course of Vivo-morpholinos targeting *Vmat2*.

Panels A, B, and C represent soleus samples while panels D, E, and F represent nucleus accumbens samples. Panel A represents western blot data probing for *Vmat2* in the soleus for both unlocked wheel and locked wheel groups. Panel B is the optical density of the individual western blot bands from panel A. A nonlinear regression was run on the data in panel B which generated an $R^2=0.65$ for the animals on unlocked wheels and an $R^2=0.55$ for animals on locked wheels. Given there was no difference ($p=0.42$) in the slope or y intercept of the unlocked wheel and locked wheel groups, the data were pooled at each Day (Panel C). Panel C shows that there was a significant knockdown ($^+p=0.001$) in *Vmat2* on days 2-6 and a significant ($*p=0.001$) over expression in *Vmat2* on day 9 in the soleus. The same methodologies were applied to Panels D, E, and F for the nucleus accumbens. The nonlinear regression resulted in $R^2=0.99$ for the unlocked wheel group and $R^2=0.99$ for the locked wheel group, and there was no difference ($p=0.66$) in the slope and y intercepts of the lines in panel E. Additionally *Vmat2* was only significantly knocked down on Days 5 and 6 ($^+p=0.001$) with a significant over expression ($*p=0.001$) on Day 11. The mouse in the locked wheel group representing data for Day 11 was removed from analysis because it developed malocclusion in the front incisors and became malnourished, thus altering physical activity level.

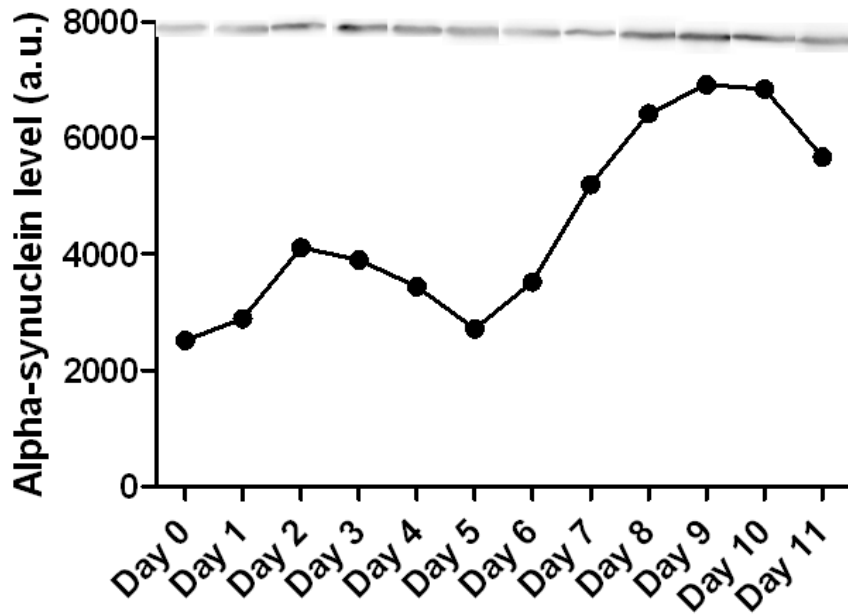


Figure 2.5: Experiment 2, α -synuclein protein level in nucleus accumbens.

Western blot analysis probing for α -synuclein to confirm the signal for the over expression of Vmat2 protein seen in the nucleus accumbens. There was an increase in α -synuclein at days 2 and 7-10. α -synuclein is an indicator of Vmat2 transcription thus when Vmat2 was knocked down by the Vivo-morpholino there was an increased stimulus placed on the cell to transcribe more Vmat2.

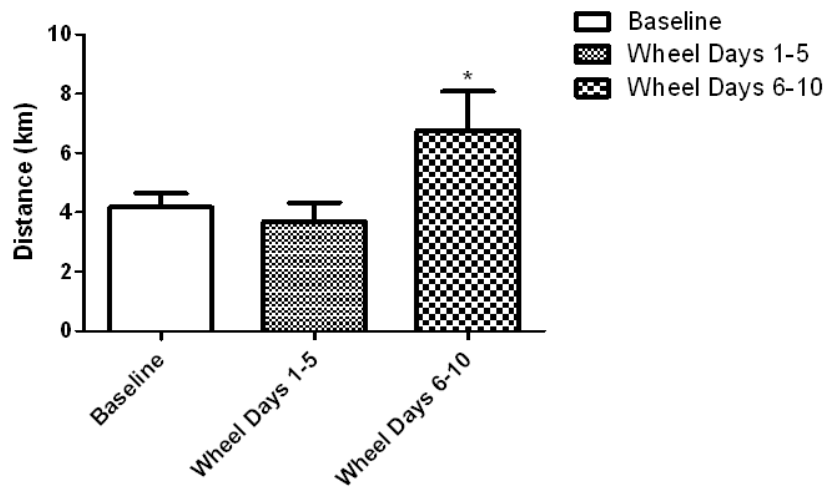


Figure 2.6: Experiment 2, mouse wheel running.

Average daily distance ran for animals treated with Vivo-morpholino targeting *Vmat2* for the baseline week, injection week (Days 1-5), and recovery week (Days 6-10) of washout protocol. Physical activity was significantly (* $p=0.0016$) increased in Days 6-10.

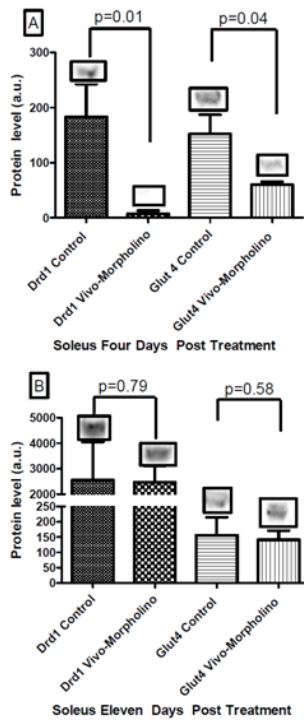


Figure 2.7: Experiment 3, Drd1 and Glut4 protein level.

Western blot and mean \pm standard deviation of optical densities of soleus tissue that underwent the Vivo-morpholino cocktail treatment. Panel A represents four days post treatment of Drd1 and Glut4 expression comparing controls to Vivo-morpholino cocktail treated animals. There was a significant knockdown for both Drd1 ($p=0.01$) and Glut4 ($p=0.04$). Panel B represents eleven days post treatment of Vivo-morpholino cocktail. There was no difference between control and Drd1 ($p=0.79$) and Glut4 ($p=0.58$) expression.

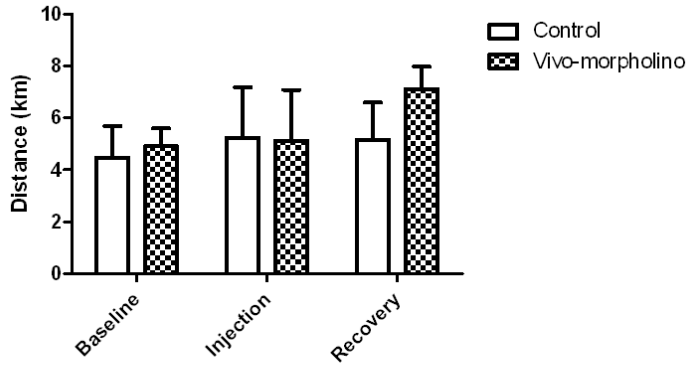


Figure 2.8: Experiment 3, mouse wheel running.

Average daily distance ran for baseline, injection, and recovery week for animals treated saline (control) and the morpholino cocktail targeting *Drd1* and *Glut4* (Vivo-morpholino). There was no difference ($p=0.15$) between the activity of the control group and the morpholino group.

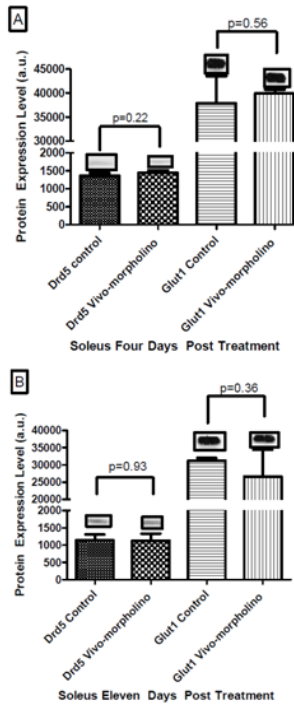


Figure 2.9: Experiment 3, Drd5 and Glut1 protein level.

Western blot and mean \pm standard deviation of optical densities of soleus tissue that underwent the Vivo-morpholino cocktail treatment. Panel A represents four days post treatment of Drd5 and Glut1 protein expression comparing controls to Vivo-morpholino cocktail treated animals. There was not a significant knockdown for either Drd5 ($p=0.22$) or Glut1 ($p=0.56$). Panel B represents eleven days post treatment of Vivo-morpholino cocktail. There was no difference between control and Drd5 ($p=0.93$) and Glut1 ($p=0.36$) expression.

III The Differential Skeletal Muscle Proteome in High and Low Active mice

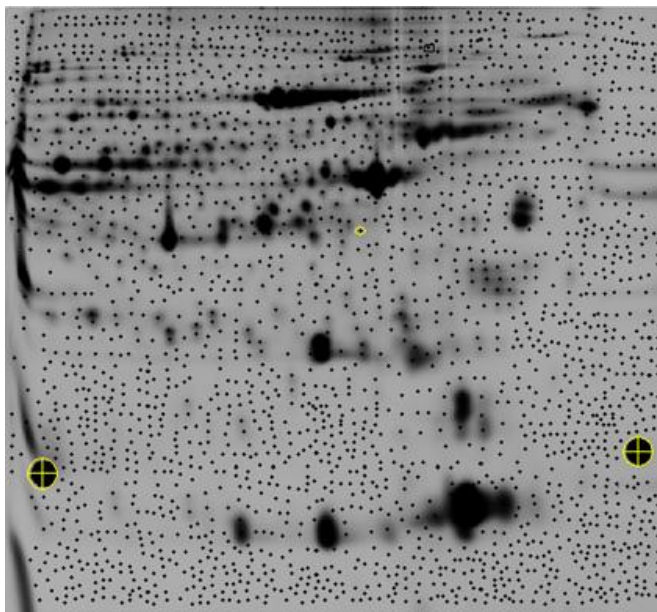


Figure 3.1: Representative 2D gel of soleus skeletal muscle (chosen as the “pick” gel by DeCyder)

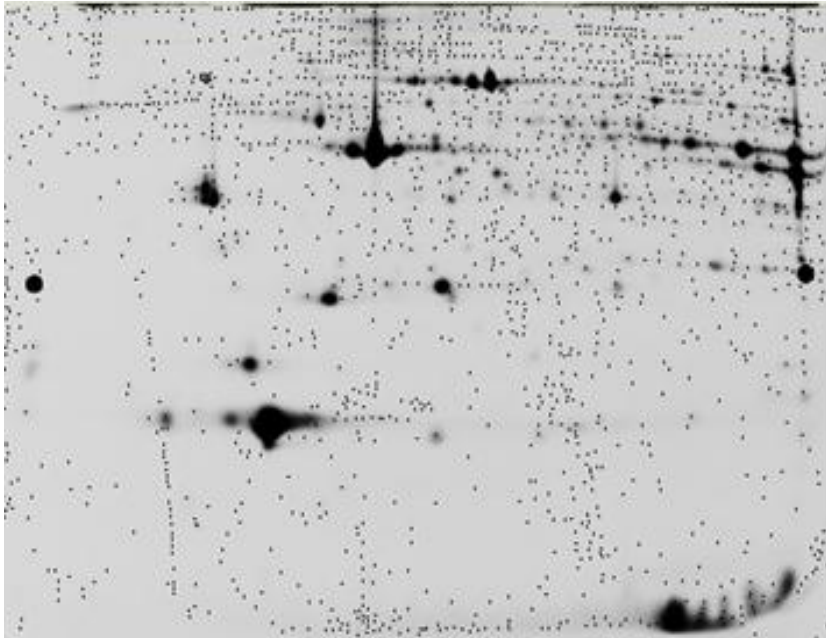


Figure 3.2: Representative 2D gel of extensor digitorum longus (EDL) skeletal muscle (chosen as the “pick” gel by DeCyder)

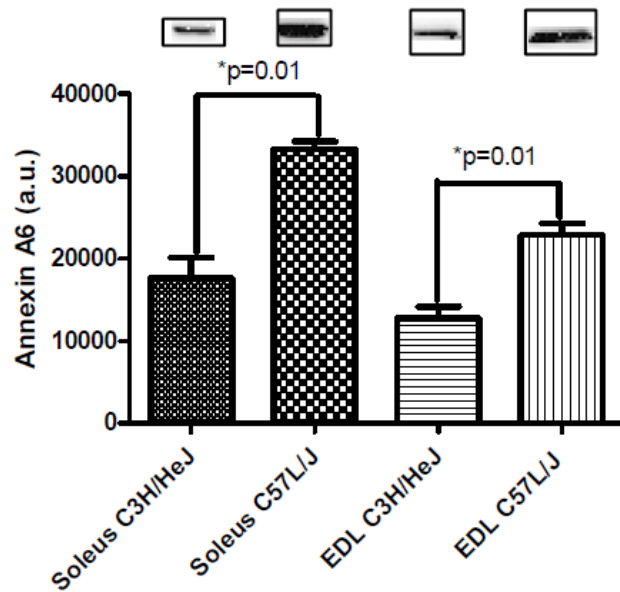


Figure 3.3: Mean \pm standard deviation of confirmatory western blots for Annexin A6 in high active (C57L/J) mice and low active (C3H/HeJ) mice for soleus and EDL tissue. The optical density of the blot is represented as mean \pm standard deviation along with a representative blot. The high active animals significantly ($p=0.01$) over expressed Annexin A6 in the soleus and EDL.

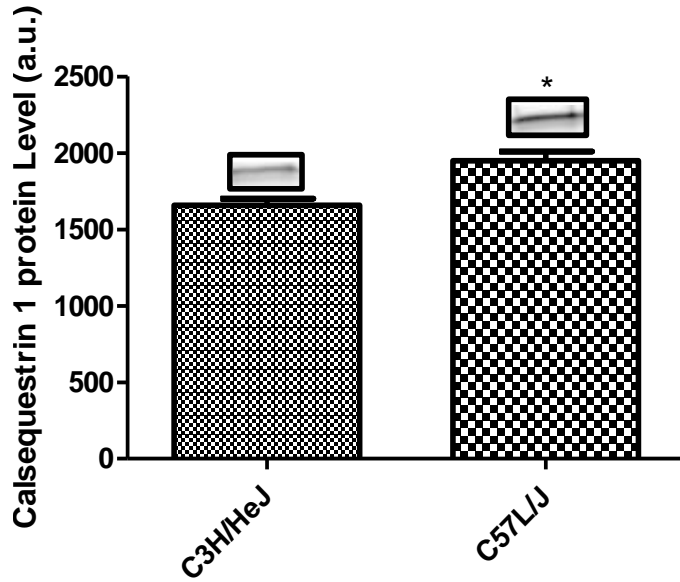
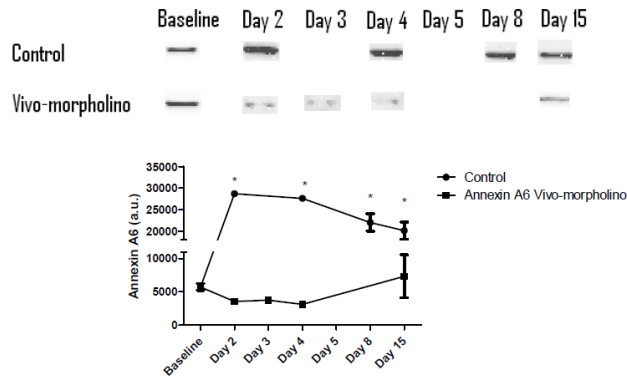


Figure 3.4: Mean \pm standard deviation confirmatory western blots for Calsequestrin 1 in high active (C57L/J) mice and low active (C3H/HeJ) mice. The optical density of the blot is represented as mean \pm standard deviation along with a representative blot. The high active animals significantly ($p=0.0024$) over expressed Calsequestrin 1 in the soleus.

A



B

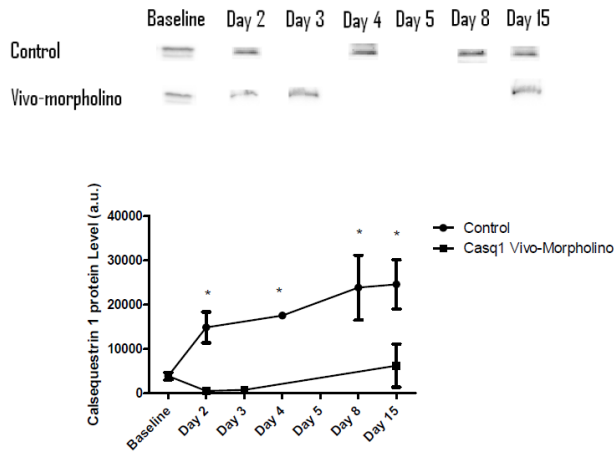


Figure 3.5: Panel A: Mean \pm standard deviation. Western blot data and a representative western blot image for Annexin A6 expression in the soleus for control and Annexin A6 Vivo-morpholino treated animals. There was a significant ($*p=0.0048$) decrease from baseline in the Annexin A6 protein expression in the Vivo-morpholino group and an increase in Annexin A6 protein expression in the control group from baseline. Panel B: Western blot data and a representative western blot image for Calsequestrin 1 expression in the soleus for control and Calsequestrin 1 Vivo-morpholino treated animals. There was a significant ($*p=0.0152$) decrease from baseline in the Calsequestrin 1 protein expression in the Vivo-morpholino group and an increase in Calsequestrin 1 protein expression in the control group from baseline.

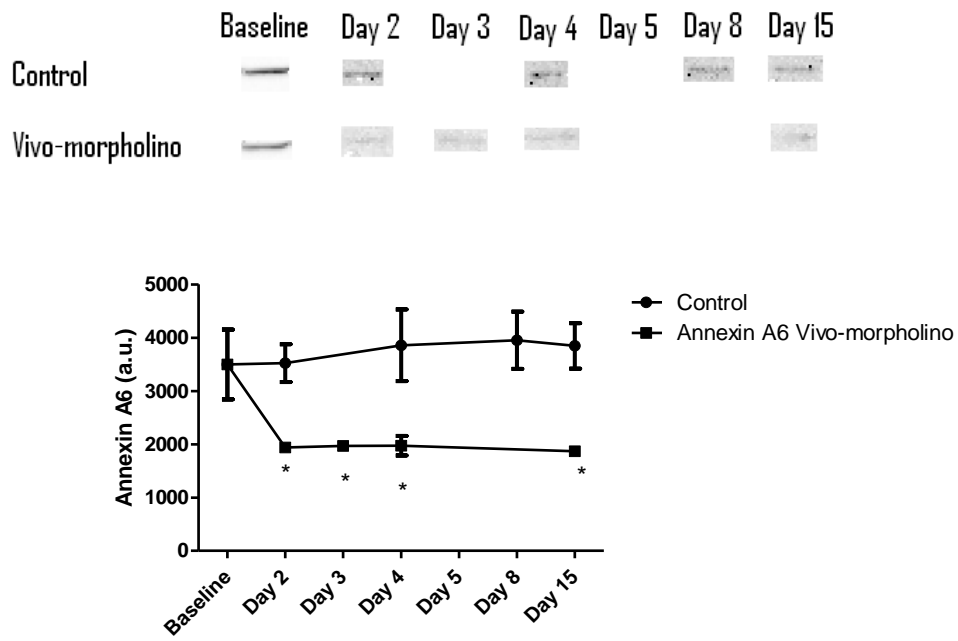


Figure 3.6: Mean \pm standard deviation. Western blot data and a representative western blot images for Annexin A6 expression in the EDL for control and Calsequestrin 1 Vivo-morpholino treated animals. There was a significant ($p=0.0019$) decrease from baseline in the Annexin A6 protein expression in the Vivo-morpholino group.

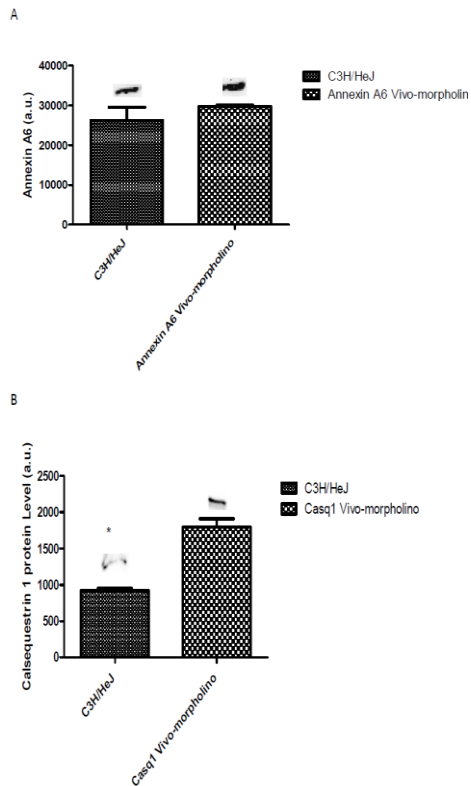


Figure 3.7: Panel A: Mean \pm standard deviation. Western blot data and a representative western blot image for Annexin A6 expression in the soleus of C3H/HeJ mice and Annexin A6 Vivo-morpholino treated animals on Day 3 of treatment. There was no difference in Annexin A6 protein expression ($p=0.14$). Panel B: Western blot data and a representative western blot image for Calsequestrin 1 expression in the soleus of C3H/HeJ mice and Calsequestrin 1 Vivo-morpholino treated animals on Day 3 of treatment. C3H/HeJ mice had significantly ($^*p=0.002$) less Calsequestrin 1 than Vivo-morpholino treated animals.

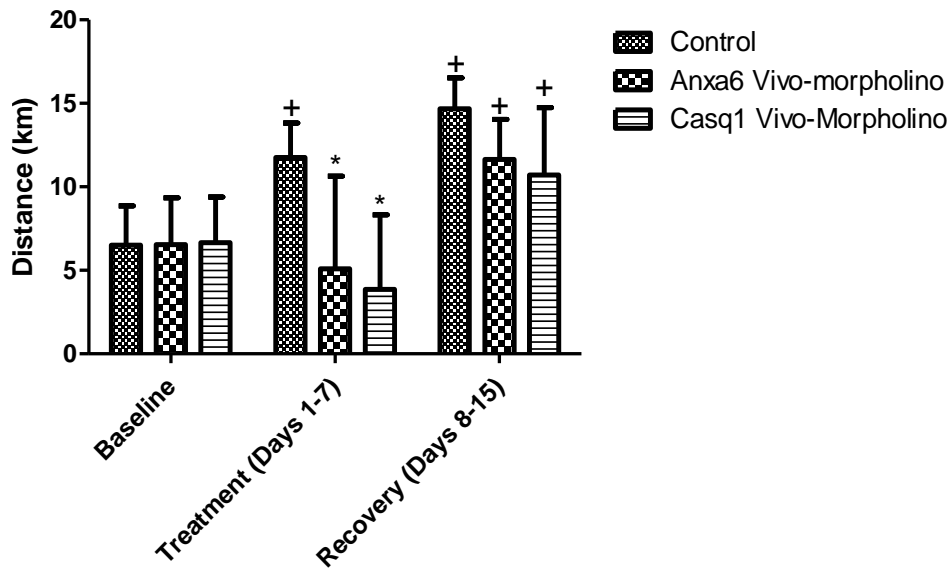


Figure 3.8: Mean \pm standard deviation. Physical activity responses (Average km ran per day) of C57L/J mice receiving Vivo-morpholino treatment knocking down Annexin A6 or Calsequestrin 1. There was a significant decrease ($*p=0.001$) in activity for the Annexin A6 and Calsequestrin 1 Vivo-morpholino treated animals. Additionally there was a significant ($^+p=0.01$) increase in activity in the control group during the treatment week and all groups in the recovery week as compared to baseline.

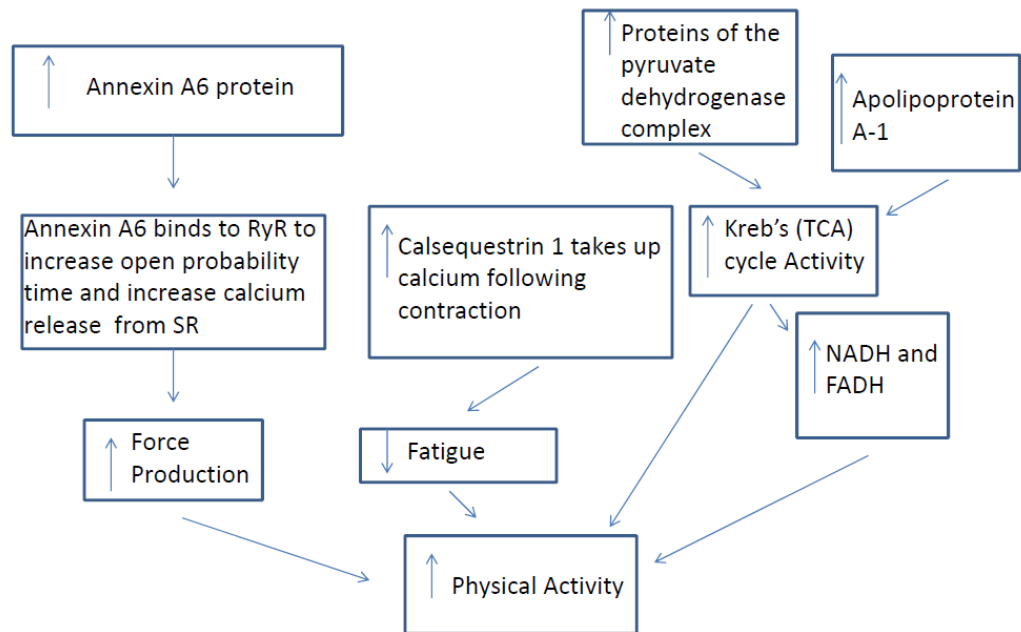


Figure 3.9: Proposed schema of peripheral skeletal muscle protein mechanisms increasing capability for physical activity in high-active animals. 1: As calcium levels rise during EC coupling Annexin A6 binds to the RyR increasing the open probability time, thereby releasing more calcium. 2: Calcium binds to troponin C allowing for actin myosin cross bridge formation. The higher concentration of calcium results in high force production and fatigability. 3: Energy in the form of ATP is generated by the Kreb's (TCA) cycle and Electron Transport Chain (ETC). A higher amount of proteins in the pyruvate dehydrogenase complex leads to high Acetyl CoA levels which results in more turns of the Kreb's (TCA) cycle. 4: This leads to more NADH and FADH, which yields more ATP from the ETC chain. 5: Following contraction there is elevated calcium in the myoplasm, which causes fatigue. 6: Increased levels of calsequestrin 1 bind free calcium and store it in the sarcoplasmic reticulum, thereby reducing fatigability. The combination of increased forced production, increased substrate availability by the Kreb's (TCA) cycle, and decreased fatigue leads to increased physical activity.

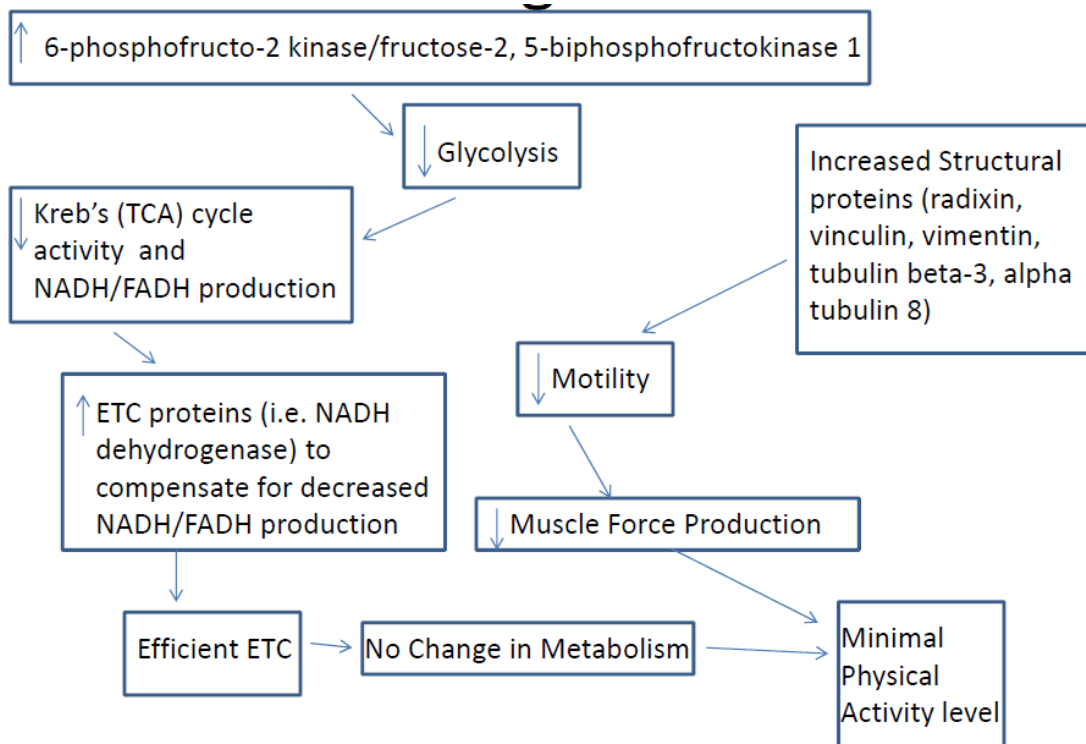


Figure 3.10: Proposed schema of peripheral skeletal muscle protein mechanisms reducing capability for physical activity in low-active animals. 1: With a decrease in Krebs's (TCA) cycle proteins, there is a decrease in NADH and FADH production, which in turn decrease ATP production and physical activity. 2: However, with an increase in the ETC proteins electron transfer flavoprotein ubiquinone oxidoreductase and NADH dehydrogenase there is an increase in the efficiency of the ETC thereby compensating for the decrease in Krebs's (TCA) cycle activity. 3: The structural proteins, radixin, vinculin, vimentin, tubulin beta-3, and alpha tubulin 8 decrease mobility of actin and thereby reduce force production and physical activity.

IV Lessons Learned from Vivo-morpholinos: How to avoid Vivo-morpholino toxicity

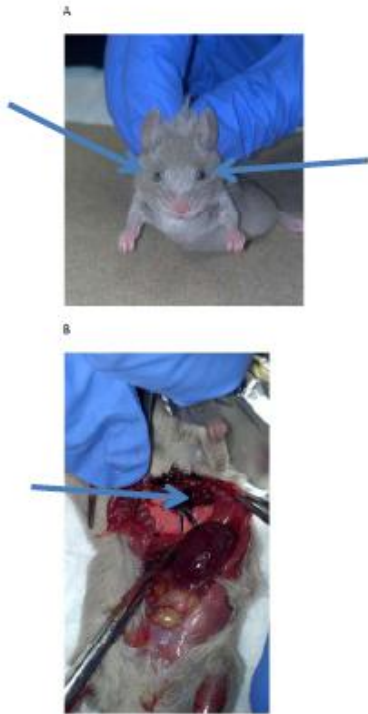


Figure 4.1: Panel A: Mouse that has received Vivo-morpholino treatment and presents with an opaque cloudy appearance to the eyes. Panel B: Dissected Vivo-morpholino treated mouse with necrotic tissue in the left ventricle.

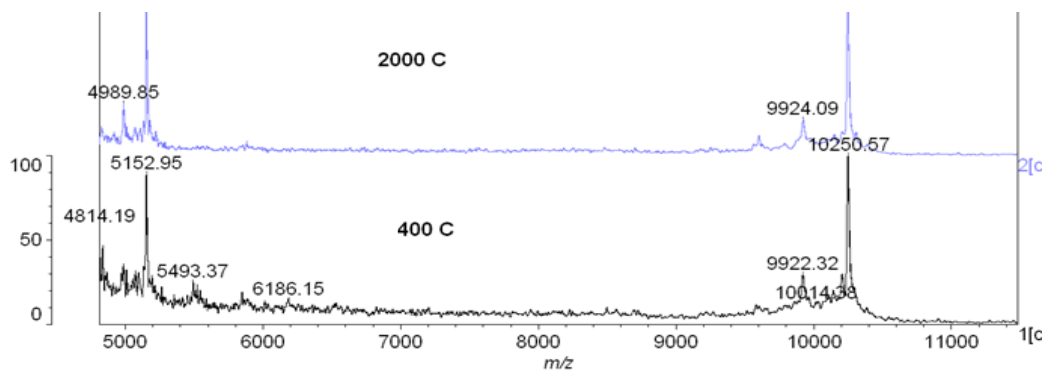


Figure 4.2: MALDI-TOF results of *Casq1* Vivo-morpholino at 400 nmol and 2000 nmol concentrations (C). There was no difference between the spectra.

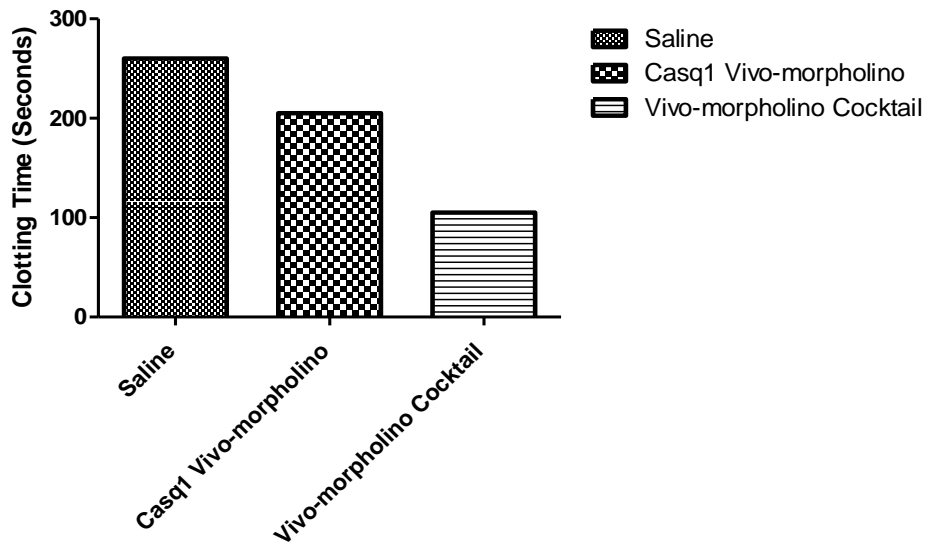


Figure 4.3: Clotting time of whole blood treated with saline, *Casq1* Vivo-morpholino, and Vivo-morpholino cocktail. Blood treated with Vivo-morpholino cocktail had an increased clotting time compared to saline control.

A: Cocktail Treatment

Anxa6

5' TGCAGCAGAAACCA**CGCGCTAGGGA** 3'

3' CTAACATGATGGAGGTA**CTCTCGAT** 5'

Casq1

B: Calsequestrin 1 Treatment

5' T**AGCTCTCATGGAGGTAGTACAA**TC 3'

3' C**TAA**CAT**GATGGAGGTA**CTCTCG**A** 5'

C: Annexin A6 Treatment

5' **I**GCAGCAGAAACCA**CGCGCTAGGGA** 3'

3' **A**GGGATCGCGCACCA**AAAGACGACGT** 5'

Figure 4.4: Nucleotide base pairing of 5' and 3' ends of the Vivo-morpholino treatments. Bold and underline nucleotides indicate location of base pairing. There was a direct relationship to the number of nucleotide base pairs and the number of fatalities.

APPENDIX B:

TABLES

Table 1: Soleus differentially expressed proteins between high- and low-active mice.

Protein	Strain Expressed in	p	Avg Ratio	No. of Identified Peptides	% Sequence Coverage	QTL
Calsequestrin 1	C57L/J	0.000025	1.78	2	5	N/A
Radixin	C3H/HeJ	0.00028	1.28	2	3	N/A
Annexin A6	C57L/J	0.00031	1.53	15	26	Mini Muscle ¹⁴
phosphoenolpyruvate carboxykinase	C3H/HeJ	0.00042	1.5	6	15	N/A
Peroxiredoxin-6	C3H/HeJ	0.00079	1.46	8	32	N/A
[Pyruvate dehydrogenase [acetyl-transferring]]-phosphatase 1	C57L/J	0.0022	1.37	2	4	N/A
Transferrin	C3H/HeJ	0.0026	1.44	12	17	N/A
Lumican	C57L/J	0.004	1.49	3	9	N/A
Synaptic vesicle membrane protein VAT-1 homolog	C57L/J	0.0046	1.27	3	10	N/A
Serine protease inhibitor A3K	C57L/J	0.005	1.91	6	15	N/A
Epoxide hydrolase 2	C57L/J	0.0051	1.21	8	13	Duration ¹²
Thioredoxin reductase 1	C57L/J	0.0051	1.21	3	5	Duration ¹²
myosin, light polypeptide 3	C57L/J	0.0062	1.9	3	14	N/A
Apolipoprotein A-I	C57L/J	0.0062	1.9	3	12	N/A
Atp5b	C3H/HeJ	0.007	1.38	12	31	Speed ¹²
Tubulin beta-3	C3H/HeJ	0.007	1.38	2	12	Duration ¹²
Vimentin	C3H/HeJ	0.007	1.38	2	5	N/A
Hemopexin	C3H/HeJ	0.018	1.34	2	4	Distance/Duration ³⁵
Phosphomannomutase 2	C57L/J	0.018	1.31	4	19	N/A
Hypothetical protein Hoch_2831	C57L/J	0.023	2.09	2	1	N/A
Annexin A4	C57L/J	0.023	1.16	8	27	N/A
pyruvate dehydrogenase E1 component subunit beta	C57L/J	0.023	1.16	6	18	N/A
Alpha-2-HS-glycoprotein	C3H/HeJ	0.026	1.26	2	24	N/A
NADH dehydrogenase [ubiquinone] iron-sulfur protein 3	C3H/HeJ	0.027	1.31	4	17	Average Speed ¹⁸³
Vinculin	C3H/HeJ	0.028	1.23	3	3	Duration ¹²
Tripartite motif-containing protein 72	C57L/J	0.029	1.27	7	16	N/A
Sarcalumenin	C57L/J	0.029	1.27	7	15	N/A
pyruvate dehydrogenase protein X component	C57L/J	0.029	1.27	3	7	N/A
FK506 binding protein 4	C57L/J	0.029	1.27	2	5	N/A
Alpha-1 protease inhibitor 2	C3H/HeJ	0.031	1.28	4	21	N/A

Table 1. Continued

Protein	Strain Expressed in	p	Avg Ratio	No. of Identified Peptides	% Sequence Coverage	QTL
alpha-1-antitrypsin 1-4	C3H/HeJ	0.031	1.28	4	21	N/A
Serpina1c protein	C3H/HeJ	0.031	1.28	7	16	N/A
Alanyl-tRNA synthase	C3H/HeJ	0.031	1.15	8	8	N/A
ATPase	C3H/HeJ	0.031	1.15	7	8	N/A
Aldehyde dehydrogenase	C3H/HeJ	0.031	1.14	5	10	N/A
6-phosphofructo-2-kinase/fructose-2,6-biphosphatase 1	C3H/HeJ	0.031	1.14	2	4	N/A
2-oxoglutarate dehydrogenase	C3H/HeJ	0.035	1.16	5	6	Mini-muscle ¹⁴
Annexin A5	C3H/HeJ	0.036	1.25	9	29	N/A
14-3-3 protein gamma subtype	C57L/J	0.036	1.2	5	16	N/A
Ubiquinone biosynthesis protein COQ9	C57L/J	0.042	1.24	4	16	Distance ³⁵
Dihydrolipoylysine-residue succinyltransferase component of 2-oxoglutarate dehydrogenase	C57L/J	0.22	1.24	5	11	Distance ³⁵

Protein = Name of the identified protein, strain expressed in = the mouse strain that the identified protein was expressed in, p= significance level of differential protein expression as obtained from DeCyder, Avg Ratio = derived from the normalized spot volume standardized against the intra-gel standard provided by Decyder-software analysis thus providing a measure of the magnitude of expression differences between identified proteins, No. of Identified Peptides = the number of peptides identified from the picked gel spot, % Sequence Coverage = the percentage of the number of amino acids identified in comparison to the total number of amino acids in the protein sequence, thus allowing for a confidence interval of 95% that the peptide sequence corresponds to the identified protein, QTL = if the identified protein is in a Quantitative Trait Loci for a coding gene associated with voluntary physical activity along with the literature reference for that QTL.

Table 2: EDL differentially expressed proteins between high and low-active mice.

Protein	Strain Expressed in	p	Avg Ratio	No. of Identified Peptides	% Sequence Coverage	QTL
v-type proton ATPase catalytic subunit A	C57L/J	0.0016	3.72	2	4	N/A
Annexin A6	C57L/J	0.0016	2.11	15	24	Mini Muscle ¹⁴
Sdha	C3H/HeJ	0.0016	1.43	6	10	N/A
electron transfer flavoprotein-ubiquinone oxidoreductase	C3H/HeJ	0.0016	1.43	3	6	N/A
Alpha-actinin-2	C3H/HeJ	0.0044	1.82	2	2	Speed ¹²
Apolipoprotein A-I	C57L/J	0.0046	2.2	2	7	N/A
T-complex protein 1 subunit zeta	C3H/HeJ	0.035	1.28	4	7	N/A
Alpha-tubulin 8	C3H/HeJ	0.05	1.45	3	6	Speed ¹²

Protein = Name of the identified protein, Strain expressed in = the mouse strain that the identified protein was expressed in, p= significance level of differential protein expression as obtained from DeCyder, Avg Ratio = derived from the normalized spot volume standardized against the intra-gel standard provided by Decyder-software analysis thus providing a measure of the magnitude of expression differences between identified proteins, No. of Identified Peptides = the number of peptides identified from the picked gel spot, % Sequence Coverage = the percentage of the number of peptides identified in comparison to the total number of peptides in the protein sequence indicating that there is a 95% confidence level that the identified protein corresponds to the peptide sequence, QTL = if the identified protein is in a Quantitative Trait Loci for a coding gene associated with voluntary physical activity along with the literature reference for that QTL.

Table 3: Protein expression profiles based on function of the protein

Protein	Strain Over Expressed in	Tissue expressed in
Electron Transport Chain		
Atp5b protein	C3H/HeJ	Soleus
NADH dehydrogenase [ubiquinone] iron-sulfur protein 3	C3H/HeJ	Soleus
ATPase	C3H/HeJ	Soleus
electron transfer flavoprotein ubiquinone oxidoreductase	C3H/HeJ	Soleus
TCA Cycle		
pyruvate dehydrogenase protein X component	C57L/J	Soleus
pyruvate dehydrogenase E1 component subunit beta	C57L/J	Soleus
Pyruvate dehydrogenase [acetyl-transferring]-phosphatase 1	C57L/J	Soleus
dihydrolipoyllysine-residue succinyltransferase component of 2-oxoglutarate dehydrogenase complex	C57L/J	Soleus
6-phosphofructo-2-kinase/fructose-2,6-biphosphatase 1	C3H/HeJ	Soleus
phosphomannomutase 2	C57L/J	Soleus
Sdha protein	C3H/HeJ	EDL
Oxygen Transport		
Transferrin	C3H/HeJ	Soleus
Oxidative stress Response		
Hemopexin	C3H/HeJ	Soleus
thioredoxin reductase 1	C57L/J	Soleus
Peroxiredoxin-6	C3H/HeJ	Soleus
ubiquinone biosynthesis protein COQ9	C57L/J	Soleus
Protein Regulation		
Serine protease inhibitor A3K	C57L/J	Soleus
alanyl-tRNA Synthase	C3H/HeJ	Soleus
FK506 binding protein 4	C57L/J	Soleus
alpha-1 protease inhibitor 2	C3H/HeJ	Soleus
alpha-1-antitrypsin 1-4 precursor	C3H/HeJ	Soleus

Table 3 Continued.

Protein	Strain Over Expressed in	Tissue expressed in
Annexin A6	C57L/J	Soleus/EDL
Calsequestrin 1	C57L/J	Soleus
Sarcalumenin	C57L/J	Soleus
Structural Proteins		
Radixin	C3H/HeJ	Soleus
Lumican	C57L/J	Soleus
tripartite motif-containing protein 72	C57L/J	Soleus
Vinculin	C3H/HeJ	Soleus
Vimentin	C3H/HeJ	Soleus
Tubulin beta-3	C3H/HeJ	Soleus
Cofilin-2-like	C3H/HeJ	Soleus
Alpha-actinin-2	C3H/HeJ	EDL
T-complex protein 1 subunit zeta	C3H/HeJ	EDL
Alpha tubulin 8	C3H/HeJ	EDL
Other		
Epoxide hydrolase 2	C57L/J	Soleus
aldehyde dehydrogenase	C3H/HeJ	Soleus
Hoch 2831	C57L/J	Soleus
apolipoprotein A-I	C57L/J	Soleus/EDL
myosin, light polypeptide 3	C57L/J	Soleus
phosphoenolpyruvate carboxykinase	C3H/HeJ	Soleus
Serpina1c protein	C3H/HeJ	Soleus
synaptic vesicle membrane protein VAT-1	C57L/J	Soleus
14-3-3 protein gamma subtype	C57L/J	Soleus
v-type proton ATPase catalytic subunit A	C57L/J	Soleus
Annexin A5	C3H/HeJ	Soleus

Table 4: Co-immunoprecipitation of Annexin VI and Calsequestrin 1

Identified Protein	Number of Peptides	Percent Sequence covered
<u>Annexin VI</u>		
<u>Soleus C57L/J</u>		
alpha S1 casein	3	15
<u>Soleus C3H/HeJ</u>		
beta-lactoglobulin	2	8
<u>EDL C57L/J</u>		
alpha S1 casein	3	15
<u>EDL C3H/HeJ</u>		
Actin, alpha 1	2	6
<u>Calsequestrin 1</u>		
<u>Soleus C57L/J</u>		
creatine kinase M-type	10	30
alpha S1 casein	3	18
Ldb3 protein	4	19
troponin T3	3	15
desmin	6	12
<u>Soleus C3H/HeJ</u>		
creatine kinase M-type	10	30

Table 4 Continued.

Identified Protein	Number of Peptides	Percent Sequence covered
troponin T3	3	15

Identified proteins from a Co-immunoprecipitation of Annexin A6 and Calsequestrin 1. Proteins were identified by mass spectroscopy and the number of peptides along with the sequence percentage is presented.

APPENDIX C:
PROTEIN ASSAY TECHNIQUES

Table of Contents

Biology of Physical Activity Lab

Adapted from Protein Chemistry Laboratory and Muscle Biology Lab at Texas A&M University

Protein Extraction

-Brain

-Muscle

Protein Concentration

-Bradford

-BCA

SDS Page

Staining

-Coomassie

-Silver Staining

Western Blotting

Chloroform Methanol Precipitation

Protein Extraction - Brain

1) Make Norris Buffer

Chemical	For 125 ml	For 250 ml	For 500 ml
HEPES (g)	0.745	1.489	2.979
β -glycerophosphate (g)	0.135	0.270	0.540
ATP (g)	0.014	0.028	0.055
Protease Inhibitor Cocktail (ml)	0.75	1.25	2.5
Benzamidine (g)	0.489	0.979	1.958
PMSF (g)	0.044	0.087	0.174
DMSO (ml)	0.25	0.5	1.0
EDTA (g)	0.186	0.372	0.744
MgCl ₂ (g)	0.254	0.508	1.017

- a.
 - b. Dissolve PMSF in DMSO and then add to buffer last
 - c. Fill to appropriate volume with ultrapure DI water
 - d. pH to 7.4
 - e. Freeze in 15 ml tubes
 - f. See Norris Buffer instructors for further information
- 2) Aliquot 300 ul of Norris buffer into the required number of 1.7 ml tubes
 - 3) Add 30 ul of 10% Tritton X 100 if there is difficulty in viewing proteins.
 - 4) Put froze brain tissue in buffer solution and using tissue homogenizer grind the tissue by pulsing for 10 seconds and resting for 15 seconds. Continue until tissue is fully homogenized avoid excessive foaming.
 - a. Cleaning homogenizer with 50/50 Ethanol/water solution and rinse with DI water
 - 5) Put homogenized tissue on ice for 1 hour and vortex every 15 minutes
 - 6) Centrifuge at 4 degrees C for 30 minutes at max speed
 - 7) Protein will be in the supernatant
 - 8) Remove supernatant and put new 0.6 ml tube
 - a. Additionally aliquot necessary sample for protein concentration
 - 9) Place protein in -80. Move on to protein concentration or store aliquot in -20 for later protein concentration

Protein Extraction – Muscle

- 1) Make Dangott Lysis Buffer
 - a. 24.6mg CHAPS
 - b. 100ul 1M Tris 7.5
 - c. 1 complete tablet (Rousch)
 - d. 9.9 ml DI water

- 2) If sample is > 100ug aliquot 1000ul of Dangott lysis buffer into 1.7ml tubes. If it is <100ug aliquot 500 ul of buffer
- 3) Remove motor and pestle from freezer
- 4) Pour liquid nitrogen into motor
- 5) Add sample
- 6) Grind sample in until fine powder
- 7) Using an autoclaved spatula scrap sample into tube with buffer
- 8) Let sample sit on ice for 1 hour with vortexing every 15 minutes
- 9) Centrifuge for 30 mins at high speed at 4 degrees C
- 10) Remove supernatant (protein) and aliquot into new tubes
 - a. Additionally aliquot necessary sample for protein concentration
- 11) Place protein in -80. Move on to protein concentration or store aliquot in -20 for later protein concentration

Protein Concentration – Bradford

Note: for use with Dangott lysis buffer

- 1) Using a 96 well plate aliquot 300 ul of coomassie into the necessary number of wells.
 - a. Add additional wells for 2000ug/ml BSA standard, 1000 ug/ml BSA standard, 500 ug/ml, 250 ug/ml standard, and 125 ug/ml standard.
- 2) Make dilution series for sample
 - a. Typically use Neat, 2x, 4x, 8x, 16x
 - b. Combine equal volume of sample with water to achieve dilution (ex: 2x=20ul neat and 20 ul water, 4x = 20 ul 2x and 20 ul water)
- 3) Add 10 ul of sample, dilutions and standards to the wells containing 300 ul of coomassie
- 4) Should observe a blue color change
- 5) Open the nanodrop program and protein Bradford software
- 6) Follow on screen instructions
 - a. Add 2ul of each sample to the nanodrop
- 7) Clean nanodrop with DI water when done

Protein Concentration – BCA

Note: for use with Norris buffer

- 1) Use 96 well plate and standards as above

- 2) Make dilution series for sample
 - a. Typically use Neat, 2x, 4x, 8x, 16x
 - b. Combine equal volume of sample with water to achieve dilution (ex: 2x=20ul neat and 20 ul water, 4x = 20 ul 2x and 20 ul water)
- 3) Follow instructions for pierce BCA protein assay kit
- 4) For heating place plate on heat block and cover with foil.
- 5) Should observe a purple color change
- 6) Open the nanodrop program and protein BCA software
- 7) Follow on screen instructions
 - a. Add 2ul of each sample to the nanodrop
- 8) Clean nanodrop with DI water when done

SDS-Page

A] Preparation of gel plates

1. Put the glass plates and Aluminum backing plates on a clean surface (like a paper towel).
2. Spray plates with 100% methanol and thoroughly clean with kimwipe. (PS: they are expensive so do not break them!.)

B] Putting the gel plates on the gel caster unit to create the gel- plate sandwich

1. Insert the 0.75mm spacers (black ones) on the sides of the plates (1 for each side, so 2 for 1 pair of plates).
2. Insert the gel-plates pair in the gel stand vertically with the glass surface facing you.
 - Make sure all edges are flush or it will leak.
3. Screw the clamps down on the plates
4. Using Gel seal fill the gap between the glass and AL plate
5. Line the bottom of the red gel holder with parafilm to prevent leaks
6. Put the grey gel caster in the red gel stand use black cams to lock the caster down
 - Put binder clamps on the top of the gel plates to prevent leaks
7. Spray distilled water in the gel – plate surface (in between the 2 plates) to test for leaking.

C] Preparation of the gel

Preparation of 12% RUNNING GEL – Muscle

1. In a small beaker

- 3.3 ml distilled water.
- 4ml of Acrylamide mix (Bis 30 % acrylamide brown bottle).
- 2.5 ml 1.5M Tris 8.8.
- 100µl of 10% Sodium dodecyl sulfate (SDS).
- 100µl of 10% Ammonium persulfate solution (APS).
- 4 ul of TEMED.
- MIX WELL

Preparation of 10% RUNNING GEL-Brain.

1. In a small beaker

- a. 3.9 ml water
 - b. 3.3ml Acrylamide
 - c. 2.5 ml 1.5 M Tris 8.8
 - d. 100ul 10% SDS
 - e. 100ul 10% APS
 - f. 4 ul TEMED
2. Fill gel caster with running gel up to the top of the grey caster
 3. Then fill rest of the caster with water .saturated iso-butanol.
 4. Wait for the gel to harden up. Takes approximately 15-20 minutes.
 5. After the gel is hardened dump the iso-butanol, and wash 3x with distilled water

Preparation of STACKING GEL

Get a small beaker for making the stacking gel.

- 3.4 ml of distilled water.
- 830 µl of acrylamide mix.
- 630 µl of Tris 6.8pH.
- 50µl of SDS.

-50µl of 10% APS.

-5 µl of TEMED.

Fill stacking gel to the top and add combs. Then clamp gels with binder clamps

D] Sample Preparation

Note the 0.75 mm spacers on this system can only hold 30ul of sample. Therefore you must calculate your sample volume appropriately

Example: The lowest protein concentrations for your samples are 1.3ug/ul. You need to mix your sample with 4x SDS sample buffer to reach a volume of 30 ul. Therefore 1/4th of 30 ul is 7.5 ul (the amount of 4x SDS sample buffer you must add for this sample.) Which means you can add 22.5 ul of your sample. Thereby you will be adding 29.25 ug of protein for this sample (22.5*1.3ug/ul). Thus, you must add the same amount of protein for all your samples. So if your next sample has a concentration of 2.5ug/ul. You would divide 29.25ug by 2.5ug/ul telling you that you will add 11.7 ul of that sample to get the same protein concentration. Then you would add 7.5 ul of 4x SDS sample buffer to 11.7 giving you 19.2 ul. Fill the remainder to 30 ul (in this case add 10.8ul of water). REMEMBER LOAD THE SAME AMOUNT OF PROTEIN PER SAMPLE AND EACH WELL SHOULD CONTAIN 30 UL OF WATER. THIS WILL GIVE A CLEAR RESULT

- 1) Once you have added the appropriate amount of sample, 4x SDS buffer and water to 0.6 ml. Vortex then quick spin the tubes. Heat the samples at 90 C for 12 minutes. Then quick spin the samples.
 - a. 200ul Beta mercaptoethanol
 - b. 800ul 5x Sample buffer
 - i. 150ml water
 - ii. 50g glycerol
 - iii. 70ml water
 - iv. 3.78g Trizma base
 - v. pH to 6.8 with HCL
 - vi. 30 water
 - vii. 10g SDS
 - viii. 25ml 0.04% bromophenol blue
- 2) Pull the combs from gel casters as slowly as possible. Wash it with distilled water three times. Clip the gel-plates to the buffer chamber using the red clamps (longer side facing you).
- 3) Fill the upper and lower buffer chambers with 1x SDS running buffer. Also, fill the gel wells. Make sure you completely fill the back of the AL plate with buffer

- a. 900 ml water
- b. 100ml 10x SDS sample buffer
 - i. 30.28 g Trizma base
 - ii. 144.1gm glycine
 - iii. 10gm SDS
 - iv. 1000 ml water
- 4) Place the well decal on the glass plate,
- 5) Disable gel caster and
- 6) Add your samples to the wells.
 - a. Avoid the outer lanes. In lane 2 add your maker
 - b. Add 30ul of 1x SDS sample buffer to the lanes with no sample
- 7) Put the top on the gel chamber matching red to red and black to black. If running 2 gels set system to constant volts at 22 mA. If running 4 gels set to constant volts and 50 mA.
- 8) Let gel run until dye front reaches end of the gel plate DO NOT LET IT RUN OFF
- 9) When done disable chamber and remove gels CAREFULLY
- 10) Remove stacking gel and cut bottom left corner of gel
- 11) Proceed to staining or Western Blotting

Staining-Coomassie

Note: for use if over 20ug of protein have been load on gel.

- 1) Fix gels for 1 hour with Fixative
 - a. 100ml Glacial Acetic Acid
 - b. 300 ml Ethanol
 - c. 600 ml water
- 2) Remove from fixative and wash for 1 hour in new fixative
- 3) Add Coomassie to properly cover the gel
- 4) Wash until bands are blue
- 5) Rinse with DI water

Staining – Silver

For use if less than 20 ug of protein have been load on gel

- 1) Fix gels for 1 hour and then fix in clean fixative for additional hour
 - a. 100ml Glacial Acetic Acid

- b. 300ml Ethanol
- c. 600 ml water
- 2) Rise gel in Rinse solution for 20 mins
 - a. 200ml ethanol
 - b. 800ml water
- 3) Rinse gel in water for 10 mins
- 4) Soak gel in Sensitizer for 1 min
 - a. 200mg sodium thiosulfate
 - b. 1000ml water**
- 5) Rinse gel in water 3 times for 30 seconds
- 6) Soak gel in silver nitrate solution for 45 mins (MAKE DEVELOPER)
 - a. 2gm silver nitrate
 - b. 1000ml water
- 7) Rise gel in DI water for 5-10 seconds
- 8) Soak gel in developer until bands appear (DO NOT OVER EXPOSE)
 - a. 15gm sodiam carbonate
 - b. 25 ml Sensitizer
 - c. 125ul 37% formaldehyde (add right before developing)
 - d. 500 ml water
- 9) Soak gel in stop solution for 15 minutes
 - a. 50g Tris base
 - b. 25 ml glacial acetic acid
 - c. 1000ml water
- 10) Soak gel in water

Western Blotting

- 1) If using a PVDF membrane: Spray methanol on it.
- 2) Place gel, membrane, sponges, and filter paper in transfer buffer working solution
- 3) . Rock the membranes and the gel in transfer buffer for 20 minutes.
- 4) Assemble the transfer cassette
 - a. Black side
 - b. Sponge
 - c. 2 pieces of filter paper
 - d. Gel
 - e. Membrane which has been labeled for lane 1 and 10 and the back top left portion
 - f. 2 pieces of filter paper

- g. Sponge
 - h. White side
- 5) using a pipette pressed on the filter paper to remove air bubbles
 - 6) Place stir bar in transfer tank and turn on when tank is closed
 - 7) Place cassette in transfer tank with the black side facing the back
 - 8) Fill with Transfer buffer working solution
 - a. 800 ul water
 - b. 100 ul Methanol
 - c. 100 ul Transfer buffer stock
 - i. 1000 ml water
 - ii. 22.13 g CAPS
 - iii. pH to 11.0 with NaOH
 - 9) Putt cap on and make sure back matches to black and red matches to red
 - 10) For muscle run at constant volts and 100mA for 3 hours
 - 11) For brain run at constant volts and 100mA for 2 hours and 20 minutes
 - 12) Remove gel from transfer and block for 1 hour muscle or 40 minutes brain
 - a. 500 ul Tween 20
 - b. 25 g NFDm
 - c. 500m TBS
 - 13) Make antibody solution and cut plastic bags
 - a. The bag will hold 5ml
 - b. Mix 5m of blocking buffer with appropriate antibody amount for protein of interest
 - 14) Wash 3x for 5 mins with TBS
 - 15) Seal membranes in plastic pouch and rock over night in 4 degree C
 - 16) Next morning remove membranes and wash 3 times for 5 mins in TBS
 - 17) Add secondary antibody
 - a. 5ml blocking buffer
 - b. 2.5 ul Secondary Rabbit HRP antibody
 - 18) Seal pouch and rock for 1 hour at room temp
 - 19) Wash membrane 3 times for 5 minutes with TBS
 - 20) Image in Fluckey's lab (use supersensitivity setting if weak signal)
 - a. Use Pierce HRP kit
 - i. 7ml brown bottle and 7 ml white bottle
 - ii. Image for 5 mins on setting 1 for the flurochem
 1. Use plastic sheet to cover membrane while in imager

Chloroform Methanol Precipitation

If you have too low of a protein concentration you can concentrate your sample with this.

- 1) Remove enough volume of each sample to equal your desired protein concentration.
Note the protein content of the volume you remove must be the same
- 2) Place volume in 1.7ml tube
- 3) Add 600ul MeOH
- 4) Vortex
- 5) Add 150 ul Chloroform
- 6) Vortex
- 7) Add 450 ul water
- 8) Spin at high speed for 1 min
- 9) Protein at interface
- 10) Remove upper layer
- 11) Add 450 ul MeOH
- 12) Vortex
- 13) Spin at high for 2 mins
- 14) Proteins in Pellet
- 15) Remove supernatant
- 16) Wash pellet with 500 ul of MeOH
- 17) Vortex
- 18) Spin for 1 min
- 19) Remove MeOH
- 20) Air dry pellet for 5 mins
- 21) If you are going to use this sample on 2 gels add 30 ul 2x sample buffer and 30 ul of water
 - a. Adjust for larger number of gels
- 22) Vortex until pellet dissolves
- 23) Freeze at -20 or load on gel

APPENDIX D:

VIVO-MORPHOLINO DOSE CALCULATOR

Mass per injection (mg) = [Dose per injection (mg/kg) * Animal mass (g)] / 1000

Nanomoles per injection = [Mass per injection (mg) / 1000] / [*Est. Formula (mass g/mole)⁹]

Vol per injection at 0.5 mM (ul) = (Nanomoles per injection * 10⁹) / (0.0005 * 10⁶)

*Note estimated formula mass is established by GeneTools as 10000 g/mole